FACULTY OF HEALTH AND MEDICAL SCIENCES
UNIVERSITY OF COPENHAGEN

PhD Thesis

Andreas Herchenhan

Collagen Fibril Development

Factors influencing cells and extracellular matrix during *in vitro* human tendon construct formation

This thesis has been submitted to the Graduate School of
the Faculty of Health and Medical Sciences, University of Copenhagen

Academic advisor: Professor Michael Kjaer

Co-advisor: Professor Peter Magnusson

Submitted: 12/11/14

“Das Leben ist wie ein Fahrrad, man muss sich vorwärts bewegen um das Gleichgewicht nicht zu verlieren”

– Albert Einstein, 05.02.1930

“Life is like a bicycle. To keep your balance you must keep moving”

– Albert Einstein, 05.02.1930

Preface

During my four-year period at the Institute of Sports Medicine Copenhagen I met many people without whom I would have been lost from the first day.

At first I owe deep gratitude to my supervisor Michael Kjaer. You gave me an unconditional offer to conduct my PhD studies at your Institute and supported me ever since. Your office is always open for everyone and your leadership is exemplary. I would like to express my special thank for your scientific and not least personal support. Similarly, I need to thank my Co-supervisor Peter Magnusson. You stay calm whatever happens– a skill that is truly inspirational. Every time I was struggling you put matters into perspective, which made me feel better from the spot.

Pernilla Eliasson, you joined the lab some time after me, but had a sustainable impact on my scientific and personal struggles. You would always lend me your ear and helped me get past whatever issue. Your positive, hands-on approach to problems is motivating and I wish I could keep up with your speed. I would like to thank all members of the tendon cell group, Katja, Monika, Rie and all intercalating students for motivating discussions and instructive journal clubs. Likewise, the biomechanics group always added a different perspective to matters. Particularly thank you to Rene Svensson, no one knows more about collagen than you and you are always happy to share your knowledge. Your helpfulness is admirable. The entire scientific staff at ISMC welcomed me warmly from the first day and during my entire time I never experienced a request remaining unanswered. The friendly and open, but also scientifically critical atmosphere was truly stimulating to my work.

Working at ISMC is purely luxurious. I would like to acknowledge all technicians, secretaries and cleaning staff. The entire lab is superbly organised and I almost feel embarrassed how few I contributed apart from giving my best to disturb this order. I also got the possibility to pursue my cell work in the dermatology department. I would like to thank everyone there for keeping up with my rushing in and out about 15 times per day. Specifically, I want to thank Vibeke Pless. Your commitment to supporting the lab is unmatched and your laughter brings joy to every day.

At the University of Copenhagen, Klaus Qvortrup gave me the possibility to use any commercially available microscopical equipment without restrictions. Thank you very

much for your support and not least for inviting me on an exciting bike tour to Paris, which helped me connecting to the Copenhagen cyclists-community. Which leads to two colleagues who became friends – Kasper and Søren, I really enjoyed our countless discussions on our favorite non-scientific topic – bikes! Even more I will always remember our many mind-relaxing but body-wrecking training rides. Jakob Agergaard, you patiently accompanied my first steps with the Danish language. If it hadn't been for you, I would still not understand a word during Julefrokost. You became a friend and we shared various activities and our passion for skiing. My office partner Christian Couppe, it was a pleasure being your neighbour and I want to thank you for always being there when I needed advice.

At the University of Manchester I met scientists who sustainably impacted my career and still were of exceptional help during my PhD studies. Karl Kadler, thank you for being truly inspiring and for sharing your motivation and ideas with me, which are beyond imagination. Another very big thanks to David Holmes. You are a true scientist and probably the most patient person in the world. Thank you for sharing your wisdom and technical skills with me, but also for your legendary PS messages. Finally, Nick Kalson, we were friends from the first day we met. We had countless discussions on science and bikes, and you always backed me up when I needed it.

All my life my family was there for me. Vielen Dank meine lieben Eltern, dass ihr mich immer mit all eurer Energie unterstützt habt und mir die Freiheit gegeben habt meine Träume zu verfolgen. Alex und Chrissi, ihr seid die weltbesten Geschwister und ich bin sehr stolz auf unseren Zusammenhalt. Wenn man so eine Familie im Rücken hat wirken viele Aufgaben nur halb so schwer!

Thank you my dear Franziska, love of my life. Words cannot tell how much your support means to me. You are always there for me and make my life complete.

Table of Contents

Abbreviations

αSMA	α-Smooth Muscle Actin
ADAMTS-2	A Disintegrin and Metalloproteinase with Thrombospondin Motifs-2
AGE	Advanced Glycation Endproducts
BAPN	ß-Aminoproprionitrile
BMP-1	Bone Morphogenic Protein-1
COX	Cyclooxygenase
DMEM	Dulbecco's Modified Eagle Medium
DTT	Dithiothreitol
ECM	Extracellular Matrix
EDS	Ehlers Danlos Syndrome
EGF	Epidermal Growth Factor
ER	Endoplasmic Reticulum
FACIT	Fibril-Associated Collagens with Interrupted Helices
FBS	Fetal Bovine Serum
FIB	Focussed Ion Beam
FGF	Fibroblast Growth Factor
GDF	Growth/Differentiation Factor
GH	Growth Hormone
HPLC	High Performance Liquid Chromatograph
IGF-I	Insulin-Like Growth Factor I
LOX	Lysyl Oxidase
LOXL	Lysyl Oxidase-Like
MAP	Mitogen-Activated Protein
Mkx	Mohawk Homeobox
MMP	Matrix Metalloproteinase
MSC	Mesenchymal Stem Cell
NFκB	Nuclear Factor Kappa-light-chain-enhancer of Activated B Cells
OCT-4	Octamer-Binding Transcription Factor-4
PBS	Phosphate Buffered Saline
PDGF	Platelet Derived Growth Factor
PRP	Platelet Rich Plasma
RT-qPCR	Reverse Transcriptase-Quantitative Polymerase Chain Reaction
Scx	Scleraxis
SDS-PAGE	Sodiumdodecylsulfate-Polyacrylamid Gelelectrophoresis
SEM	Scanning Electron Microscopy
SLRP	Small Leucin-Rich Repeat Proteoglycans
SSEA-4	Nucleostemin and Stage-Specific Embryonic Antigen-4
TEM	Transmission Electron Microscopy
TGF-ß	Transforming Growth Factor-ß
TIMP	Tissue Inhibitor of Metalloproteinases
Tnm	Tenomodulin
VEGF	Vascular Endothelial Growth Factor

Summary

Collagen fibrillogenesis is a key aspect of tendon development and healing. In order to augment the production of functional tendon tissue, the meticulously regulated collagen synthesis needs to be better understood. Moreover, factors influencing this process need to be evaluated for their beneficial or antagonising function, respectively. This PhD project aimed to expand common knowledge on how tendon cells produce collagen fibrils *in vitro* and the effect of specific interventions on this process.

In the first study, a three-dimensional cell culture system termed tendon construct was evaluated for its developmental potential over five weeks. To create a construct, primary adult human tendon cells are seeded in a fibrin gel between two anchor points to form a rod-shaped structure. Over time, the constructs showed a significant increase in tensile mechanical properties, accompanied by a rise in average collagen fibril diameter. Despite being larger in size, the cells were aligned similarly to tendon *in vivo*.

The aim of the second study was to investigate the effect of insulin-like growth factor-I (IGF-I) on construct development. The standard growth factor-rich cell supplement fetal bovine serum (FBS) was thereby varied between 0.5% and 10%. Tendon constructs showed increased collagen production and fibril development due to IGF-I treatment. Interestingly, high levels of FBS had a decreasing effect on collagen production, while very low FBS increased collagen expression. However, this increase was not translated to functional collagen fibrils and the cells were impaired. IGF-I could rescue this effect, and the combination of IGF-I with low serum was thus the most enhancing treatment to sustain the tendon phenotype.

Lysyl oxidase (LOX) is known as the essential enzyme during collagen cross-link formation. The third study focused on the effect of LOX-inhibition during collagen fibrillogenesis. Due to the lack of collagen cross-links, construct mechanical development was disabled. Moreover, the collagen fibrils showed irregular shapes, which points towards a new role for LOX as fibril regulator. Notably, no change in gene expression or protein modification was found, suggesting that the cells lack a mechanism to control correct collagen fibril formation.

Taken together, this project confirms the tendon construct as a suitable model system for tendon development and extends the knowledge on IGF-I and LOX in this context.

List of Papers

This thesis is based on the following original papers:

1. Herchenhan A, Bayer ML, Svensson RB, Magnusson SP, Kjaer M (2013) In Vitro Tendon Tissue Development From Human Fibroblasts Demonstrates Collagen Fibril Diameter Growth Associated With a Rise in Mechanical Strength. *Developmental Dynamics* **242**: 2-8

2. Herchenhan A, Bayer ML, Eliasson P, Magnusson SP, Kjaer M (2014) Insulin-like growth factor I enhances collagen synthesis in engineered human tendon tissue. *Growth Hormone & IGF Research* (http://dx.doi.org/10.1016/j.ghir.2014.09.001)

3. Herchenhan A, Uhlenbrock F, Eliasson P, Mary Ann Weis, David Eyre, Kadler KE, Magnusson SP, Kjaer M (2014) Lysyl Oxidase controls collagen molecule aggregation during fibrillogenesis. *In preparation*

Introduction

Tendons and ligaments are frequently subjected to injuries and irritations that cannot be fully explained by the scientific community to date. The fundamental element in understanding these issues is how collagen fibrils are formed, maintained and repaired during development, pathology and ageing. Current knowledge has already been transferred to *in vivo* studies to further increase understanding of tendon regulation. However, these studies are restricted in regards to invasiveness and developmental potential. Therefore, *in vitro* studies are required.

An *in vitro* model for tendon development would be beneficial in order to investigate collagen fibrillogenesis. Moreover, factors influencing this development could be isolated and their effect could be monitored in detail. A recently developed tendon construct from adult human tenocytes appears to be a promising tool for this purpose. Treatment of tendon related injuries is often conducted by means of humoral stimulation such as application of platelet rich plasma, human growth hormone (GH) or IGF-I. However, for many of these substances the exact effects and/or formulation remain unknown. Therefore, the tendon construct provides the opportunity to investigate the influence of the humoral milieu on collagen fibril formation by manipulation with FBS and IGF-I amongst others. A different, often neglected, factor for functional collagen fibrils is inter- and intrafibrillar cross-linking of collagen molecules. The key player to establish these cross-links in early collagen development is LOX. It is well established that LOX is responsible for establishing cross-links and thereby securing the collagen's mechanical stability and reducing solubility. However, the effect of LOX during fibrillogenesis as well as the timing of cross-links formation during development is so far unknown.

The objective of this PhD project was to evaluate the tissue-engineered tendon like structure – termed tendon construct – on its developmental potential. Showing that the human tenocytes develop the structure over time would confirm the validity of the construct as a model for tendon development and collagen fibrillogenesis *in vitro*. Thereafter, the effect of IGF-I and FBS on collagen fibrillogenesis was studied. Finally the influence of LOX on collagen fibrillogenesis was investigated providing new insights into this research field.

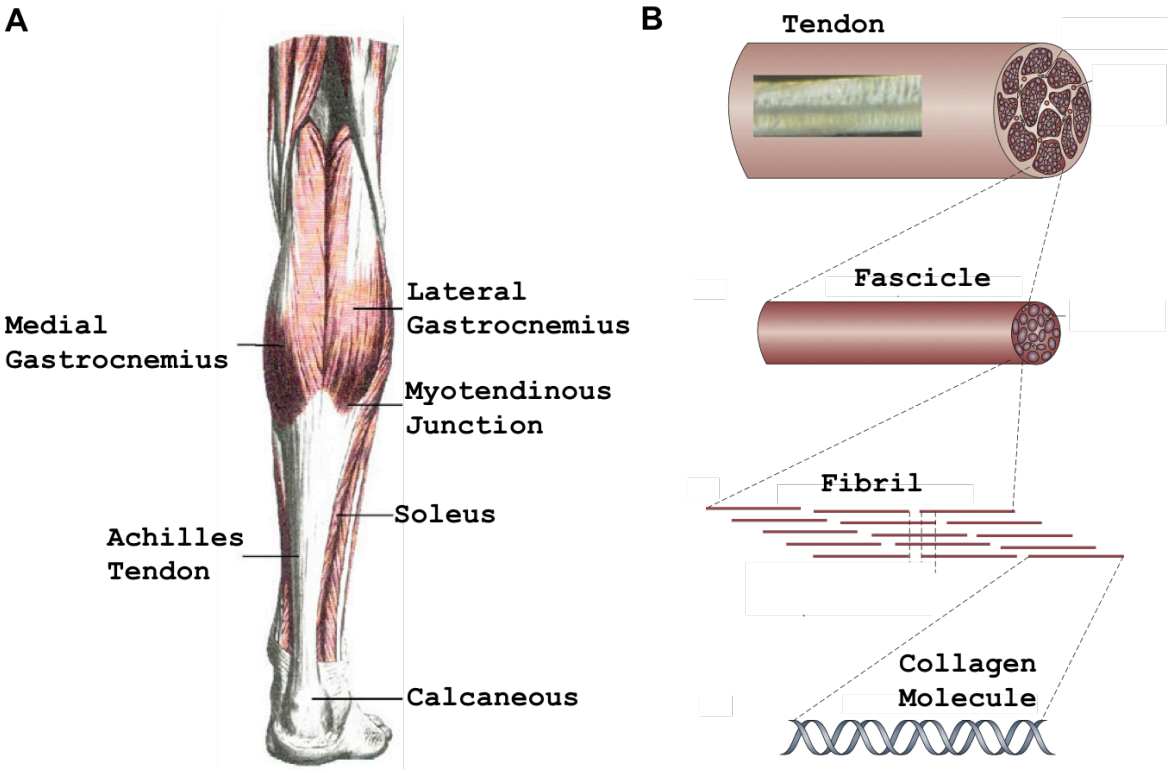

Figure 1. Overview of the tendon structure. A) The Achilles tendon is the thickest and strongest tendon of the human body and transfers loads from the calf muscles to the calcaneous (adapted from Grey´s Anatomy [76]). B) The hierarchical setup of tendon ranging from the tendon to fascicles, fibrils and ultimately collagen molecules. Cells are squeezed in between fascicles (adapted from Magnusson et al.[134]).

Tendon

Tendon is the connective tissue transferring muscle-generated forces to bones (Fig.1). Throughout the body tendons and ligaments are essential for locomotion, and their tasks can vary substantially between different sites [175]. The rotator cuff tendon, for instance, has a sheet-like structure and transmits forces across different angles [42], while the patellar tendon transfers the force produced by the quadriceps muscles unidirectionally to the tibia [44; 67]. The Achilles tendon is the largest weight-bearing tendon in the human body and transfers loads of up to 5000 N during high intensity activities such as jumping [128]. Ligaments on the other hand join one bone to another such as the anterior cruciate ligament, linking femur to tibia within the knee capsule [18; 189]. Their major function is to keep the skeleton in place and function as a buffer for impacts or strains [154; 189].

Despite their differing functional requirements, tendon and ligament share a very similar structural organisation, consisting mostly of extracellular matrix (ECM), which is

dominated by longitudinally aligned collagen type I fibrils [25; 135; 189]. Since these structural analogies are very close, this thesis will focus on the term tendon, although the main outcomes can similarly be applied to ligament tissue.

Approximately 70-80% of tendon dry weight consists of arranged collagen, with the major fraction being collagen type I [23]. Single collagen fibrils are combined in fibril bundles, which in turn aggregate in fascicles to create the tendon (Fig.1) [117]. This highly hierarchical arrangement gives rise to the typical tendon properties and ensures mechanical function [68; 117; 134]. Cells make up a minor portion of the tissue and speculation suggests that the cells of adult tendon are in a rather inert state, which might explain slow tissue repair [33].

Tendon Development

Tendons originate from the mesoderm, particularly from somites that are located near the neural tube and notochord [131]. Chaplin and Greenlee observed human digital tendons of 40 to 120 day old embryos and found that the tissue's development mechanism is remarkably different to known tendon repair mechanisms [39]. Initially, a core of tendon cells is developed while continuously more homogenous collagen fibrils are produced. Collagen fibrils are thereby "guided" by the cells to run in aligned bundles. As soon as the extracellular space is filled with fibrils the cells retract to leave space for more fibrils, which are organised in fascicles (Fig.2) [39]. This development is strikingly similar to observations in chick embryonic tendon [25].

During tendon development, two key molecules were identified that play essential roles and are therefore considered tendon markers: The basic helix-loop-helix transcription factor scleraxis (scx) and the transmembrane glycoprotein tenomodulin (tnm). Cserjesi et al. [47] first described scx as a regulator of gene expression in cartilage and connective tissue precursor cells. At first, scx-null mice were shown to die at embryonic day 8.5 by failing to gastrulate [31]. Subsequent to the initial detection, scx was established as the first tendon- and ligament-specific marker both during early development and up to differentiated tendons [179]. In contrast to initial findings, Murchison et al. [145] described viable scx-null mice. The study showed elegantly that scx mainly regulates the differentiation of force-transmitting tendons such as in limbs and tail. Interestingly, ligaments and positional tendons were not affected to the same degree, ensuring viability of the animals. Scx was furthermore shown to affect both cellular

development and ECM development in tendon [145]. Tnm was initially described and characterised as tendon specific by Shukunami et al. [182]. Tnm knockout mice are viable and show a reduced quantity of tenocytes but intact matrix composition [53]. Three different tnm isoforms were isolated and one theory suggests its main function to be anti-angiogenic [91; 169]. Connecting these two tendon markers, it was shown that scx positively regulates tnm expression [183].

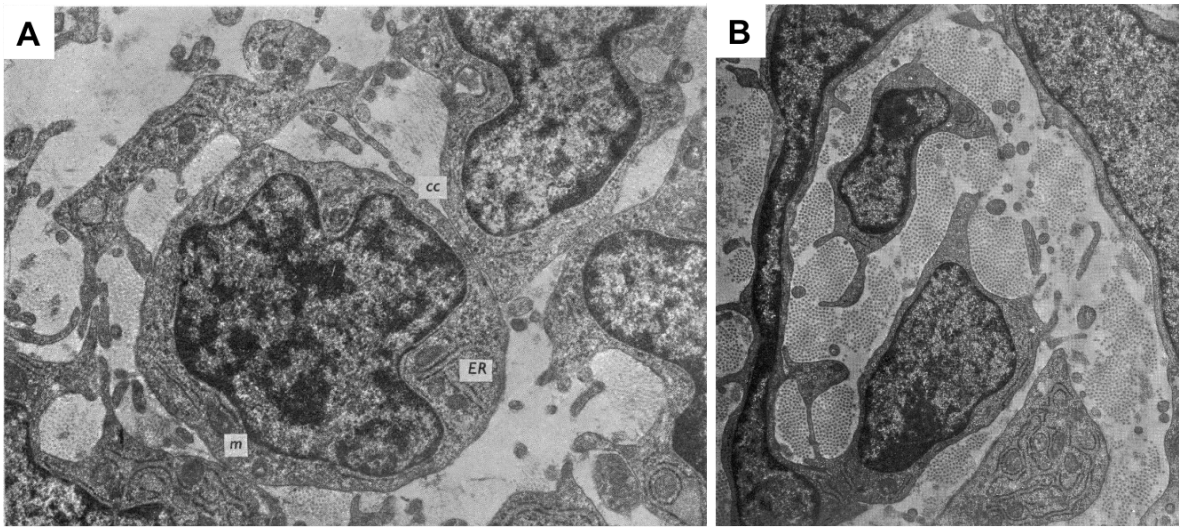

Figure 2. Human embryonic tendon. A) Cross sectional image of human tendon at 40 days of age in transmission electron microscopy. Cells take up most space and are closely connected. The ECM (light areas) contains small amounts of collagen fibrils. B) Human tendon at 95 days. The ECM is almost entirely filled with collagen and cells start building fibril bundles (adapted from Cahplin et al. [39]).

Knockout mouse studies focussing on tendon development have further proven that the transcription factor mohawk homeobox (Mkx) and transforming growth factor ß (TGF-ß) signalling are essential for proper tendon formation [132; 167]. Mkx is highly expressed during early tendon differentiation and its absence is associated with downregulation of collagen type I, fibromudulin and tenomodulin, as well as significantly smaller collagen fibrils [132]. Though Mkx is independent of scx expression [132], TGF-ß signalling strongly regulates scx expression [167]. Moreover, tendons and ligaments were absent in knockout mice with impaired TGF-ß signalling [167].

Mechanical stimuli are a key factor during tendon development. Beckham et al. [15] demonstrated the importance of movement for tendon development during embryogenesis. The chick muscles were inactivated with D-tubocurarine, which resulted in non-functional tendons, stiffened joints and disarranged cells [15]. Since tendon consist

mostly of ECM and only a minor cell fraction, a link between cells and ECM is vital in order to transmit forces to the cells. The key components in this respect are integrins. Integrins are transmembrane proteins consisting of varying α and ß subunits [96]. Different integrin subtypes bind to a variety of ECM proteins, amongst others collagens, laminin and fibronectin [96]. Mechanical signals are transferred via both the MAP kinase and the NF-κB pathways [41]. It has been suggested that the α subunit binds to the ECM molecule, while the ß subunit connects to the actin filaments of the cytoskeleton [204]. Different *in vitro* studies have shown that strain-deprivation results in increased matrix-metalloproteinase (MMP) expression, increased apoptosis, loss of tendinogenic gene expression and even inflammatory phenotypes, which can in turn be rescued by mechanical stimulation [13; 56; 70].

Mechanical Properties of Tendon

Tensile mechanical properties of biological tissues can be distinguished between structural properties such as stiffness (unit: N/m), load (N) and elongation (m), and material properties such as elastic modulus (Pa), stress (Pa) and strain (%) [71]. Stress is defined as the load divided by the cross-sectional area of the sample and strain depicts the elongation divided by the initial length. The elastic modulus is the stress/strain ratio and determines the stiffness of the material (Fig.3). Hence, the material properties are the result of normalising the structural properties by the geometric dimensions of the sample [71]. Material properties are therefore the method of choice in order to compare biological samples of varied dimensions.

Tendon's main function is unidirectional force transmission, so tensile mechanical properties play a key role and determine the tissue's organisation. Tendon has a characteristic force elongation curve under tensile loading with a large initial deformation, termed "toe-region", and increased stiffness under higher loads (Fig.3). The response can be divided into different sections from 1) the initial toe region where collagen fibrils are uncrimped, to 2) the linear rise of the curve representing the tissues' elastic modulus, and finally 3) the point of rupture [68; 208]. Moreover, tendons show viscoelastic properties under tensile strain [64; 98]. The characteristic properties of viscoelastic materials are higher strain when stretched slowly, opposed to reduced strain under fast stretch, i.e. the material stiffens under faster and increasing loads [68]. A challenging anatomical element is that tendon transfers forces from the very soft material muscle to the very stiff material

bone [17; 158]. This mechanical mismatch needs to be absorbed by the tendon in order to guarantee efficient load-transfer and avoid regional damage to the tendon [4]. It was suggested that this damping is achieved due to the viscoelastic properties of the material [58]. Under fast movements such as sprinting or jumping tendons can store and release energy, thereby acting similar to a spring [2; 21].

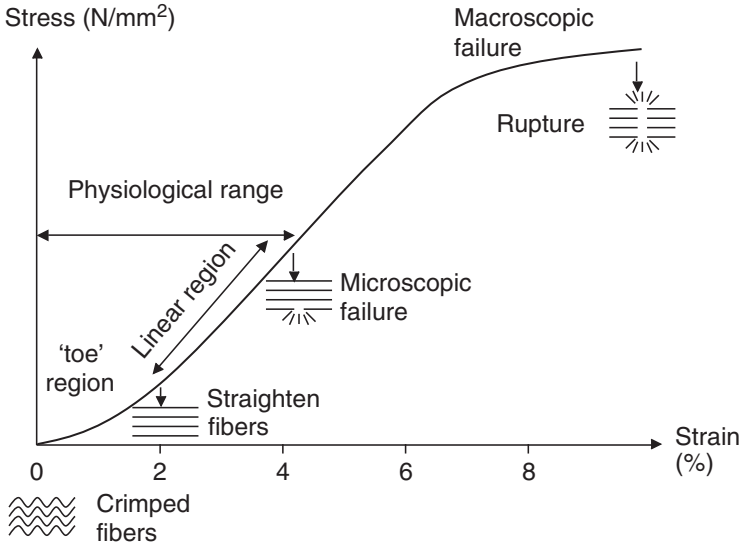

Figure 3. Mechanical stretching of tendon. The stress/strain graph shows the characteristic phases during tensile stretching of tendon. In the toe region the collagen fibrils are straightened, the linear region defines the elastic modulus of the tissue and leads to the point of rupture, which defines the ultimate stress and failure strain (adapted from Wang et al. [208]).

Values for distinct mechanical properties for identical tendons vary considerably among the literature. This can to some extend be explained by specimen status (*in vivo* vs. cadaver studies) and methodological differences. *In vivo* studies measure tendon elongation by ultrasound and measure forces directly. With this method, the elastic modulus for human patellar tendons was reported to be 1.0 or 1.9 GPa, respectively [37; 122]. *In vitro* approaches, however, also vary considerably. Hammer et al. [80] recently published data on iliotibial band samples that showed an elastic modulus of about 700 MPa. Another study tested mechanical properties of various animal tendon and showed values between 1.0 and 2.0 GPa [16]. Yet another study determined the elastic modulus for human Achilles tendon to be about 800 MPa [217].

More recent studies have been able to measure mechanical properties of single collagen fibrils. Svensson et al. [192; 193] showed that single collagen fibrils from human patellar tendon have a tensile modulus of 3.5 GPa and show a viscoelastic stress/strain

response. This discrepancy between single fibril mechanics and gross tendon mechanical properties might be due to tendon composition or interfibrillar sliding. However, this issue is still under current scientific debate. Tendon is considered a biological composite material, with collagen fibrils embedded in a soft matrix [168]. Determining the exact material properties, however, requires knowledge of the different components. Since collagen fibril tensile strength exceeds the strength of the inter-fibrillar matrix by many orders of magnitude, their structure is of particular interest in order to understand tendon function. If collagen fibrils are discontinuous as proposed by certain studies, shear forces in between fibrils would constitute for a major portion of the tendon's strength [69; 168; 195]. In case fibrils span across entire tendons as proposed by other studies, the mechanical properties of the single fibrils would determine the entire tendon's mechanical properties [45; 166]. In summary, collagen fibrils are the weight bearing structure in tendon tissue and are therefore key for proper tendon function. However, the load-bearing mechanism is complex and remains to be fully clarified.

Tendon Cells

The cellular fraction of tendon is reduced gradually during embryogenesis with the ECM covering the major fraction in adult tissue [39; 114; 117]. The exact composition of the tendon cell population remains elusive and requires further investigation. ECM-producing fibroblasts are the predominant population and comprise approximately 90% of all cells [114; 120]. Other cell types include chondrocytes, synovial, smooth muscle and endothelial cells [114]. Different studies have described varying markers for tendon fibroblasts such as CD90.2 [19], which, however, is also used as progenitor cell marker [33]. Other studies have suggested PH4B and vimentin [129], Tcf4 [139] or [1B10] [12], but a generally established marker remains to be found. Cadby et al. [33] characterised cell populations from peritenon and tendon core and found that cells from both regions have adipogenic and osteogenic differentiation potential. This ability of differentiation pinpoints a major challenge when trying to characterise primary tendon cells. Unpublished data from our laboratory showed that primary tendon cells stain positive for the stem cell markers octamer-binding transcription factor-4 (OCT-4), nucleostemin and stage-specific embryonic antigen-4 (SSEA-4), which leaves doubts about antibody specificity but also underlines the issue (Bayer and Herchenhan, unpublished data). Furthermore, a distinct population of mesenchymal stem cells was recently discovered in tendon [19; 221]. These

cells are reported to be dependent on biglycan and fibromodulin [19]. The presence of multipotent stem cells gives room to new concepts about how tendons are maintained and healed. One theory suggests that tendon cells are in general inert, which in combination with the relatively low cell fraction might explain slow tissue turnover and poor healing capacity of the tissue [86; 199]. However, further studies are required in order to decode the role of tendon cells in healthy and diseased tissue.

Despite the low cellular fraction and scattered distributions, cell communication in tendon is important and the cells constitute a broad network [141; 207]. Tenocytes establish gap junctions, whereby connexin 32 is located at cell body connections and connexin 43 is found at cell process-gap junctions [141]. Ralphs et al. [171] showed that adherence junctions connect tendon cells and, further, that the adherence junction associated molecules n-cadherin and vinculin are regulated by mechanical strain. Furthermore, they describe that these junctions, in combination with stress fibres, help maintaining the cell-cell network as well as cell-matrix connections under tensile loading [171]. Finally, the current key markers to distinguish tendon cells are the earlier described tendon specific transcription factor scx and transmembrane glycoprotein tnm [179; 182]. In this study tendon derived cells are referred to with the more general term “tenocytes” to overcome the general problem of tendon cell discrimination.

Collagen

Collagen is the major building block of tendon ECM and is responsible for most of the tissue’s mechanical properties [117]. The human body contains at least 27 forms of collagens that can be divided into different functional categories [68; 147]. Fibril forming collagen types I, II, III, V, XI, XIV and XXVII are the basis for material integrity in many organs such as skin, bone, blood vessels, cornea and tendon [68; 117; 186; 209; 210]. Fibril-associated collagens with interrupted helices (FACITs), among others type IX, XII and XIV are closely bonded to collagen fibrils and can modulate surface properties of the fibrils [23; 104].

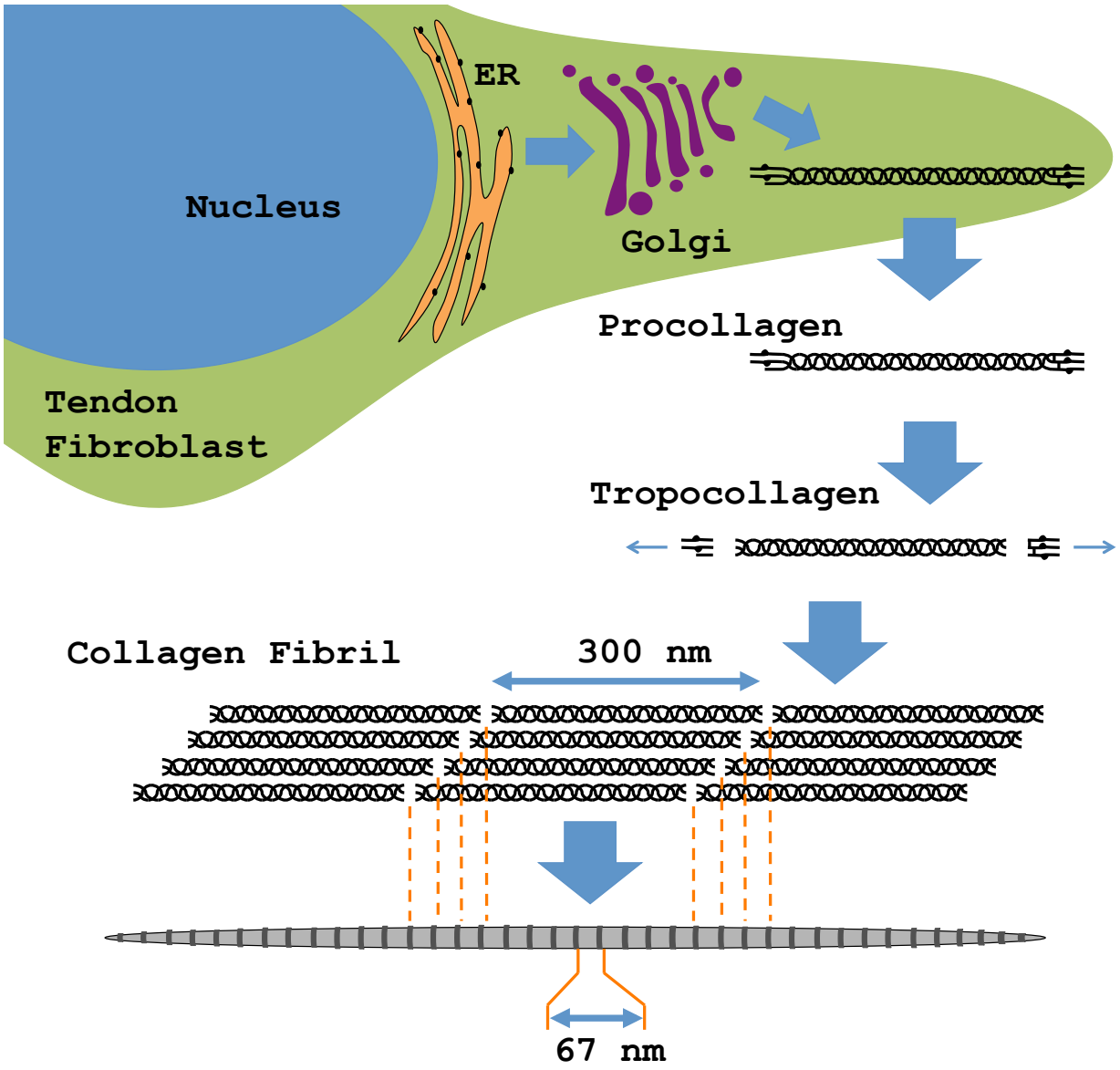

Figure 4. Collagen synthesis and fibrillogenesis. Procollagen molecules are synthesised at the endoplasmic reticulum (ER), transported to the Golgi apparatus and from there transported to the extracellular space. Subsequently, N- and C-propeptides are cleaved off and the resulting tropocollagen molecules are accumulated into fibrils in a highly controlled pattern. This results in the collagen-specific 67 nm banding pattern termed “D-period”.

Collagen Synthesis

Fibroblasts are matrix-producing cells in tendon and are linked directly to the ECM. The collagen α chains are synthesised, modified and assembled into triple helix molecules in the ER [146]. The structure is stabilised by a characteristic Gly-X-Y amino acid residue setup, where every third residue is glycine followed by interchangeable amino acids. These

varying residues are frequently proline or hydroxyproline [68; 104]. Modification of the residues includes hydroxylation of specific proline and lysine residues as well as glycosylation of other residues. The helical arrangement is initialised at the C-terminal end and folded towards the N-terminus. C-terminal and N-terminal propeptide domains flank the helical region in procollagen molecules and prohibit from spontaneous collagen aggregation within the cell [104; 146]. Procollagen molecules are transported via the Golgi network to the cell surface and secreted into the extracellular space (Fig.4). The N-terminal propeptide is subsequently cleaved by a disintegrin and metalloproteinase with thrombospondin motifs-2 (ADAMTS-2) and the C-propeptide is cleaved by bone morphogenic protein-1 (BMP-1) [77]. This leaves an approximately 300 nm long triple helix structure with short non-helical ends, called telopeptides (Fig.4 and Fig.8) [23; 68; 104].

Collagen Fibrillogenesis

Cleaved and solubilised type I collagen molecules have the remarkable feature of spontaneously forming fibrils when heated to 30-40°C at physiological pH [78; 102]. Furthermore, fibril fragments can serve as nucleators for new fibril formation when cultured in a collagen solution [94]. Collagen molecules within fibrils are assembled in a highly controlled quarter-staggered array where each molecule is shifted by 67 nm. This arrangement gives rise to gap and overlap regions, visible as a 67 nm banding pattern, named D-period (Fig.4) [68; 104].

Collagen fibrils are roughly circular rod-shaped structures with diameters from about 20 nm in embryonic tissue up to 400 nm in some adult tissues [74; 135; 157; 223]. The fibril diameter distribution plays a particular role for the function of the tissue and changes during development and ageing, respectively [73; 135; 189]. The mechanism of lateral growth of collagen fibrils is not fully understood yet. The most common theory suggests lateral accumulation of collagen molecules to existing fibrils, explaining the gradually increasing diameter of early fibrils during development [93; 185]. Moreover, this is supported by the fact that fibril spectra during early development show unimodal distributions (Fig.5A) [140]. An alternative theory suggests lateral growth of fibrils by fusion of existing fibrils [26; 75]. The two mechanisms are, however, not mutually exclusive and they might both play important roles during collagen fibrillogenesis. Fibrils may be produced as short small-diameter fibrils that fuse in order to quickly create larger

fibrils. This would be accompanied by constant accumulation of collagen in order to gradually develop these fibrils further (Fig.5B). Finally, mature tendon contains two populations of fibrils [74; 140]: The large diameter fibrils are suspected to be the most weight bearing, while a small diameter fraction assures optimal packing density and may play a role in load transfer. These steps are delineated in Fig.5, where the fibril diameter development is related to the overall tendon development from highly cellular to ECM dominated.

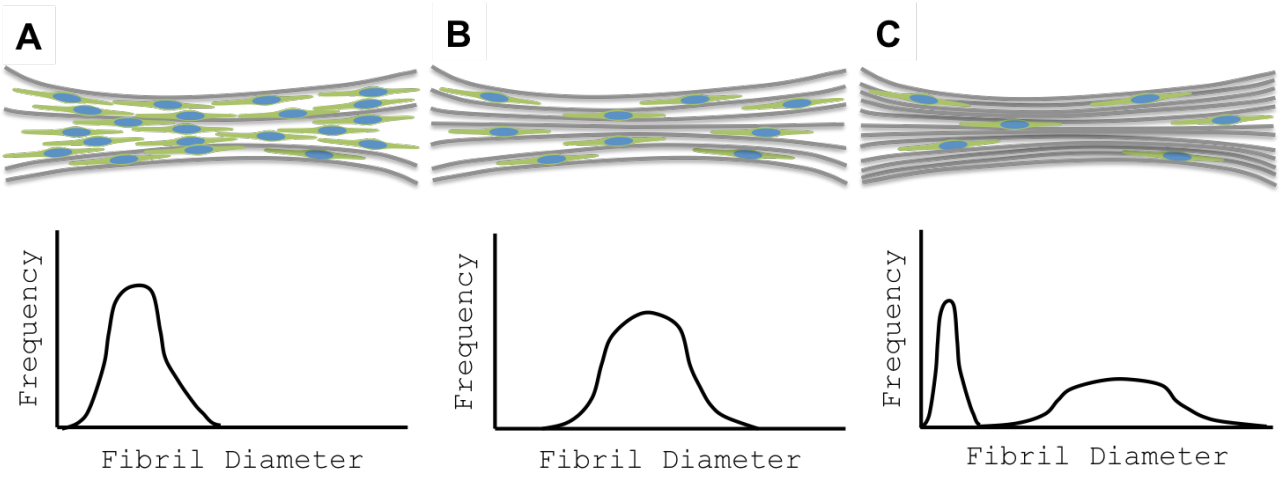

Figure 5. Schematic tendon development. A) Embryonic tendon is highly cellular with low ECM fraction (grey bars represent ECM, green and blue structures show cells and nuclei, respectively). The collagen fibrils (bottom graph) are unimodally distributed at low fibril diameters. B) During development the cell number is reduced and more fibrils are produced. The diameter distribution shifts towards higher values (bottom graph). C) Adult tendon is ECM-dominated and only contains few cells. The collagen fibrils show two fractions, a group of very low diameter fibrils and a broad distribution of larger diameters (bottom graph).

Fibril length, however, is under on-going scientific debate due to methodological difficulties to image entire fibrils in their natural surrounding. Statistical approaches, interpretations of mechanical responses and microscopic studies have attempted to estimate fibril length and reasoned the actual value to be between 0.1 and 10 mm, while other theories propose continuous fibrils throughout the tissue [45; 94; 166; 172]. As described before, this debate is fundamental in order to explain the response of tendons to mechanical loading. Along their length, fibrils are assumed to have a consistent diameter. The ends of early collagen fibrils were, however, shown to taper off [75; 92; 103]. The advantage of this system is that fibrils are able to “lean” on to the ends of adjunct fibrils, thereby promoting fibril elongation [103]. This mechanism is linked to the alignment of

collagen molecules within the fibril, which can be either unipolar – with all N-termini pointing in the same direction – or bipolar. Bipolar fibrils contain a switch region in their centre and show N-termini on both ends [75]. Kadler et al. [92; 103] found that only unipolar fibrils are able to fuse laterally in order to promote fibril elongation.

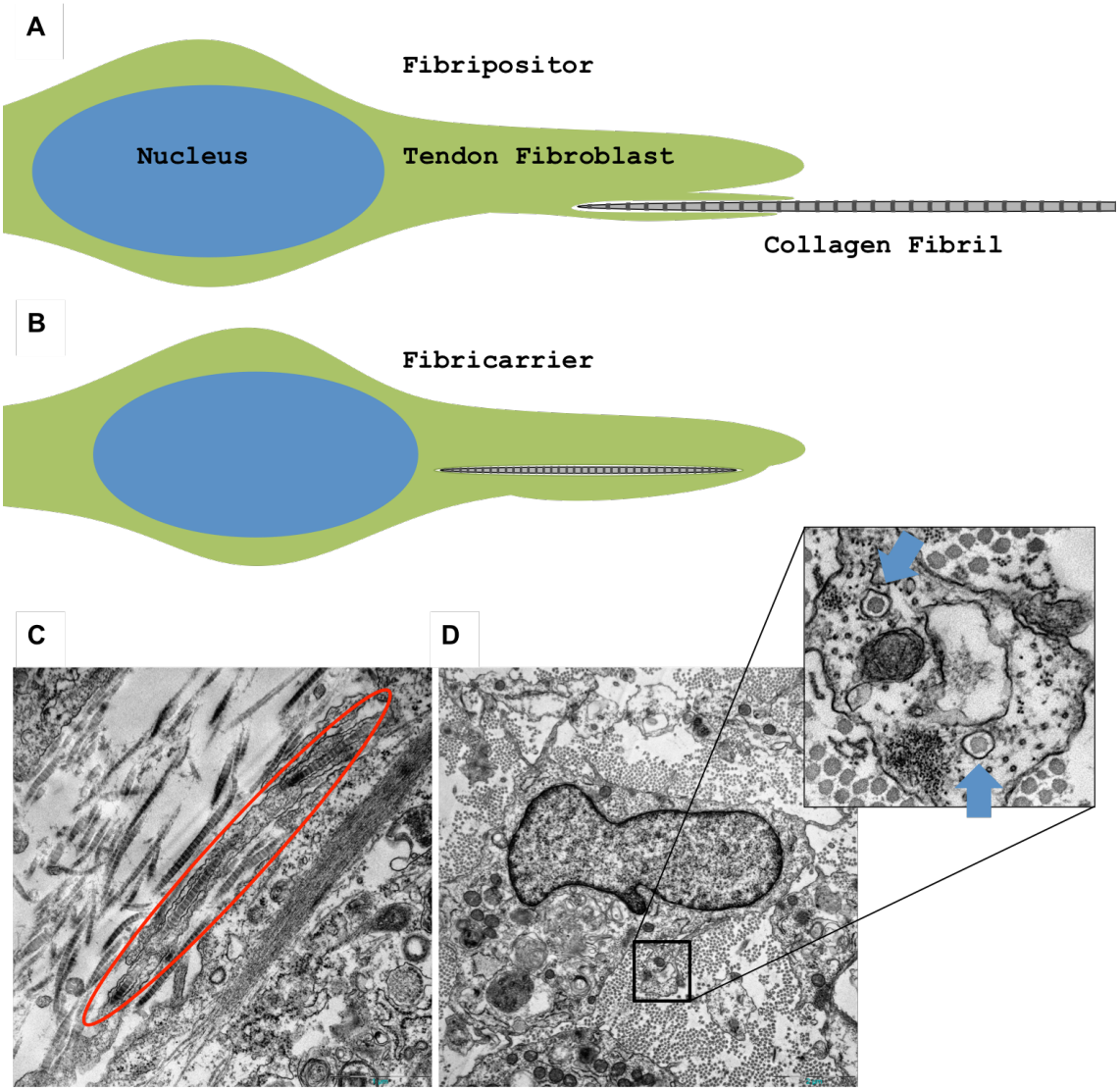

Figure 6. Collagen fibripositors and fibricarriers. Tendon fibroblasts are closely connected to extracellular collagen fibrils via cell protrusions termed "fibripositors" (schematic in A) and can even incorporate extracellular vesicles carrying entire fibrils termed "fibricarriers" (schematic in B). C) Longitudinal section of a fibripositor in a tendon construct (red ellipse). D) Cross section of a tendon construct with fibripositors (highlighted by blue arrows in magnifying insert of D: the fibril (grey spot) is surrounded by the cell membrane (dark ring) and thus partly included in the cell).

How collagen fibrils are formed, and how this process is controlled by the cells has not been resolved in detail to date. Finger-like cell protrusions were discovered that release

collagen fibrils into the extracellular space (Fig.6). These protrusions were named fibripositors and assumed to be fibril-generating structures [36]. More recent work shows, however, that fibroblasts besides extruding fibrils also pull on fibrils via fibripositors [111]. This points rather towards a matrix-organising function. Moreover, single fibrils are entirely pulled inside the cell in external vesicles termed fibricarriers to either be degraded or extruded at another location (Fig.6) [111]. Hence, the clear function of these cell-protrusions remains to be revealed.

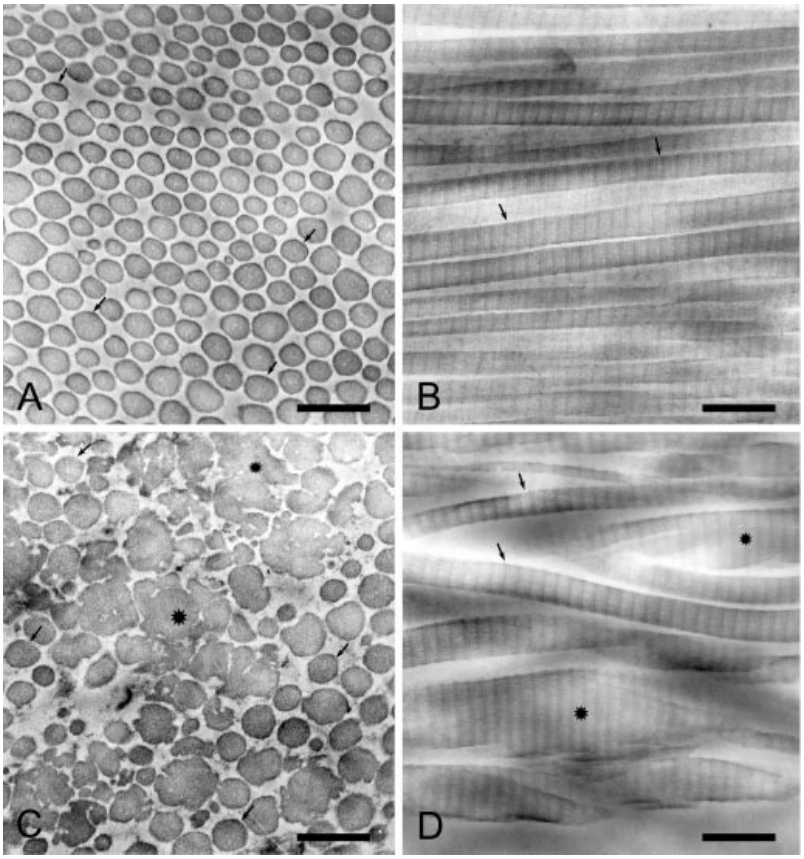

Figure 7. Effect of collagen V knock-out in mice. A+B) Cross sectional and longitudinal electron micrographs of healthy mouse tendon collagen. C+D) Cross-sectional and longitudinal images of collagen V haploinsufficient mouse tendons. Collagen fibril shapes are distorted and of highly variable diameter compared to controls. (adapted from Wenstrup et al. [212])

Apart from direct cell-collagen connections, several other extracellular molecules control collagen fibrillogenesis. Specifically collagen type V plays a major role in fibril assembly and regulation, which is why it is also called a fibril nucleator [101]. Complete collagen type V knockout mice are not viable, but studies with haploinsufficient collagen knockout mice for collagen types V and XI have shown that collagen fibrils show abnormal fibril shapes in cross-section and large variations in diameter distributions (Fig.7) [212; 215]. This phenotype is associated with extensible skin, weak tendons and hypermobile joints [212; 215]. In fact, these characteristics are similar to the Ehlers-Danlos syndrome

(EDS) in humans [161], which was shown to be caused by variations in collagen V genes [136; 213; 214] and can be distinguished morphologically from healthy and hypermobile subjects [150]. Collagen V was shown before to be incorporated in collagen I fibrils [24] and the N-terminal domain of collagen V contains a non-collagenous region that protrudes from the regular structure [130]. This led Wenstrup et al. [212] to propose the mechanism that incorporated collagen type V regulates fibril shape by sterical hindrance of collagen accretion. However, recent studies revealed comparable phenotypes in knockout mice for the proteoglycans decorin [55; 220] and fibromodulin [61; 190], as well as the glycoprotein tenascin-X [30; 137; 177]. The function of these extracellular proteins will be discussed in further detail in the next paragraph.

Taken together, these studies show that collagen fibrillogenesis is a tightly regulated process in which cells can interact and control the developing network directly (via fibripositors) or indirectly (via expression of regulating ECM proteins). The detailed mechanism, however, remains elusive and requires further investigation.

Non-Collagenous Tendon Extracellular Matrix

Although the tendon ECM consists mostly of fibrillar collagen, many other molecules play major roles for tendon development and function. The inter-fibrillar space is occupied with a highly hydrated matrix, where proteoglycans serve as the fluid-binding component [219]. Proteoglycans consist of a core protein with covalently bound glycosaminoglycan chains [219]. It has been discussed whether shear-load transfer between collagen fibrils is supported by glycoproteins, but recent studies dismissed this hypothesis [191].

As briefly mentioned above, the proteoglycans decorin and fibromodulin and the glycoprotein tenascin-X play distinct roles during collagen fibrillogenesis. Decorin and fibromodulin belong to the group of small leucine-rich repeat proteoglycans (SLRP) that are located in the ECM and fulfil various functions [219]. SLRPs are divided into 4 classes, while in tendon four SLRPs from two classes are mostly present. Decorin and biglycan represent class I, while fibromodulin and lumican belong to the group of class II SLRPs [108].

Decorin was shown to be highly abundant in tendon and it is closely associated with collagen fibrils [50; 66; 165], but inhibits collagen fibrillogenesis *in vitro* [205]. The molecule is horseshoe-shaped and can bind tightly to the surface of the round fibrils [181]. A more recent study proposed that each decorin monomer binds to at least four collagen

molecules [155]. A potential mechanism is that decorin coats the fibril and prevents collagen molecules from random accumulation. At the fibril tips, however, fewer decorin molecules are present allowing the fibril to grow and thereby controlling a constant diameter along the fibril [75].

Biglycan, fibromodulin and lumican were also shown to be horseshoe-shaped. The resulting gap from this configuration is approximately 2 nm wide, reaching from one collagen molecule to a second molecule and thereby organising fibril assembly [181]. Biglycan, the second member of class I SLRPs present in tendon, interacts with fibrillar collagen [178] and biglycan knockout mice show an osteoporosis phenotype with irregular fibrils [218]. Similar to decorin deficient mice, fibromodulin and lumican knockout mice show reduced mechanical integrity of their skin and tendons due to irregular collagen fibrils comparable to the collagen V knock-out phenotype (Fig.7) [61; 190]. Interestingly, lumican is the only SLRP that does not affect collagen fibrillogenesis in tendons but in cornea instead [38].

Fibromodulin and decorin are co-localised by binding to distinctly different binding sites along the collagen fibril [84]. In contrast, fibromodulin and lumican compete for the same binding site, but fibromodulin has the higher affinity and can also bind via a second binding site [107]. A double knockout mouse study for these two SLRPs has shown that a time-dependent shift – first lumican and subsequently fibromodulin – is a potential mechanism for collagen fibrillogenesis regulation [61]. Furthermore, SLRPs have been speculated to play a role in collagen cross-linking regulation [108]. More recent work has shown that tendons from fibromodulin knockout mice are – despite being mechanically weaker – more intensely cross-linked. This suggests that fibromodulin interacts with LOX in order to modulate collagen cross-linking (discussed in more detail within the next paragraph) [106]. Notably, there is another ECM molecule that is essential for collagen fibrillogenesis. Knockout mice lacking the glycoprotein tenascin-X show an EDS phenotype [137] and further studies have confirmed a recessive form of EDS linked to defects in tenascin-X [177]. However, neither the specific function nor the precise mechanism of tenascin-X has been resolved to date and is therefore subject of on-going scientific debate.

Enzymes and their antagonists constitute another important fraction of the non-collagenous proteins in tendon. MMPs are a family of zinc-dependant proteases that degrade a variety of ECM proteins [148; 149]. Particularly MMP1, MMP8 and MMP13,

known as collagenase type I, II and III, respectively, play a distinct role in digesting fibrillar collagen [120]. Although recent studies showed that tendon is supposedly not turned over at all after reaching adulthood [86; 199], it is known that a fine balance between MMPs and their antagonists is crucial for ECM development [148]. The group of MMP inhibitors are called tissue inhibitors of metalloproteinases (TIMPs). MMPs and TIMPs are key factors specifically during matrix repair [173].

An enzyme that is not engaged in degenerative processes of the ECM is LOX. LOX is present in the ECM and has the primary role of inducing collagen cross-links in order to stabilise the tendon structure as detailed in the following section [105].

Collagen Cross-linking

In order to stabilise collagen fibrils and the entire ECM network, inter- and intrafibrillar cross-links are vital for the structure of tendon [5]. In general, enzymatically derived cross-links and cross-links through advanced glycation endproducts (AGE) are distinguished [5; 6; 59]. AGEs are considered a major factor during ageing [6]. Due to the incorporation of sugar molecules, irreversible cross-links are established that stiffen the ECM and thereby reduce the flexibility of tendon tissue [6; 7]. A recent study shows that AGEs inhibit fibre sliding, which is compensated by increased fibril stretching. Despite higher yield and braking stress the linear modulus of AGE cross-linked tissue did not vary compared to control tissue [201].

The predominant cross-links in developing collagen fibrils are enzymatically derived by the enzyme LOX [59; 104; 105]. The enzyme acts by deaminating specific lysine residues in the telopeptide region of collagen fibrils to form allysines (Fig.8) [59; 105]. This specific modification leads to a self-assembly of cross-links between allysines and lysines at predetermined sites. Due to the controlled stacking pattern of collagen fibrils, one molecule is covalently cross-linked to another collagen molecule 4 D-periods away, connecting one telopeptide to the helical region of the other molecule (Fig.8) [82; 211]. Two pathways of cross-links can be distinguished, based on whether the involved telopeptide region has an allysine or hydroxyallysine residue [59]. Both allysine and hydroxyallysine can bind to an allysine or hydroxyallysine of the helical region of the other molecule, leaving four possible covalent binding sites (Fig.8) [59]. These initial cross-links are considered “immature” and are able to mature over time by bonding to the telopeptide of a third collagen molecule [5; 8].

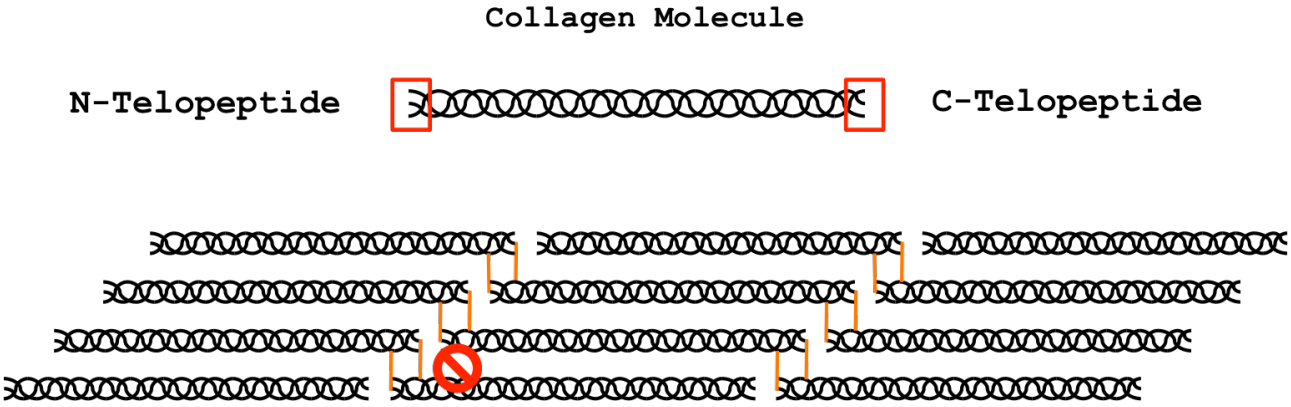

Figure 8. Collagen cross-links. Top: Scheme of a single collagen molecule with highlighted N- and C-telopeptides. Bottom: Cross-links among collagen molecules are arranged in a defined manner (orange connections): The C-telopeptide of a collagen molecule is bound to a specific lysine residue of the N-helical part of another molecule. The N-telopeptide is likewise connected to a defined lysine residue of the C-helical region. Single D-period staggered molecules cannot be cross-linked (indicated by forbidden sign).

LOX is secreted as a 50 kDa pro-protein into the extracellular space and is cleaved by BMP-1 to become the active 32 kDa protein [200; 201]. It specifically binds to fibrillar collagen, preventing non-arranged collagen from being cross-linked [46]. Apart from LOX, the so-called “LOX family” contains LOX-like 1 (LOXL1), LOXL2, 3 and 4, which all share the C-terminal domain and thereby the enzymatically active site of LOX, but differ at their N terminus. This might hint towards different functions for each member within the ECM [144]. LOX expression is stimulated by TGF-ß in rat cardiac fibroblasts [206], which in turn is induced in mechanically loaded tendon cells [85]. Recently, LOX also caught attention in the field of cancer research [11]. One theory suggests that LOX “primes” potential sites for metastases by stiffening through cross-links [9]. However, to date specific functions for the single LOX family members in tendon remain elusive.

One characteristic LOX family members have in common is that they can be irreversibly blocked by the lathyrogen ß-Aminoprorionitrile (BAPN), which binds to the enzymatically active site of LOX and the LOXLs [197]. Manipulation with LOX and BAPN has therefore been of interest in various studies. Injection of BAPN into fertilised chick eggs led to extremely fragile embryos, reduced mechanical properties of their connective tissues and easily soluble collagen [127; 162]. Furthermore, it was shown that BAPN, despite leading to weak tendons, does neither affect collagen production nor cell fate in chick embryos [138]. For tendon engineering, LOX transfected cells effectively increased

the mechanical resistance of a construct due to cross-linking [57]. Similarly, LOX strengthened the ECM in a healing wound model both *in vitro* and *in vivo*, while BAPN treatment served as a negative control [125].

Humoral Milieu of Tendon

Although tendons are sparsely perfused, the humoral milieu does play a major role during tendon development and significantly impacts tendon maintenance and particularly repair [143]. Various growth factors have been widely studied concerning their impact on tendon cells both *in vitro* and *in vivo*. Current literature suggests six different growth factors influence tendon: IGF-1, TGF-ß, platelet derived growth factor (PDGF), vascular endothelial growth factor (VEGF), fibroblast growth factor (FGF) and growth/differentiation factor 5 (GDF-5) [35; 143]. PDGF, VEGF, FGF, GDF have been addressed with *in vivo* animal healing models and *in vitro* studies. It is suggested that these growth factors initiate tendon cell proliferation, collagen synthesis, cell migration, tendon vascularisation and overall tendon healing [35; 43; 79; 112; 198].

Despite these data, TGF-ß and IGF-I are considered the most beneficial for tendon development and healing. TGF-ß is part of the TGF-ß superfamily, and three isoforms of TGF-ß with 60-80% homology are known, which share the same intracellular pathway. In cells derived from the mesenchyme (such as tendon cells), TGF-ß can induce proliferation and ECM production [121]. TGF-ß binds to four different TGF-ß receptors (two type I and two type II) and signals both through a SMAD-dependant and a SMAD-independent pathway [52]. *In vitro* TGF-ß was investigated both in cells and cell derived constructs and proved to initiate collagen synthesis [3; 79; 142]. This finding was transferred to a multitude of *in vivo* animal tendon healing studies. Overall, TGF-ß showed improved, faster healing and increased collagen production [87; 112; 121].

IGF-I is named due to its structural similarity to proinsulin, and has been shown to play a role both during growth and healing. It binds to two receptors, IGF-receptors type I and II, and is synthesised by various cell types. However, the predominant IGF-I producing cells are macrophages [216]. In tendon cells, IGF-I induces collagen synthesis and proliferation *in vitro* [1; 10]. Moreover, Scott et al. [180] have shown that IGF-I prevents tendon cells from apoptosis by activating the protein kinase B signalling pathway. Animal models for tendon healing confirmed the proliferation- and collagen-stimulation effect *in vivo* [49; 123; 174]. Recent studies applied IGF-I in humans *in vivo*, where

injection into patellar tendons led to an upregulation of ECM related genes and subsequent protein synthesis, such as collagen type I [81; 151]. Moreover, injection with GH results in increased IGF-I production, which in turn rescues from ECM degradation during a period of immobilisation [27].

Hence, TGF-ß and IGF-I are considered beneficial by most studies for tendon development and regeneration. However, TGF-ß also facilitates fibrosis, i.e. uncontrolled collagen production [203]. Therefore its application for tendon aetiologies needs to be considered carefully. IGF-I in contrast, appears to stimulate functional tendon maintenance as the recent study on immobilised patients suggests [27]. The mentioned study was the first to investigate effects on the tendon ultrastructure due to unloading and GH administration. Despite an increase in collagen gene expression the study could not detect changes in tendon ultrastructure [27]. Nevertheless, it needs to be taken in to consideration that the intervention period of two weeks was perhaps too short in order to expect structural changes in the rather inert adult human collagen matrix. The effect of IGF-I on early fibrillogenesis has not been investigated to date. Resolving this question would help understanding whether IGF-I is beneficial for tendon engineering or long-term tendon healing, respectively.

In recent years, the lack of established treatment options for tendon rupture and chronic tendinopathy have resulted in various proposed approaches. Among those, the application of preparations rich in growth factors such as platelet rich plasma (PRP) became a widely applied method both *in vivo* [51; 65] and *in vitro* [62; 133]. The rationale behind this technique is a “the more the better” approach, reasoning that a highly concentrated mix of various growth factors might improve the situation. However, the major drawback with this approach is that the applied substance is neither controlled in terms of composition, nor carefully evaluated prior to use. As PRP originates from the subject, components can vary highly both in concentration and composition [113]. So far clinical outcomes have not proven consistent either, so PRP is viewed more critically in the recent scientific debate [113]. *In vitro*, a similar approach is adapted by using FBS as a gold standard supplement in cell culture [202]. Similar to PRP, composition of different FBS batches can vary substantially [28; 222]. Therefore, the uncontrolled situation during PRP-treatment *in vivo* can be mimicked by the application of FBS on tendon cells *in vitro* to further evaluate effects on collagen fibrillogenesis.

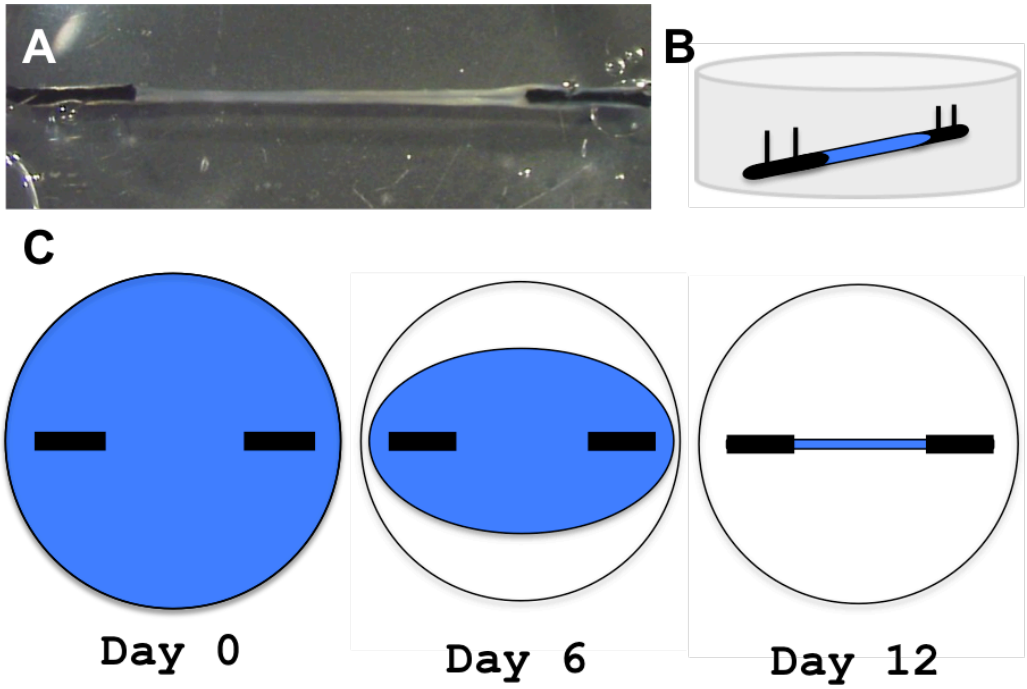

Figure 9. The human tendon construct. A) Picture from the top and B) Schematic of the tendon construct. The black bits at the ends are pieces of suture that are pinned to the bottom of the well. In between is the tendon construct containing cells and ECM. C) Schematic of the construct formation. The fibrin gel (blue) is contracted by the tendon cells to a rod-shaped structure in between the anchor points over an approximately 12 day time period.

In vitro Tendon Engineering

Engineering of tissues has been an emerging field of interest within the last decade. Novel techniques combined with better understanding of cells and *in vitro* tissue culture offer the opportunity to develop and study various tissues. In the research field of tendon, tissue engineering is used with two main focuses: 1) In order to create replacement tissues for damaged tissue and 2) as a tool to investigate tendon development and factors influencing this. However, tendon development cannot be entirely reproduced *in vitro*, which is why applicable approaches rely on artificial scaffolds or decellularised allografts [40; 48; 63; 164; 170]. As the work in this thesis is centred on the use of engineered tendons as a tool to investigate tendon development, studies within this field will be further discussed here.

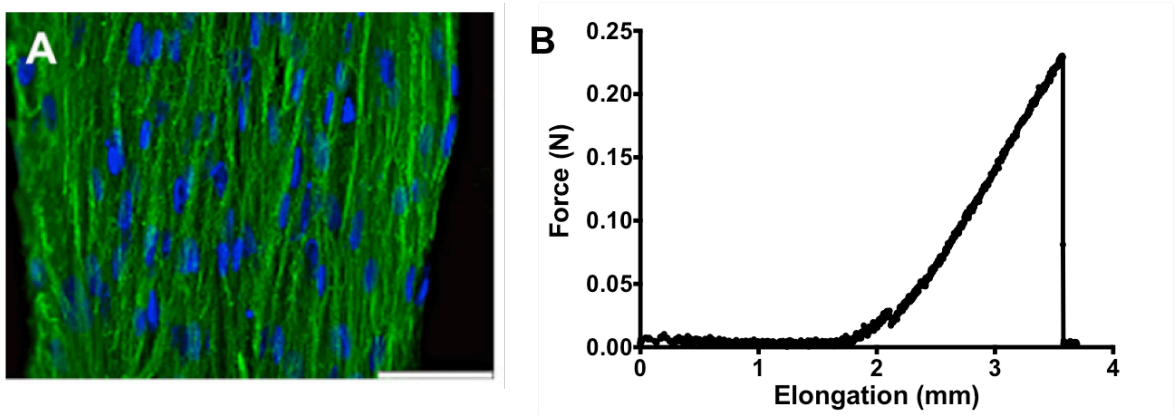

Figure 10. Characteristics of tendon constructs. A) The tendon constructs contain longitudinally aligned collagen type I fibrils (green=Type I collagen; blue=nuclei; adapted from Bayer et al. [14]). B) Response to tensile stretching from tendon construct. Typical phases of tendon force/elongation curves are seen with toe region, linear rise and point of failure.

Developing a 3D tissue model for tendon development *in vitro* usually requires a biocompatible scaffold. Most common approaches therefore make use of collagen [100; 152] or fibrin gels [14; 115; 194]. The advantage of collagen gels is their mechanical integrity and easy maintenance. However, a major disadvantage with this technique is that collagen gels or sponges contain randomly arranged collagen fibrils as opposed to the perfectly aligned fibrils in mature tendon tissue. Moreover, it is not possible to distinguish pre-existent collagen and new cell-derived collagen. Fibrin gels on the other hand are mechanically weak, but were shown to be potential scaffolds for tendon engineering with one major advantage: All collagen existing in the system is produced and aligned by the cells [14; 115]. Furthermore, a recent study found improved tendon-like development in fibrin based constructs compared to collagen based constructs [29].

The second main component to successfully engineer tissues is the cell. Clearly, differentiated cells from the desired tissue are a logical choice and also widely used in tendon engineering [14; 35; 110; 176]. Despite their natural potential to build tendon tissue, tenocytes are difficult to access from healthy patients and are therefore no option for future tissue engineering applications. Mesenchymal stem cells (MSCs), on the other hand, are derived from bone marrow or adipose tissue and therefore much easier accessible [32; 72; 163]. Hence, many studies attempted to use these multipotent cell types for tendon engineering approaches [40; 99; 116; 152].

In this project a tendon construct based on human adult tenocytes seeded in a fibrin gel was used (Fig.9). The system was first described and termed “tendon construct” by

Kapacee et al. [115] and adapted with human tenocytes thereafter by Bayer et al. 2010 [14]. In order to form the construct, tenocytes are allowed to contract a fibrin gel between two anchor points (Fig.9). The tenocytes produce and align collagen fibrils and keep the structure under constant tension (Fig.10A). Strikingly, tenocytes isolated from adult donors in this model show embryonic-like behaviour with formation of fibripositors, which are normally not present in adult tendon tissue [14]. The tenocytes exhibit tendon-typical gene expression profiles with upregulation of collagen types I and III, and the tendon markers scx, tnm and mkx as opposed to when cultured in 2D [13]. As ultimate functional proof, the tendon constructs show stress/strain response of similar shape to tendon *in vivo* (Fig.10B) [14; 44].

Tendon constructs have been shown to be stress responsive. Mechanical stretching leads to an upregulation of collagen and higher collagen fibril diameters, respectively [109]. Releasing the structure from tension, in contrast, leads to reduced collagen gene expression with upregulation of the inflammatory markers COX 1 (cyclooxygenase 1) and COX 2 and the collagen network loses orientation [13]. These data indicate that a baseline level of loading needs to be present in order to ensure proper tendon formation, and further mechanical stimulation has advantageous effects on construct development. Another influence on construct development is the humoral milieu, i.e. culture medium and growth factor supplementation. As described earlier growth factors play key roles in tendon development and have also been implemented in tendon engineering approaches before [34; 43; 116]. Hagerty et al. [79] showed that in constructs from human anterior cruciate ligament cells an optimised growth factor combination of IGF-I, TGF-ß and GDF-7 can improve total collagen content and construct mechanical strength.

Taken together, construct development can be triggered by different stimuli such as mechanical stretching or manipulation of the humoral milieu. This makes the system a valid tool to investigate the effect of diverse factors on tendon development and collagen fibrillogenesis.

Methodological Considerations

This section will introduce key methods used during the studies. Special focus is set on adaptations that were necessary in order to overcome specific challenges. Routine methods will be described in the end for the purpose of reproducibility.

Primary Human Tendon Cell Culture

Gracilis and Semitendinousus tendon tissue was obtained from patients undergoing anterior cruciate ligament reconstruction. Specific attention was given to cleaning the tendon from any remaining muscle tissue. Primary tenocytes were isolated by enzymatic digestion with 20 mg/ml collagenase type II in DMEM/F12 culture medium supplemented with 20% FBS over night. Subsequently, cells were cultured in DMEM/F12 culture medium supplemented with 10% FBS.

As described in the introduction section, tendon fibroblasts are difficult to characterise since no generally accepted marker has been found to date. However, simple light microscopy can help distinguishing among different cell types in 2D culture. The here used tenocytes show similar appearance to fibroblasts with elongated cell bodies and protrusions reaching out in different directions (Fig.11A+B). This makes them distinguishable from for example tendon-derived stem cells, which are small and have a square-shaped cobblestone-like appearance (Fig.11C)[221]. Myoblasts, on the other hand, are very long rod-like structures (Fig.11B). Therefore, cell populations that displayed contamination with myoblasts were not used for construct formation. Tendon stem cells are more difficult to locate and no attempt was made to exclude them due to their potential as tenocytes. An important fact about fibroblasts is that when cultured on plastic and supplemented with TGF-ß, fibroblasts get activated and turn into myofibroblasts [90]. The transformation is commonly characterised by *de novo* expression of α-smooth muscle actin (α-SMA). In the current study this was not further addressed, however, initial tests confirmed the expression of α-SMA and it can therefore be assumed that the cells used in the current study have a myofibroblast phenotype (Bayer et al. unpublished data). The population doubling time was approximately 7 days and cells were used for experiments between passages 2 and 5.

Finally, when working with primary cells variation among different donors needs to be addressed and accounted for. It has been shown in human dermal fibroblasts and arterial smooth muscle cells that donor age has a significant influence on the phenotype [20; 160]. Furthermore, natural variation among donor cell lines is an often-neglected fact, which has for example been shown in mesenchymal stem cells [184]. In order to reduce these variances, each experiment was repeated with tendon cells from at least 5 different donors in the current projects. Moreover, all donors were male, aged 18-30 and had no chronic diseases.

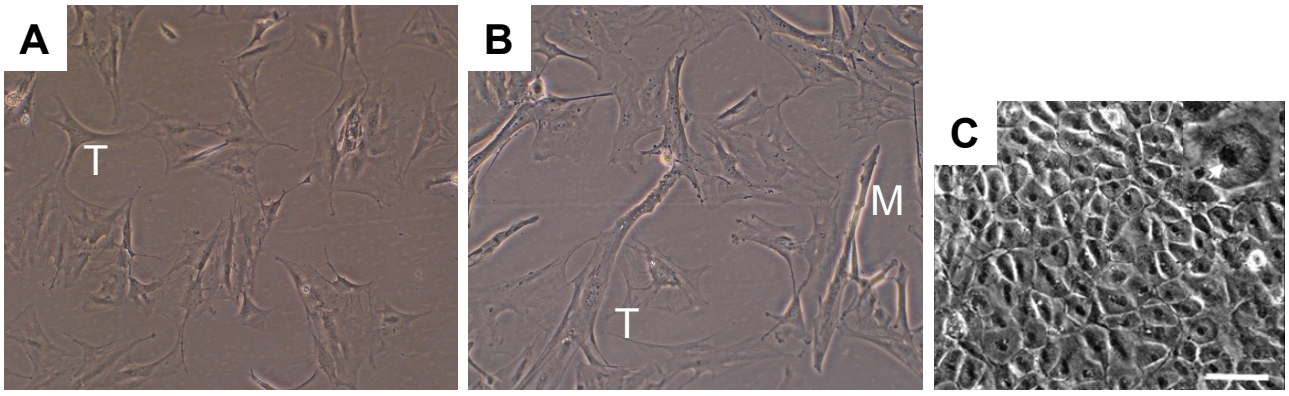

Fig.11. Primary cells from tendon tissue. A) Tenocytes with fibroblast-like appearance (T) develop star-shaped protrusions in 2D culture. B) Tenocytes (T) that are contaminated with the elongated myoblasts (M). C) Tendon derived stem cells show cobblestone-like appearance but are very small and thus difficult to spot in tenocyte cultures. (C adapted from Zhang et al. [221])

Tendon Construct Preparation

Tendon constructs are prepared by seeding tenocytes in a fibrin gel, which is constrained by two anchor points. Two 0.3 cm long silk sutures were therefore pinned either 10 or 15 mm apart in each well of a sylgard elastomer coated six well plate to act as anchors (Fig.9). Empirical testing revealed that 40 mg fibrinogen polymerised with 0.8 U thrombin in 800 µl volume provide a suitable environment for the cells. Too low concentrations lead to unstable gels, while too high fibrinogen concentration results in very stiff gels that prohibit cell migration and communication. Cell number can be varied from as low as 50.000 to 250.000 cells per construct. A reduction in cell number extends construct formation time since a critical cell number is required for gel-contraction. Within study I, constructs with 15 mm anchor point distance and 250.000 cells were used. For study II and III, the distance was reduced to 10 mm and the cell number was reduced to

200.000 cells per construct. The reduction of anchor distance was due to easier handling during mechanical testing and the cell number reduction enabled more efficient use of cells at comparable construct formation rates. The culture medium for constructs was slightly modified from the cell culture medium. DMEM/F12 (50:50) medium was supplemented with 10% FBS, 200 μM ascorbic acid and 50 μM L-proline. When constructs are initially seeded the gel covers the entire well. During approximately 14 days the gel is contracted by the cells to form a cylindrical structure between the anchor points. It can, however, frequently occur that the gel sticks to the sides of the well leading to irregular shapes. These attachments need to be loosened in order to accomplish proper construct formation, which is termed “scoring”.

Unsuccessful construct formation can have various reasons. First, there can be cell-culture infections that can occur mostly from the invasive scoring process. To account for this problem 1% penicillin/streptomycin was added routinely to the construct culture medium. A more challenging problem is cell-line variation. In rare cases the cells digested the fibrin gel faster than desired. In these instances the gel developed visible holes and was fully degraded before the time point of formation. To alleviate this problem, 0.1 mg of the trypsin inhibitor aprotinin was added to the fibrinogen solution before polymerisation. A third mode of construct failure is complete detachment of fibrin gels from the well. In these instances the outer part of the circular gel detaches and no contraction is visible, which was caused by apoptotic cells. Overall, construct survival rate during these projects was approximately 75%.

Tendon Construct Manipulation

Tendon constructs are well suited for manipulations of all kinds. As usual for cell cultures, the medium is easily accessible for interventions using cytokines or other chemical compounds. The standard medium containing 10% FBS can thereby be varied as in study II, where the FBS level was reduced to 0.5% in order to focus on the effect of IGF-I on construct development. Moreover, the effect of high FBS levels could be investigated.

Another chemical intervention took place in study III, where BAPN was added to the culture medium. Initial testing showed that constructs supplemented with 50 μM BAPN or more ruptured spontaneously at the timepoint of formation. Since ruptured constructs can no longer be analysed, a new protocol was developed. Constructs were allowed to form under standard conditions until 14 days post seeding. At this stage constructs were either

left as control or supplemented with 50 µM BAPN until day 21. The constructs did not rupture under these conditions and the desired analysis methods could be applied.

One major advantage of the system is that the construct does not stick to the bottom of the well. Two ways of removing the constructs from the 6 well plates were established: 1) The construct was simply unpinned (e.g. for RNA extraction or collagen content assay), or 2) The entire elastomer base containing the pinned construct was lifted out of the well. This technique was particularly useful for methods that require intact structures such as electron microscopy and mechanical testing.

Construct Mechanical Testing

Tensile mechanical testing of biological tissues always faces the dilemma of keeping the tissue in a physiological surrounding and at the same time clamping the structure rigidly enough in order to determine its breaking stress. With tendon in particular, this issue can become extensive, as tendons, and specifically collagen fibrils, can withstand considerate amounts of force [118; 192]. However, the tendon constructs break at rather low forces they are is similar to embryonic material. So in order to clamp the construct on the mechanical testing rig (200 N tensile stage, 20 N load cell, Petri dish version, Deben, Suffolk, UK), standard super glue is sufficient to keep the structure in place. A downside to the mechanical weakness is that determining the point where the force initially starts rising becomes more difficult. As visible in Fig.9, the toe region of the tendon construct is rather long until the linear region starts. The initial length of the construct needs to be controlled as the clamping and suture length are not standardised between constructs.

Hence, the constructs were clamped using super glue, kept in phosphate buffered saline (PBS) soaked gauze until the glue was dried and were subsequently submerged in the PBS bath of the uniaxial tensile testing machine. Constructs were tested at a constant rate of 2 mm/min until the point of failure. In order to determine stress and strain, geometric dimensions also need to be measured. The mechanical testing rig was therefore mounted on a stereomicroscope fitted with a digital camera. A video of every test was recorded and the construct length at the onset of force was measured after testing. Moreover, the construct diameter was measured at three points along the length of the structure and the cross-sectional area was calculated assuming a circular shape. The minimal area was used for ultimate tensile stress calculations. The tensile modulus was calculated from the slope of the linear region in the stress/strain curves.

Transmission Electron Microscopy

Transmission electron microscopy (TEM) has been the method of choice for analysing collagen fibrils since the 1950s. Until very recently, no other imaging technique allowed for sufficient resolution in order to investigate collagen fibrils in detail. As TEM has been widely applied over such a long time span, the method has become highly reproducible and technical advancement has improved the data output significantly. However, the downside of TEM is the extensive tissue handling, which is both very time consuming and costly. Moreover, the preparation process might change the structure of very delicate samples and the method is static, as it cannot be applied to living tissues.

The tendon construct is a rather robust structure and can readily be used for TEM. Fixation can easily be done in the culture dish, where the culture medium is, after two washing steps with PBS, replaced by 2% glutaraldehyde solution in 0.15 M phosphate buffer. After 30 minutes, the construct was divided into 3 pieces of equal size and the fixative was refreshed. Post fixation was conducted in 1% OsO_4 in 0.12 M cacodylate buffer for 2 hours at room temperature. After extensive washing in H_2O, the samples were en bloc stained with 1% aqueous uranyl at 4°C over night, dehydrated in a graded series of ethanol and embedded in Epon (Hexicon, Houston, Texas, USA) according to standard procedures.

Ultrathin cross- and longitudinal sections were prepared using a Reichert-Jung Ultracut E microtome equipped with a diamond knife. Images were acquired using a Philips TM 100 transmission electron microscope at 80 kV equipped with a Megaview 2 camera. The magnification was varied to acquire a range from overview images to high magnification images for detailed analysis (Fig.12).

Focussed Ion Beam/ Scanning Electron Microscopy

Serial block-face imaging is a new method in the field of electron microscopy combining sectioning and imaging within the chamber of a scanning electron microscope (SEM; Quanta FEG 3D, FEI, Eindhoven, Netherlands). In this case, a focussed gallium ion beam (FIB) is used in order to mill away material and make the underlying tissue visible. A high-resolution detector for backscattered electrons is used to visualise the structure at the block face. The technique is commonly known as FIB/SEM.

A detailed description on the preparation and imaging steps for serial block face imaging has been published by Starborg et al. [188]. The preparation of tendon constructs

for the method is a moderate modification of the standard TEM embedding procedure in order to enhance the staining. More precisely, during postfixation the osmium solution was complemented with 1.5% potassium ferrocyanide. After one hour, the samples were treated with 1% tannic acid (in 0.12 cacodylate buffer) for 1 h, followed by staining in 1% Osmium solution for 1 h. Thereafter, the process continued as described for TEM.

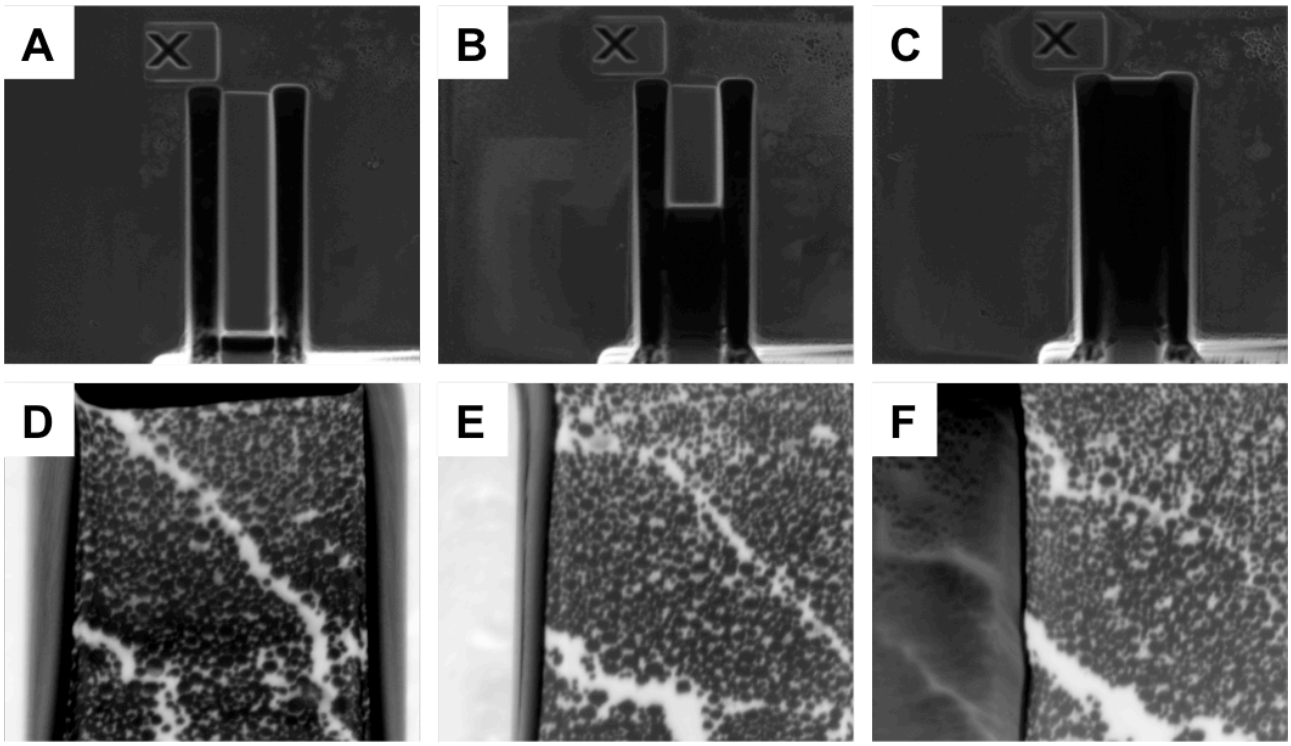

Figure 12. FIB/SEM procedure. A-C show images from the view of the ion beam with the area of interest in the center. The cross at the top left is used for beam alignment and the range in this sample is 400 slices with 50 nm slice thickness. The images progress in time from A to C as more material is milled away. D-E depict the corresponding E-beam images of human adult gracilis tendon. The drift in image center is one of the major problems when trying to investigate a long range at high magnification.

Standard ultrathin sections were prepared to evaluate the area of interest in TEM. Subsequently, preparing the specimen block for FIB/SEM included further important steps. The sample needs to be directly accessible from both front- and top-side of the block, thus the top needed to be trimmed. Thereafter the block was mounted on a stub using carbon paste and gold coated to reduce charging effects. After aligning the ion and electron beam, trenches around the area of interest were milled in order to leave room for milled-away material, reduce charging effects and create a defined area of interest (Fig.12A-C).

Fig. 12D-F shows images from the electron beam and thereby depict one of the major challenges with FIB/SEM. Particularly when attempting to image a long structure such as tendon at high magnification over longer distances, the electron beam tends to drift. A possible reason is that the electron beam needs to travel passed the longer growing stretch of uncoated sidewalls. This results in a reduced field of view over the entire z-range that needs to be accounted for during image post-processing. The image processing and analysis were undertaken using the dedicated 3D image software package Amira (v.5.4.0, FEI, Eindhoven, Netherlands). When investigating tendon in FIB/SEM, the resolution is another major concern. As visible in Fig.12 D-F, adult tendon collagen fibrils are of sufficient size to be well resolved with the method. Tendon construct collagen fibrils on the other hand are of significantly smaller diameter and can therefore not be resolved with the method at present. However, with additional improvements to the preparation and imaging process, this issue can hopefully be solved in the future.

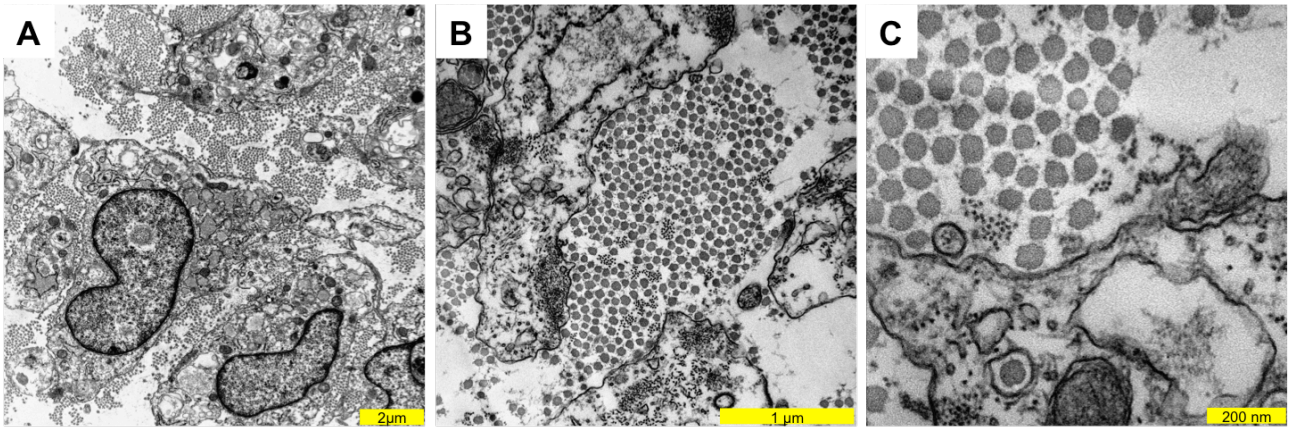

Figure 13. Tendon construct cross-section in TEM. A) A tendon construct cross-section at 7800x magnification. Most space is occupied by cells (nucleus membrane is heavily stained), while a part of the extracellular space is covered with collagen fibrils (round structures in white open spaces). B) Electron micrograph focussing on the collagen matrix at 34500x magnification. C) An image typically used for fibril diameter measurements at 93000x magnification. There are still cellular structures visible at the bottom of the image.

Collagen Fibril Analysis

Different laboratories, including our institute, have developed automated systems for collagen fibril diameter analysis in tendon or other tissues. In the current projects, however, tendon constructs were investigated that are more challenging in this aspect. Since adult tendon consists mostly of collagen fibrils, images that contain purely fibrils are

easy to obtain. Furthermore, collagen fibrils in adult tissue have large diameters ranging from 65 to over 300 nm. In order to analyse these, moderate magnifications in TEM are sufficient. Constructs, however, contain only low amounts of collagen fibrils, which are always located in close proximity to cells (Fig.13). Therefore, even high magnification images of constructs contain both cellular structures and fibrils (Fig.13C). Moreover, the extracellular space of tendon constructs contains non-collagenous structures with round shape. These variations can at present only be recognized by a human investigator. In order to guarantee objectivity across the studies and treatments within this thesis, the same investigator undertook all measurements in a blinded fashion. At least 300 fibrils per specimen were analysed using the image analysis software package ImageJ (NIH, Bethesda, Maryland, USA). As visible in Fig.12, collagen fibrils in the construct are not perfectly round in shape. However, in order to simplify the analysis circular shapes were assumed and the minimal diameter was measured. Average fibril diameters were calculated for each specimen and collagen fibrils were collected in 5 nm groups in order to create fibril spectra.

SDS-PAGE and Western Blotting

Because direct measurement of collagen cross-links requires specialised equipment and also sufficient quantities of pure collagen within samples, an indirect estimation of collagen cross-linking was used in this study. Because collagen solubility is directly linked to cross-link quantity, constructs were heated to 95°C for 3 min in sodiumdodecylsulfate-polyacrylamid gelelectrophoresis (SDS-PAGE) sample buffer (5 mg/ml). Samples were run on 5% SDS-PAGE according to standard procedures [124]. For detection of type III collagen we used delayed reduction. Therefore, the gel was stopped after 20 min and 10 µl 0.5 M DTT (in water with 10% glycerol) were added. The gel was subsequently washed, stained with commassie brilliant blue, washed again and analysed. Because the gel was set to run until proteins between 75 and 500 kDa were separated, the large collagen proteins dominated the gel. Collagen type I is the most abundant type in tendon and also the tendon construct, and the collagen I alpha 1 and 2 chains can be distinguished. At larger sizes, the three possible dimers from these alpha chains are visible and a variety of larger trimer bands can also be seen. Collagen cross-linking can be estimated from the proportioning of these bands and the overall signal intensity depends on the cross-link-dependant collagen solubility.

For western blotting experiments, tendon constructs were lysed by mechanical disruption with a pistil and sonication for 3x5 s in sample buffer (NuPAGE® LDS sample buffer, Invitrogen, Carlsbad, CA, USA). Subsequently the samples were heated to 95°C for 10 min and centrifuged at 10000xg for 10 min and stored at -80°C until further use.

Samples were incubated at 70°C for 10 min and separated on a NuPAGE® criterion XT 4-12% Bis-Tris gel using 1xNuPAGE® MES SDS running buffer (Invitrogen) at 700 V for 70 min, blotted with an iBlot™ device (Invitrogen) on PVFD membranes (GE-healthcare, Little Chalfont, UK) and blocked with 5% milk powder in PBS plus 0.1% tween 20. Primary antibodies against LOX (1:1000; NB100-2530), collagen V (1:500; NBP1-19633), decorin (1:500; NBP1-84970), fibromodulin (1:500; NBP2-16494) and tenascin-X (1:500; H00007-D01P) were incubated over night at 4°C (all acquired from Novus biologicals, Littleton, CO, USA). The complementary HRP-conjugated secondary antibody (anti-rabbit, 1:1000 dilution, swine, DAKO, #P0399) was incubated for 1 h. Membranes were analysed using an Odyssey® FC system with complemented software (LI-COR Biotechnology, Lincoln, NE, USA).

Digression: The Tension Stepper

The Tension Stepper was developed by Dr. David Holmes in the laboratory of Prof. Karl Kadler at the University of Manchester who kindly provided a copy of their version for our lab. The system provides a unique opportunity to study the mechanical response of tendon constructs and its compartments, respectively. The equipment makes it possible to stretch the construct longitudinally and to observe mechanical forces in real time. This principle is not unique per se, but the newly developed system provides major advances over commercially available systems. First, it is fully integrated in the cell culture incubator, which allows construct manipulation under standard culture conditions. Second, the sensitivity reaches a force resolution of approximately 0.5 mN, which is sufficient in order to measure cell-derived contraction forces.

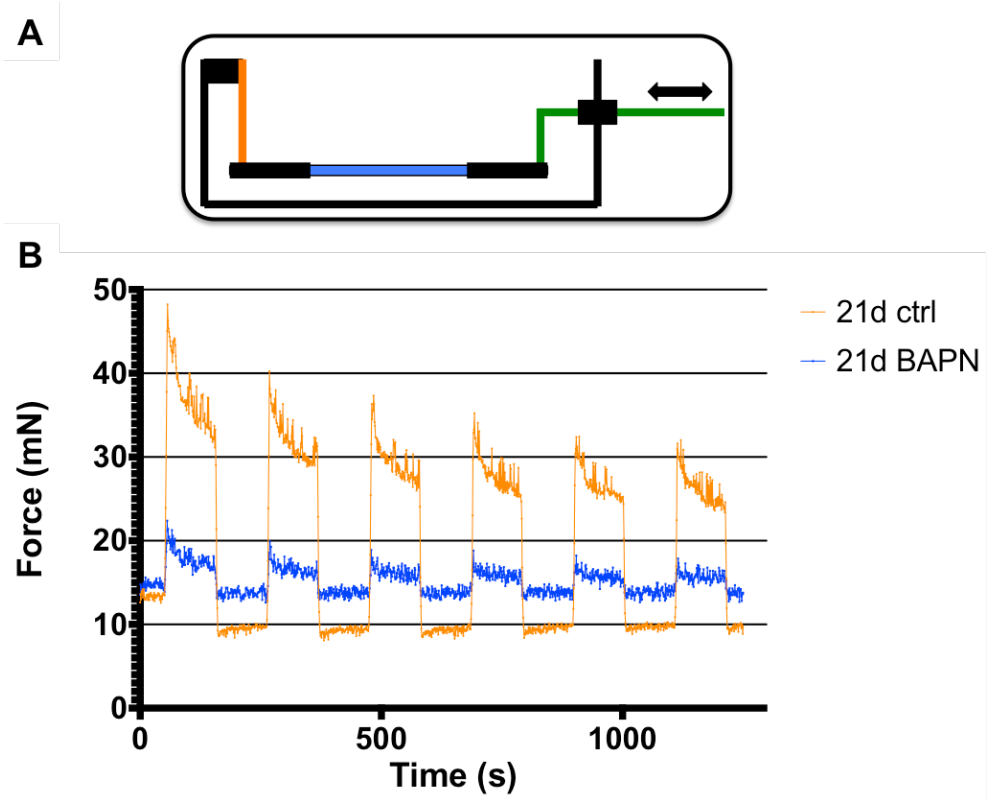

Figure 14. The tension stepper. A) Schematic of the tension stepper. The construct (blue) is mounted in between a movable rod (green) and a cantilever that can be deflected (orange). Deflections are measured by two strain gauges and converted to mechanical loads. B) Output from the tension stepper. The orange curve delineates a 21 day control construct that was stretched by 5%, left to relax for 100 s and moved back to starting position. This cycle was repeated 6 times. The same regime was applied to a 21 day BAPN treated construct (blue curve).

Within this PhD project the tension stepper was set up and preliminary data was collected. However, the system did not function reliably to collect data in a controlled fashion. Nevertheless, the method is an essential tool to study tendon constructs in future experiments. The initial results can thus be utilised to initiate new studies and further understand cell-derived forces and strain-induced behaviour in tendon cells.

A schematic of the machine is presented in Fig.14, where the construct is fixed on the right side to a movable steel rod and on the left side to a vertical cantilever. This cantilever is equipped with two strain gauges (on front and back side) that are able to convert minimal cantilever deflections into changes of resistance and thereby a change to an applied voltage. In this way the mechanical response of the construct to manipulation with the actuator is transferred into signal changes that can be recalculated into force changes. As the tendon construct is a very delicate structure, manipulations must be kept to a small level in order to not destroy its integrity.

In this context, the tension stepper was used in order to investigate the mechanical response of BAPN treated constructs over repeated loading cycles. Control or BAPN-treated constructs, respectively, were stretched by 5%, left to relax for 100 s, moved back to starting length and finally rested for another 100 s. This cycle was repeated six times and the response is presented in Fig.14. The initial level of force is the result from the cell-derived tension. The control sample showed the largest response to the first stretch of 35 mN, while the force was gradually reduced during the following cycles (Fig.14 orange curve). This decay resembles the pre-conditioning effect, which is believed to re-arrange the ECM [83]. The relaxation pattern within each cycle resembles an exponential decay, though the timespan is not sufficient to reach equilibrium. When moved back to baseline length, the force dropped by about 5 mN under the starting force. Thereafter a slight increase in force is visible during the resting phase, which represents re-tensioning by the cells. However, the force of this re-tensioning lies within the noise level of the data output and can therefore not be quantified. Variations in cell number and further effort to reduce the noise level might provide the opportunity to measure cellular contraction forces within the construct. Stretching of the BAPN treated sample, on the other hand, required significantly lower force at about 7 mN (Fig.14 blue curve). Similarly to the control construct the repeated stretching led to a gradual reduction in force, which indicates that the structure adapts comparable to repeated stretching as the control, though at much lower forces. This proofs yet again the importance of cross-links among collagen molecules

in order to build functional and strong fibrils. Assuming similar relative relaxation rates leads to the hypothesis that the cross-links neither reduce nor increase relaxation potential. However, it needs to be considered that the BAPN treated constructs were formed under control conditions for the first 14 days where a certain amount of cross-links were already established. The re-tensioning is no longer detectable, which might be due to the above-mentioned noise.

Taken together, the tension stepper is a tool that might be valuable in the future in order to gain further insight into tendon construct mechanics. Particularly, the role of the cells in mechanical properties needs to be elucidated further. Various chemical interventions can therefore be used to manipulate the system in the desired way.

Routine Methods

These methods were conducted according to well-established protocols.

RT-qPCR

The amount of mRNA for target genes was measured using quantitative real-time RT-qPCR. An overview of targets and primer sequences is provided in table 1. First, tendon constructs were harvested and transferred to RNAse free tubes containing 1 ml TriReagent (Molecular Research Centre, Cincinnati, OH, USA), 5 stainless steel beads of 2.3 mm in diameter and 5 silicon-carbide sharp particles of 1 mm for mechanical disruption (BioSpec Products, Inc., Bartlesville, Oklahoma, USA). For RNA isolation, samples were mechanically disrupted using a FastPrep®-24 instrument (MP Biomedicals, Inc., Illkirch, France) and subsequently bromo-chloropropane (Molecular Research Centre) was added in order to separate the samples into an aqueous and an organic phase. Glycogen was added to the tendon samples to improve RNA precipitation (120 µg per ml TriReagent). Following isolation of the aqueous phase, RNA was precipitated using isopropanol, washed in ethanol and dissolved in RNAse-free water. RNA concentrations were determined by spectroscopy at 260 nm and RNA quality was confirmed by gel electrophoresis.

Synthesis of complementary DNA (cDNA) was performed using Omniscript reverse transcriptase (Qiagen, Hilden, Germany) on 500 ng of tendon cell RNA. For each target mRNA, 0.25 µl of 20x diluted cDNA (in 1x Tris/EDTA buffer with 1 ng/µl salmon DNA) was amplified in 25µl Quantitect SYBR Green Master Mix (Qiagen) with specific primers (100 nM each, Table 1) on a real-time PCR machine (MX3000P, Stratagene, La Jolla, CA,

USA). The thermal profile was 95°C, 10 min → (95°C, 15 s → 58°C, 30 s → 63°C, 90 s) × 50 → 95°C, 60 s → 55°C, 30 s → 95°C, 60 s. Signal intensity was acquired at the 63°C step and the threshold cycle (Ct) values were related to a standard curve made with the cloned PCR product. Specificity was confirmed by melting curve analysis after amplification (the 55°C to 95°C step). The large ribosomal protein P0 (RPLP0) mRNA, which was stably expressed relative both to GAPDH mRNA and total RNA (data not shown), was chosen as internal control. Values were normalized by RPLP0 expression and are presented as relative difference from baseline treatments as described in the corresponding study.

Collagen Content Assay

Tendon constructs were snap frozen in liquid nitrogen and stored at -80°C until further use. Subsequent to thawing, the samples were freeze-dried and weighed at constant humidity using an ultra-microbalance scale (Mettler-Toledo GmBH, Gießen, Germany). The samples were hydrolysed in 6 M HCl at 110°C for 18 h, dried at 95°C, followed by thorough washing in H_2O. The dry hydrolysate was suspended in 600 µl acetate-citrate buffer (0.6% acetic acid, 130 mM citric acid, 440 mM sodium acetate, 425 mM sodium hydroxide) of which 150 µl were used for further analysis. Next, 75 µl chloramine-T solution (60 mM chloramine-T in 50% 1-propanol) was added and incubated for 20 min at 20°C. Thereafter 75 µl aldehyde-perchloric acid solution (1 M 4-dimethylaminobenzaldehyde, 60% 1-propanol, 22% perchloric acid (70-72%)) was added and further incubated at 60°C for 25 min. The reaction was stopped by putting the samples on ice and the absorbance was measured using a multi plate reader at a wavelength of 570 nm. The samples were correlated with a standard curve from pure hydroxyproline (Sigma, H1637) and collagen content values were calculated using the dry sample weight and an estimated hydroxyproline/collagen mass fraction of 11.4% (the multiplying factor was calculated from the measured ratio between pure bovine tendon collagen mass and hydroxyproline mass).

Table 1. PCR targets and primer sets.

Target	Sense	Antisense
RPLP0	GGAAACTCTGCATTCTCGCTTCCT	GCTCCTTGCCGAGAAGCAGAAC
GAPDH	CCTCCTGCACCACCAACTGCTT	GCATTGCCCTCAACGACCACT
COL1A1	GGCAACAGCCGCTTCACCTAC	GCGGGAGGACTTGGTGGTTTT
COL3A1	CACGGAAACACTGGTGGACAGATT	ATGCCAGCTGCACATCAAGGAC
COL5A1	AGCAGATGAAACGGCCCCTG	TCCTTGGTTAGGATCGACCCAGT
COL6A1	CACACCGCTCAACGTGCTCTG	GCTGGTCTGAGCCTGGGATGAA
COL11A1	ACCCTCGCATTGACCTTCCTCTT	ATCCCGTTGTTTTTGATATTCCCTCTG
COL12A1	CCCAGGTCCTCCTGGATACTGTGA	GCAGCACTGGCGACTTAGAAAATGT
COL14A1	AGCATGGGACCGCAAGGC	GACGCGCCACTGATCTCACC
Scleraxis	CAGCCCAAACAGATCTGCACCTT	CTGTCTTTCTGTCGCGGTCCTT
Tenomodulin	GAAGCGGAAATGGCACTGATGA	TGAAGACCCACGAAGTAGATGCCA
IGF-Ia	GACATGCCCAAGACCCAGAAGGA	CGGTGGCATGTCACTCTTCACTC
IGF-Ib	CAGGAGGGGAACAGAAGGAG	GCGCTTTCTAGGGCATTACA
IGF-Ic	GCCCCCATCTACCAACAAGAACAC	CAGACTTGCTTCTGTCCCCTCCTTC
TGF-ß1	GAGGTCACCCGCGTGCTAATG	CACGGGTTCAGGTACCGCTTCT
TGF-ß2	CCCAAAAGCCAGAGTGCCTGAA	ATGTAGCGCTGGGTTGGAGATG
TGF-ß3	CTGTGCGTGAGTGGCTGTTGAG	CTCCATTGGGCTGAAAGGTGTG
TGF-ß Receptor	TTTGGGCTTTCCCTGCGTCT	TCTGGAGCCATGTATCTTGCAGTTC
Lysyl Oxidase	CGCTGTGACATTCGCTACACAGGAC	CATTGGGAGTTTTGCTTTGCCTTCT
LOXL1	GGTGAGATGCAACATTCACTACACAGG	GCCTGCTTTGGAAGGGGAGAGA
LOXL2	CCACCGCATCTGGATGTACAACTG	GAGCCCGCTGAAGTGCTCAAA
LOXL3	CTGGGTGCACAACTGCCACAT	TCAAACCTCCTGTTGGCCTCTTC
LOXL4	TATGATGGGCACCGGGTCTG	GGAGAGTTCTGCATTGGCTGGGTA
Transglutaminase 2	CGGGAGGATATCACCCACACC	CTCCTTCTCGGCCAGTTTGTTCA
Decorin	GGTGGGCTGGCAGAGCATAAGT	TGTCCAGGTGGGCAGAAGTCA
Fibrilin-I	CGCTGCAATCATGGTTTCATCCTTT	ATTCCCATTTCCACTTGCACATTC
Elastin	GGCTTCGGATTGTCTCCCATTTT	CCAACGTTGATGAGGTCGTGAG
Caveolin-I	GAGCTGAGCGAGAAGCAAGTGTACGA	TCTGGTTCTGCAATCACATCTTCAAA
BMP-I	CAGACGGCACACAGCTCGTAAGT	TGGCAGCTGGGGGTAGAAGTGT
Fibromodulin	CAGTCAACACCAACCTGGAGAACC	TGCAGAAGCTGCTGATGGAGAA
Tenascin-C	CAACCATCACTGCCAAGTTCACAA	GGGGGTCGCCAGGTAAGGAG
Tenascin-X	GGAGGACTATGCCCATGGTTTTG	CGCATGGAGTAGTCACCTGCCTGT
Biglycan	AGGCCAAGCTGACTGGCATCC	TGGCCTGGATTTTGTTGTGGTC
Lumican	CCCTGGTTGAGCTGGATCTGTC	CCAGGATCTTGCAGAAGCTCTTTATGT

Summary of Results and Discussion

This section will give an overview of the results of the three studies and put these in perspective with current knowledge. For in depth description and discussion of the results the reader is kindly referred to the three manuscripts attached at the end of this thesis.

Study I

During the first phase of this PhD project the tendon construct model was evaluated regarding its capacity to develop over time without additional stimuli from the outside. The constructs were left under control tissue culture conditions and cell-derived tension. It was proven by FIB/SEM that the cells in the tendon construct are elongated with the longitudinal axis of the structure. However, the cells are considerably larger in the construct as opposed to their original tissue, adult human gracilis tendon. TEM investigation revealed a considerable development of the ECM and the collagen fibrils in particular. Fibrils were connected to cells by fibripositors as usually only seen in embryonic tendon. Fig.15 shows the fibril size distribution (A) and mean fibril diameter (B) at 14, 21, 28 and 35 days post seeding.

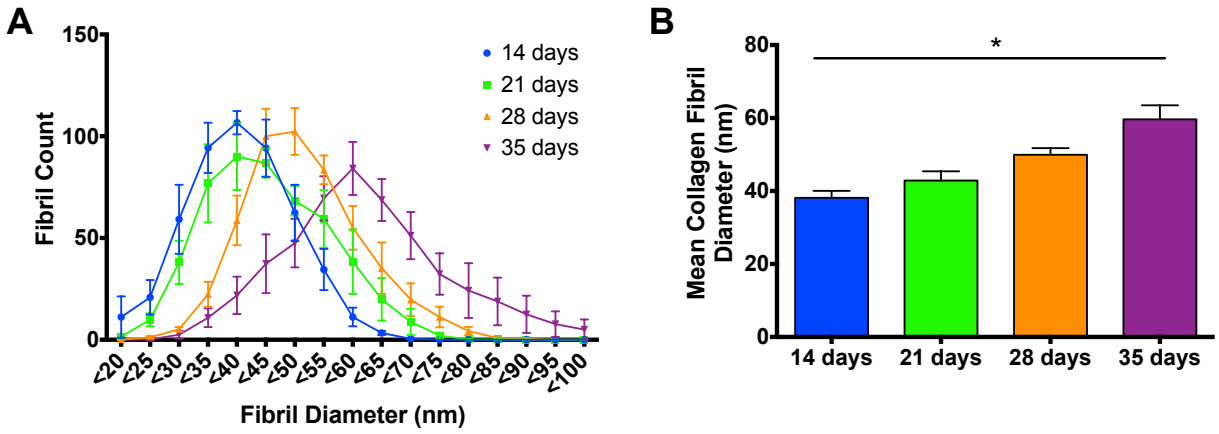

Figure 15. Collagen Fibril Diameter Development. A) Fibril diameter spectra from tendon constructs at 14, 21, 28 and 35 days. The curve shifts gradually towards higher diameters and with higher age the spectrum broadens. B) Mean fibril diameters from the spectra in A). The mean fibril diameter develops significantly from day 14 to 35. (n=6 cell lines, 500 fibrils measured per cell line, mean±SEM, *p<0.05 among groups)

The finding that the collagen fibril spectrum is unimodal and is shifted towards higher diameters with time (Fig.15A) supports the theory of collagen molecules being gradually accumulated to existing fibrils in order to develop. Fusion of small fibrils, in contrast, would lead to rapid shifts towards higher diameter, while maintaining a population of very small (<20 nm) fibrils. However, as described before, fusion of the small fibrils might be particularly important to rapidly increase fibril length [92; 103]. The largest fibril diameters in 35 days old tendon constructs reach approximately 100 nm, which is very close to fibrils found in adult human tendon where fibrils range from approximately 60 to 150 nm [135]. Moreover, human anterior cruciate ligaments contain collagen fibrils of similar diameters to 35 days old tendon constructs [189]. Nevertheless, the tendon construct has significantly lower total collagen content than adult tendon. The highest values in tendon constructs are approximately 15%, while adult tendon contains about 95% collagen of dry weight. The construct, in contrast, is mainly composed of cells.

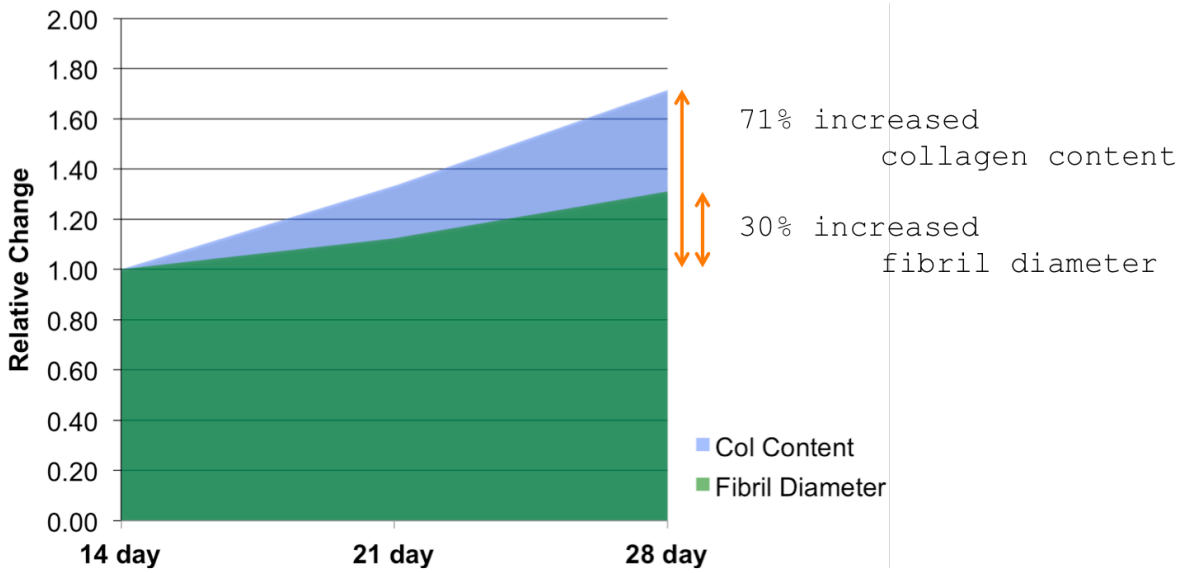

Figure 16. Collagen content vs. fibril diameter development. The mean fibril diameter increases from days 14 to 28 by approximately 30% (green curve). Meanwhile the total collagen content develops by about 71% (superimposed blue curve).

During 14 and 28 days the development is fairly linear with an increases of about 30% in mean collagen fibril diameter (Fig.15B and 16), which is equivalent with a 69% increase in fibril cross-sectional area. The total collagen content rises in this period by about 71% (Fig.16). Thus, the increase in total collagen content can almost be explained by the increase in fibril diameter. This would support the theory of the initial production of

short fibrils that merge at their tips to promote fibril lengthening, while simultaneous collagen molecule accretion increases fibril diameters. However, fibril number and fibril length are two parameters that would also need to be quantified to support this theory. Yet these values are very difficult to obtain. The challenge of fibril number measurements is the fact that collagen fibrils in the construct are accumulated locally and not evenly distributed over the entire structure. Thus in order to quantify the fibril volume fraction, very large parts of the structure would need to be analysed, which is technically difficult and very time-consuming. Collagen fibril length measurements are even more challenging. As described in the introduction, the quest after fibril length quantifications has been in the scientific debate for almost three decades with no generally accepted outcome yet. Hypotheses span from interrupted fibrils [69; 168; 195] all the way to continuous fibrils [45; 166], but no study could prove their case by a direct technique. In our laboratory, we took our own approach to address this problem by attempting to apply the direct measuring FIB/SEM approach (Svensson and Herchenhan, unpublished data). The idea was initially to follow individual fibrils by using the serial block-face imaging technique. The tendon construct seems like an ideal starting point to address this issue but the resolution of the collagen fibrils was not sufficient to distinguish the rather small construct-fibrils. Thus, adult human gracilis tendon was investigated thereafter. However, although collagen fibrils were sufficiently distinguishable at high resolutions, the

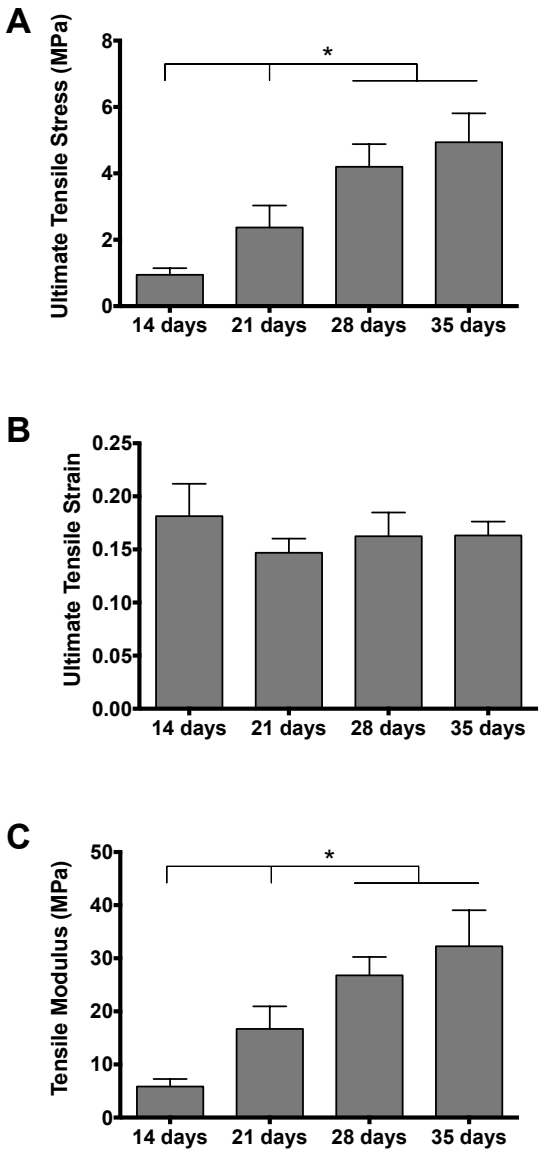

Figure 17. Mechanical development of tendon constructs. A) The braking stress of constructs develops significantly from day 14 to 28. B) Ultimate tensile strain does not develop over time. C) This leads to an approximately 5-fold increase in tensile modulus up to approximately 32 MPa at day 35. (*$p<0.05$ among groups)

physical shape of the fibrils with approximately 100 nm in diameter and >1 mm in length makes tracking of these structures exceptionally difficult. Therefore, we were forced to take a statistical approach to the problem. Individual fibrils were tracked through the dataset (images in Fig.12) and counted. To date, about 67 mm of continuous fibril was tracked and 1 fibril end was detected. Moreover, 7 fibrils were caught changing direction by 180 degrees and 4 events of fibril branching were observed (Svensson and Herchenhan, unpublished data). This proves yet again the difficulty of measuring total collagen fibril length. Improved techniques need to be applied in the future in order to solve this important question in tendon research.

The rise in collagen fibril diameter and content is accompanied by a similar increase in mechanical strength of the constructs (Fig.17). Interestingly, the tensile strain does not change over time, but purely the increased strength gives rise to an increase in tensile modulus (Fig.17). Whether this increase is mainly driven by the increased fibril diameter, longer fibrils or a combination of both is difficult to evaluate. Moreover, collagen cross-linking will affect the mechanical properties over time [59] and a time course study of the cross-link dynamics would be of high value for in depth understanding of functional collagen fibrillogenesis.

Compared to developing human digital tendon (Fig.2) [39], the construct is very similar in the initial phase. The tenocytes cover the largest fraction of the tissue and gradually the ECM is produced with collagen fibrils that are aligned longitudinally. Fibril sizes are comparable and particularly the similarity in developing of fibril populations in close proximity to the cell membranes is striking. However, at about 95 days, human tenocytes initiate the segmentation of collagen fibrils into fascicles. This step cannot be observed in the tendon construct, which suggests a stop in development. Certainly, tenocytes receive a multitude of signals and stimuli during tendon development *in vivo*. As the construct develops to a certain extend, it provides a valuable base in order to investigate several stimuli *in vitro*. Among these possible factors, mechanical stimulation and adjusting the humoral milieu are the most prominent choices. Mechanical stimulation requires specifically designed equipment, which was not available during the course of this project. Therefore, the effect of the humoral milieu with focus on the growth factor IGF-I was investigated in the next study.

Study II

Growth factors play an essential role during tendon development and maintenance [143]. It has been shown that growth factors like TGF-ß and IGF-I increase collagen synthesis both in *in vivo* and *in vitro* studies [1; 54; 81; 121]. However, the detailed effect on collagen fibrillogenesis is unknown. Moreover, combinations of growth factors such as PRP are often applied without analysing the exact composition in advance [51; 65]. Here, the tendon construct was used to evaluate the discrete effect of IGF-I on early collagen fibrillogenesis and to monitor the consequence of applying FBS, as an example for preparations rich in various growth factors.

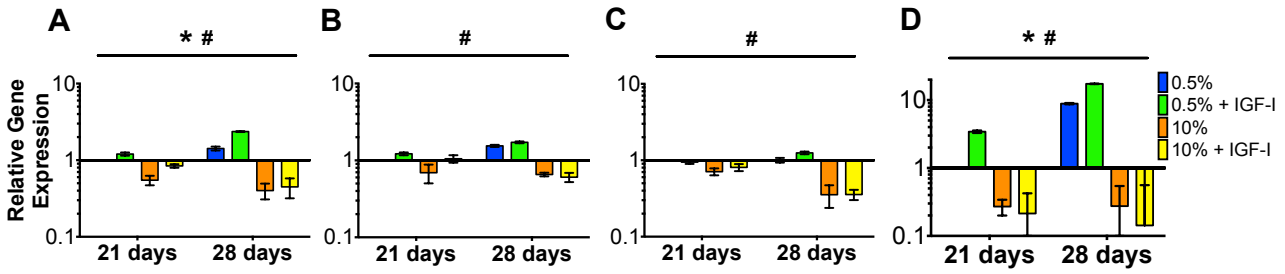

Figure 18. Gene expression analysis of the IGF-I study. A) Collagen type I expression is increased by IGF-I and reduced due to high FBS levels. B) Collagen III is not affected by IGF-I but reduced due to 10% FBS. C) Scx is similarly reduced by 10% FBS but unchanged with IGF-I. D) Tnm is highly upregulated with IGF-I, while the tnm expression is significantly reduced with high FBS. (*$p<0.05$ for an effect of IGF-I, #$p<0.05$ for an effect of high FBS)

IGF-I significantly increased the gene expression of collagen type I and the tendon marker tnm (Fig.18A+D). Moreover, there was a significant reduction in gene expression with the high FBS concentration of 10% for collagen types I and III, as well as the tendon markers scx and tnm (Fig.18). The effect of IGF-I was predicted as it was shown before that IGF-I increases collagen type I expression [1; 10]. The negative effect of FBS, in contrast, was rather unexpected since FBS is widely accepted as the gold standard for *in vitro* cell- and tissue culture. Nevertheless, a few studies saw similar effects of high levels of FBS that reduce the gene expression of important ECM components in vascular smooth muscle cells and rat cardiac fibroblasts, respectively [119; 126].

As a result the total collagen content developed accordingly, with IGF-I treated samples having significantly higher collagen contents than non-treated ones (Fig.19). Surprisingly, the mean collagen fibril diameter did not resemble this trend. At 21 days post seeding, the IGF-I treated sample with low serum had significantly increased collagen fibril

diameters compared to the other samples. However, at day 28 the non-IGF-I treated samples showed significantly increased collagen fibril diameters over the treated groups (Fig.19). Since the mean fibril diameter does not resolve the distribution of fibril diameters, fibril spectra were also analysed (Fig.20). Samples supplied with 10% FBS show the expected unimodal distribution of collagen fibrils, with the peak shifting from day 21 to day 28. Low serum groups, however, have skewed distributions and the low 0.5% FBS group at 28 days has a broad distribution without a distinct peak. Thus, the high mean fibril diameter results from a high variation in single fibril diameters, which is not according to physiological development [39; 140]. IGF-I, on the other hand, has the ability to rescue this skewing effect and lead to a more physiological unimodal distribution (Fig.20A).

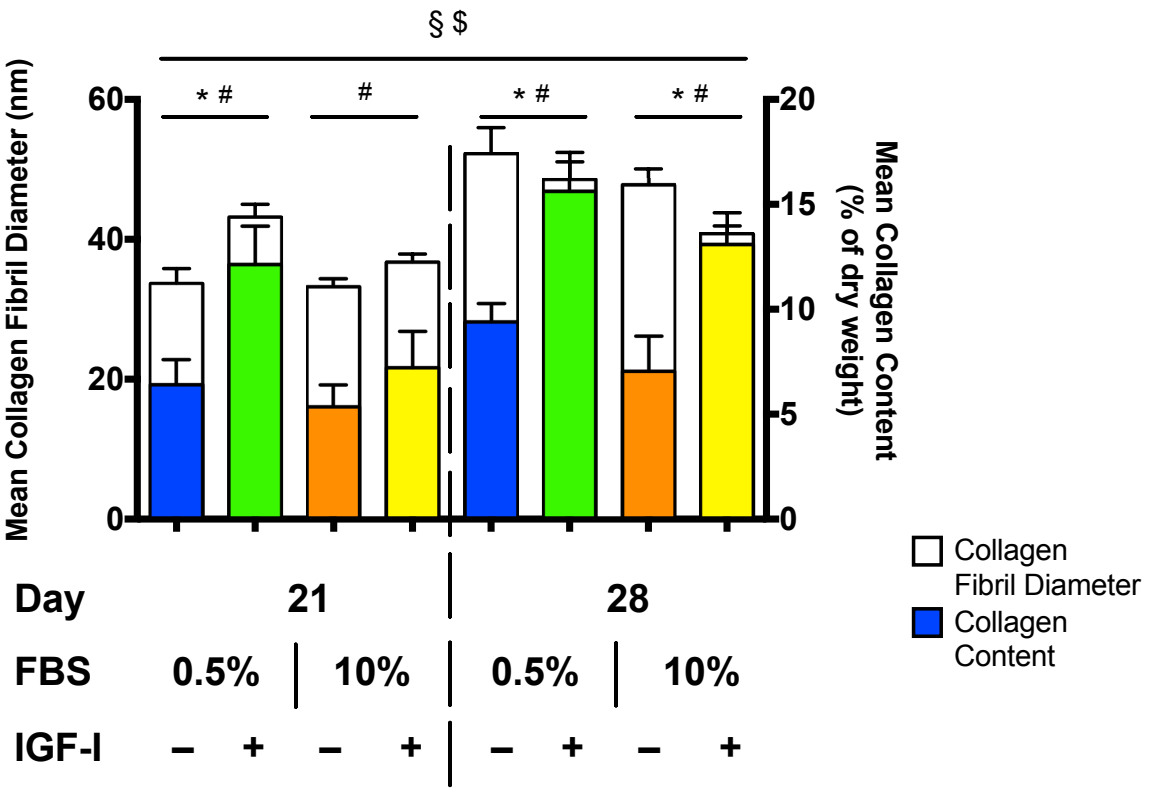

Figure 19. Collagen Quantification IGF-I study. The mean collagen fibril diameter (open bars) is superimposed with the total collagen content (coloured bars) of constructs at 21 and 28 days, respectively. The four groups are distinguished by colours and depicted in the legend below. The 0.5% FBS plus IGF-I group shows the highest collagen content, combined with a high collagen fibril diameter at both time points. 0.5% FBS without serum develops high fibril diameters, despite rather low total collagen contents. (mean±SEM; §$p<0.05$ effect of IGF-I on collagen content; \$$p<0.05$ effect of IGF-I on fibril diameter; *$p<0.05$ difference in collagen content among pairs; #$p<0.05$ difference in fibril diameter among pairs)

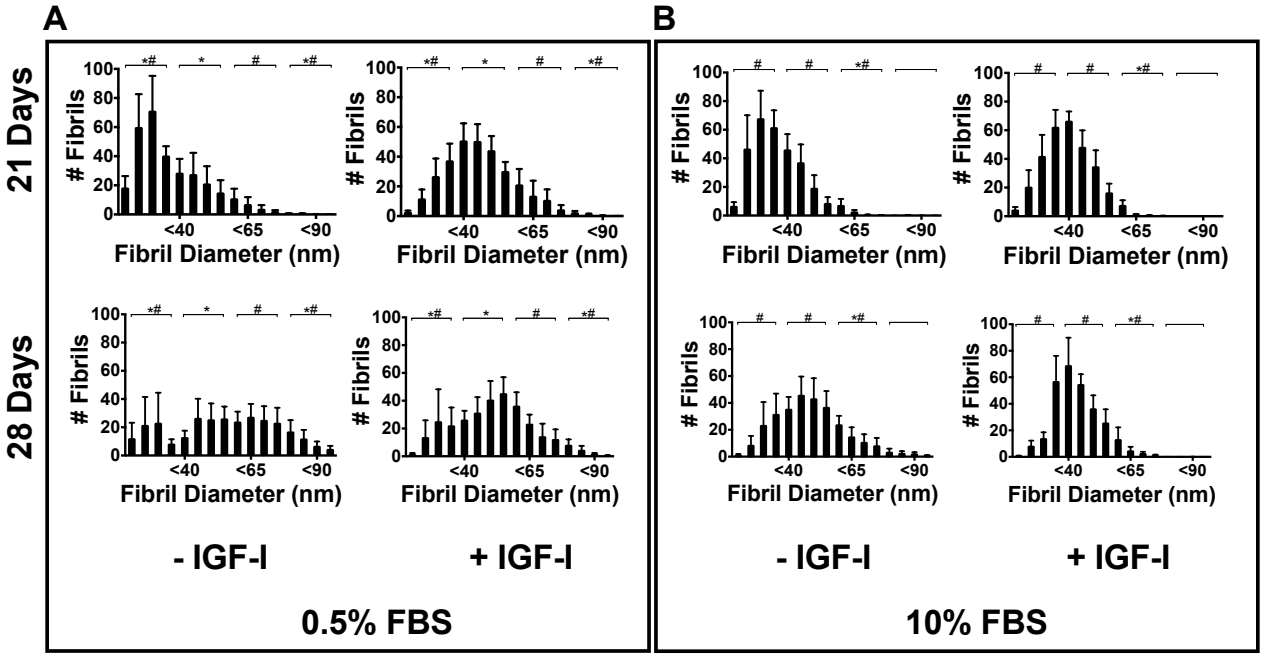

Figure 20. Collagen fibril spectra IGF-I study. A) Collagen fibril spectra of 0.5% FBS groups at 21 (top row) and 28 days (bottom row). Non-IGF-I treated groups show a skewed fibril distribution with a particularly broad range at 28 days. IGF-I rescues this effect and leads to unimodal distributions. B) High FBS groups show all Gaussian distributions that shift slightly towards higher diameters at 28 days. (*$p<0.05$ for IGF-I effect; #$p<0.05$ for time effect)

The effect of IGF-I was also investigated during tendon construct formation. It was found that the effect already starts during early development, even before full construct formation. Thus, IGF-I can be considered beneficial for early tendon development and might be stimulating for tendon healing. However, there was so far no direct effect on tendon ultrastructure detected *in vivo* [27], which might be due to short intervention periods in the rather inert adult tissue.

As indicated in the introduction, several growth factors can influence tendon development and repair [143]. The approach by Hagerty et al. [79] where multiple growth factors are taken in consideration provides valuable information. However, trying to study each growth factor and their synergies leads to extensive experiment setups. Hagerty and colleagues tried to account for this issue by using a statistical model [79]. Rather simplistic outcome measures such as mechanical testing and collagen content were acquired and the effects of single growth factors could not be resolved. Several studies have focussed before on growth factor supplementation, especially in *in vitro* studies. Apart from IGF-I, the growth factors TGF-ß, PDGF, VEGF, FGF, GDF and epidermal growth factor (EGF) were shown to have effects on tendon cells [3; 35; 43; 79; 112; 198]. These growth factors can be

grouped into factors that mostly enhance proliferation like FGF, PDGF and EGF [10; 43; 198], and those that both stimulate proliferation, tenogenic differentiation and ECM production like GDF, TGF-ß and IGF-I [1; 3; 10; 79; 97; 156]. Despite existing knowledge on growth factors and their potential, the basic building block, i.e. collagen fibrils, are hardly investigated in detail. This limitation originates partly from difficulties in assessing tendon tissue, but mostly from the fact that TEM analysis is both time and resource consuming.

From the variety of growth factors IGF-I was chosen because it is well accepted as a tendon supporting factor and is already applied in human *in vivo* studies [81; 151]. Particularly for treating tendinopathy or full tendon rupture, the effect on fibrillogenesis needs to be elucidated in order to safely apply IGF-I to tendon aetiologies. The applied IGF-I concentration was adapted from the literature. Abrahamsson et al. [1] described maximal proliferation of avian tenocytes at 100 ng/ml IGF-I and a ceiling effect of collagen synthesis stimulation at 250 ng/ml, while most other studies used lower concentrations without showing ceiling effects [43; 79]. In addition, IGF-I concentration in FBS has been described with high variation. One study could not detect IGF-I in FBS [222], while another study determined the concentration between 50-150 ng/ml [95], which would result in approximately 15 ng/ml at 10% FBS use. Thus, in order to be confident that the supplied amount of IGF-I would be sufficient to evoke the maximal effect, 250 ng/ml were chosen throughout the experiments. This was particularly important when combined with 10% FBS, since the IGF-I supplementation was supposed to exceed the existing level in FBS-treated samples significantly.

The limitation of this study to a single growth factor simultaneously represents the strength of this study. Since the setup was kept rather simplistic, it was possible to acquire quantitative data from the collagen fibrils and find that IGF-I does not only stimulate collagen production, but also supports physiological collagen fibrillogenesis. Importantly this was still true for samples treated with very low levels of FBS. While only 0.5% FBS resulted in impaired fibril spectra, IGF-I rescued the effect in order to develop the specific unimodal pattern as expected in developing tendon tissue [39; 140].

Study III

LOX is the key enzyme in the process of collagen cross-link formation [59]. Thus, LOX is critical for the development of functional collagen and thereby tendon integrity. The function of LOX on early tendon development has been well established by showing that LOX inhibition leads to mechanically inferior tissue [127; 162]. The first experiments with BAPN on tendon constructs led to construct rupture approximately at the time point of formation. This showed that the tenocytes generate sufficient force to tear the construct. Moreover, this implies that the cells do not sense the maximal force the structure can withstand. In order to obtain intact constructs for analysis, the constructs were allowed to form for 14 days and were subsequently treated with 50 µM BAPN. This treatment led to a stop in mechanical development as proven by the lack of increase in tensile modulus between day 14 and 21 (Fig.21).

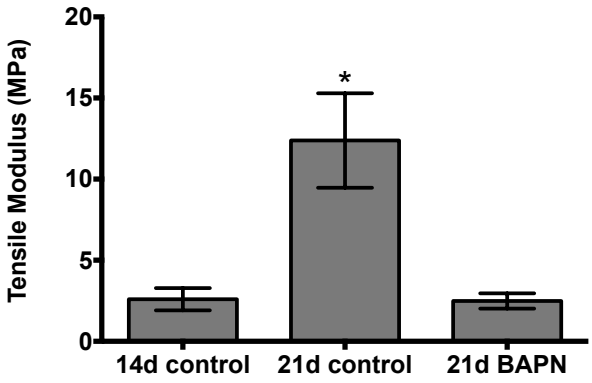

Figure 21. Tensile moduli of BAPN treated constructs vs. controls. The control constructs develop significantly from day 14 to 21. BAPN treated samples show no difference at 21 days compared to 14 day controls. Thus the development was stopped by BAPN. (*$p<0.05$ compared to other groups)

Apart from the mechanical integrity, the ultrastructure of BAPN treated samples was investigated. The collagen fibrils of control tissue had a uniform circular shape and showed a low variation in size, similar to the earlier studies (Fig.22A+C). BAPN treated samples, on the other hand, had irregular collagen fibrils and a broad distribution of varying fibril sizes (Fig.22B+D). Despite these irregular collagen fibrils, the constructs' total collagen content increased significantly compared to 14 day controls (Fig.23A). Similarly, the mean collagen fibril diameter was comparable to 21 day controls. However, it needs to be considered that the fibril diameter measurements assumed circular fibrils. Thereby the

minimal diameter is measured, which underestimates the area covered by the large, irregular fibrils (Fig.23B). The fibril diameter spectra are unimodal and show a shift towards higher diameters at 21 days. The BAPN treated samples display a flattened profile, with more small- and high diameter fibrils compared to 21 day controls (Fig.23C). These novel findings cannot be explained by the existing knowledge on collagen fibril shape regulation, since only collagen type V and the SLRPs decorin and fibromodulin as well as tenascin-X have so far been described to regulate fibril shape [137; 190; 212; 220]. Possible mechanisms might therefore include these ECM molecules in interplay with LOX in order to organise proper fibril formation.

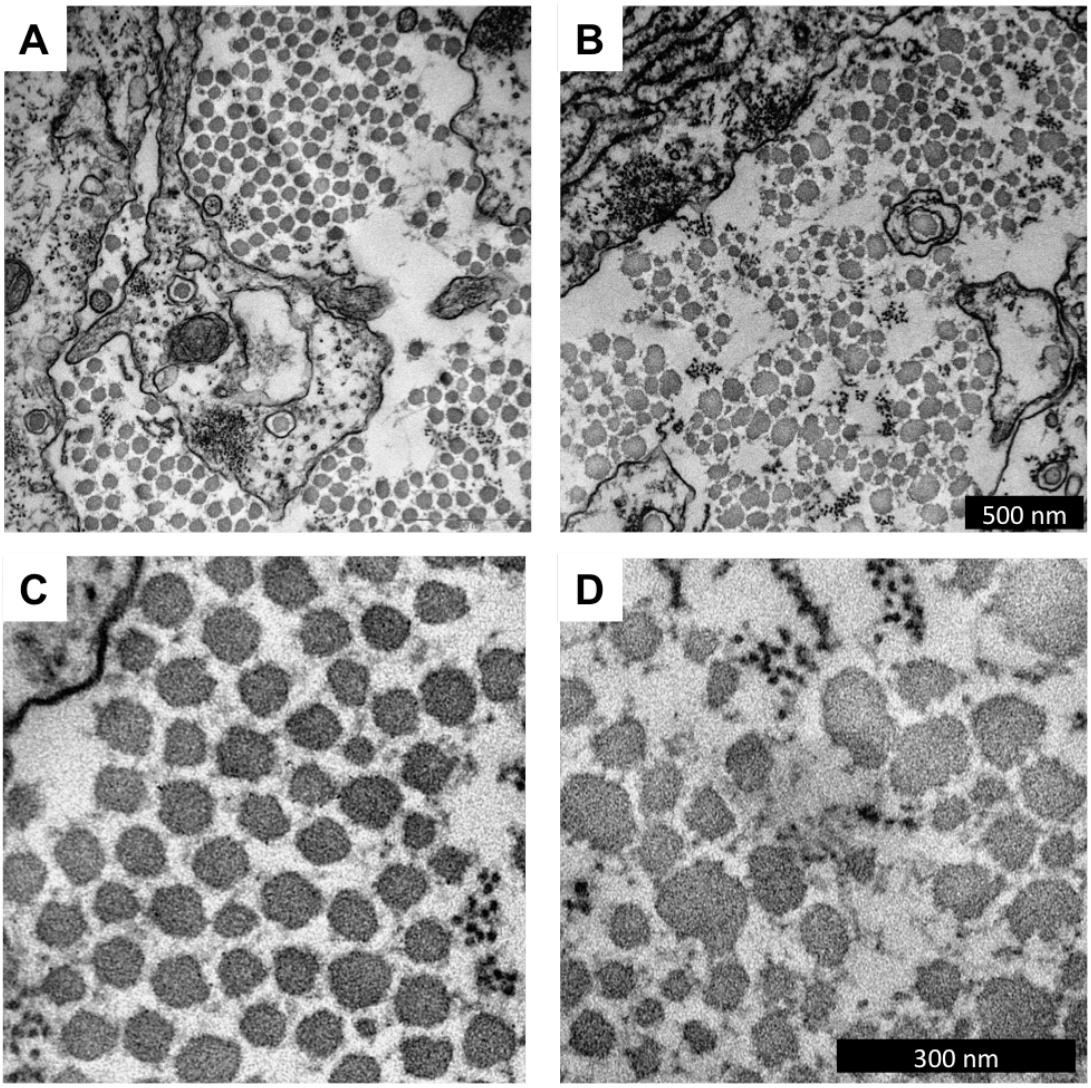

Figure 22. TEM of BAPN treated constructs. A+C) 21 day control constructs at medium and high resolution, respectively. Collagen fibrils show round outlines and are of similar size. B+D) BAPN treated constructs have irregular fibrils with a large variation among fibril sizes.

The cellular response to this severe intervention was first investigated by RT-qPCR (please refer to manuscript III for detailed datasets). However, neither the collagen cross-linking proteins, nor the fibrillogenesis regulating molecules were affected. In line with the unaltered total collagen content (Fig.23A), no change in gene expression for a broad range of essential ECM molecules could be detected. This supports the notion that the cells do not respond to LOX inhibition to rescue the weakened ECM.

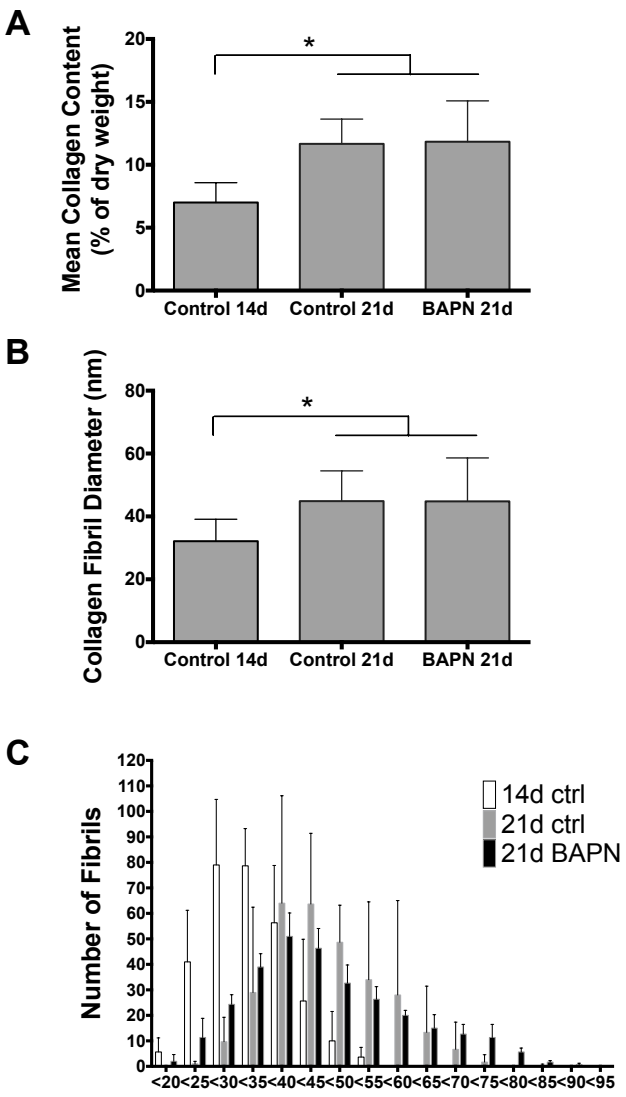

Figure 23. Collagen quantification from LOX inhibited constructs. A) The mean collagen content rises from day 14 to day 21 by approximately 5%, irrespectively of LOX inhibition. B) The mean collagen diameter develops significantly from day 14 to 21. BAPN treatment does not alter the mean fibril diameter. C) The fibril spectra show the difference between controls and BAPN treated samples. The BAPN samples have a broader spectrum of fibril diameters, with particularly a population of large diameter fibrils.

The direct measurement of collagen cross-links requires the use of HPLC (high performance liquid chromatograph), which was not available for this project. Moreover, the total amount of collagen from a single construct is very small. Tendon constructs have a dry mass of approximately 150 µg, which leads to a total collagen amount of ~15-20 µg collagen, while at least 50 µg would be required for the analysis (personal communication with Dr. David Eyre). Certainly, this critical mass might be achievable by pooling several constructs, but this was not pursued in the present work. Instead of measuring collagen cross-links directly, an indirect approach was used, whereby the solubility of the collagen per tendon construct can be estimated when run on a SDS-PAGE. Constructs were dissolved by heating in SDS-sample buffer at 95°C for 5 minutes. The resulting solution was separated by SDS-PAGE and subsequently

stained with coommasie brilliant blue. This resulted in the separation of collagen subunits that have been investigated in several studies of collagenous tissues and are usually used for further analysis in HPLC [60; 106].

The characteristic pattern shows distinct bands for the two collagen type I alpha chains, three ß-dimer bands and a group of γ-trimer (Figure 24). These bands were of significantly higher intensity in BAPN-treated samples compared to control constructs, suggesting increased solubility due to BAPN treatment. Thus, the collagen molecules are not as intensely cross-linked as in control constructs and are therefore more easily extracted by this relatively mild approach.

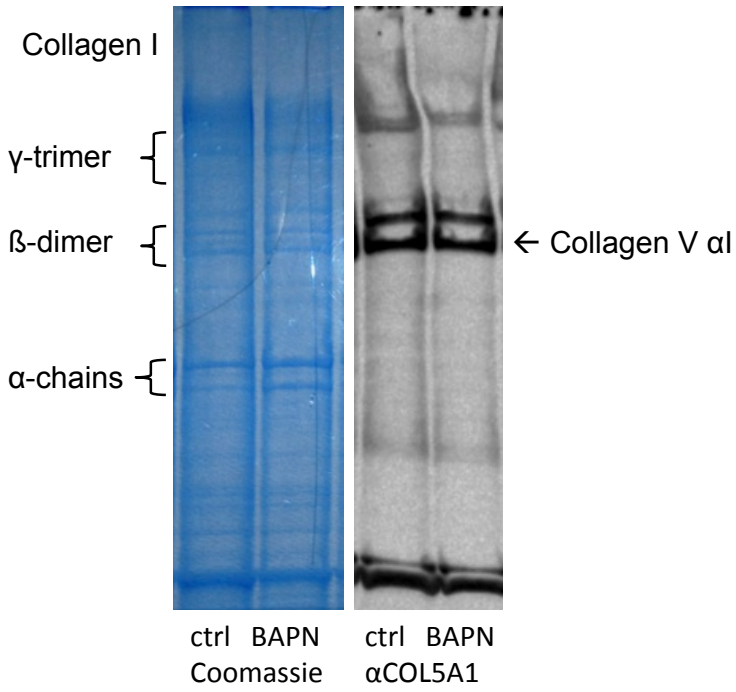

Figure 24. SDS-PAGE vs. western blot. A control and a BAPN-treated construct were analysed by commassie blue staining [196] and αColV western blot. The collagen pattern with monomers, dimers and trimers is indicated and combined with the location of collagen V. The total collagen is easier soluble in BAPN samples, but there is no visible difference in collagen V location.

As described in the introduction deficiency of collagen type V, decorin, fibromodulin and tenascin-X were shown to have similar effects during collagen fibrillogenesis. Since decorin, fibromodulin and tenascin-X were not changed in gene expression or western blotting due to BAPN treatment a novel hypothesis was developed: Collagen type V is known to be important for fibril shape regulation and has been shown to be cross-linked to collagen type I [22; 153], LOX might be essential in order to establish these cross-links and thereby bind collagen type V to the type I fibrils. Once cross-linked, collagen type V would be able to regulate fibril shape. This hypothesis was tested by comparing the coomassie blue stained gel with a western blot from the identical samples stained with a collagen type

V antibody (Fig.24). An alteration in collagen type V cross-linking would be detectable by a different location of collagen V in the samples. However, no changes could were seen between controls and BAPN-treated samples, rejecting this hypothesis.

Taking this line of thoughts to the next level – there might be a "hen and the egg" paradox. If LOX is not essential for collagen type V function, the mechanism might work the other way; hence collagen V guides LOX in a certain way in order to fulfil its function. In an attempt to combine the so far established fibrillogenesis regulators, a model is developed that might explain the roles of the different components and link their individual functions to ensure structural and mechanical integrity of collagen fibrils.

As a starting point, a recent study by Smith et al. [187] showed that collagen V is located in close proximity to the cellular surface (Fig.25). The rationale is that the quantitatively minor portion of collagen type V needs to be associated with the cell membrane where fibrillogenesis is initiated [25; 36]. Collagen type I, in contrast, is highly abundant in the ECM and it is therefore not necessary to guide this ubiquitous molecule to the area of fibril initiation. Moreover, the collagen I self-assembly mechanism will attract sufficient numbers of molecules for fibril nucleation [78; 102]. Due to its concentration at the cell surface, collagen type V is present in sufficient amounts to be incorporated into the fibrils [212]. Moreover, this is where we speculate a – so far unknown – interaction with LOX might occur. The proposed mechanism is that collagen V directs LOX to the spot where cross-linking is essential in order to create functional fibrils. In this scenario the observed importance of collagen V in controlling fibril formation would not be direct but rather mediated through LOX. Both molecules play an essential role in fibril diameter regulation (Fig.25).

Decorin, fibromodulin and tenascin-X are in this scenario rather independent from the LOX/collagen V interaction, since those are located along the already established fibrils. Decorin and fibromodulin bind to different locations within the collagen molecule [84] and can work in conjunction. Decorin has the major task to control fibril spacing [155], which is important to prohibit lateral fibril fusion. Moreover, it "coats" the fibril to encourage fibril growth at the tips [75]. Decorin is associated with tenascin-X as described earlier [30]. Fibromodulin was shown recently to sterically inhibit LOX [106] and is similarly to decorin believed to control fibril spacing [181]. Thus, here decorin and fibromodulin are believed to act in a similar way (Fig.25). Both accumulate along the collagen fibril and thereby organise fibril spacing and inhibit LOX in these finished areas.

This passive regulation leaves LOX to act in the areas of lateral and longitudinal fibril growth. As stated before this model is speculative. However, it provides an attempt to link the so far established mechanisms – in combination with LOX – to create functional collagen fibrils.

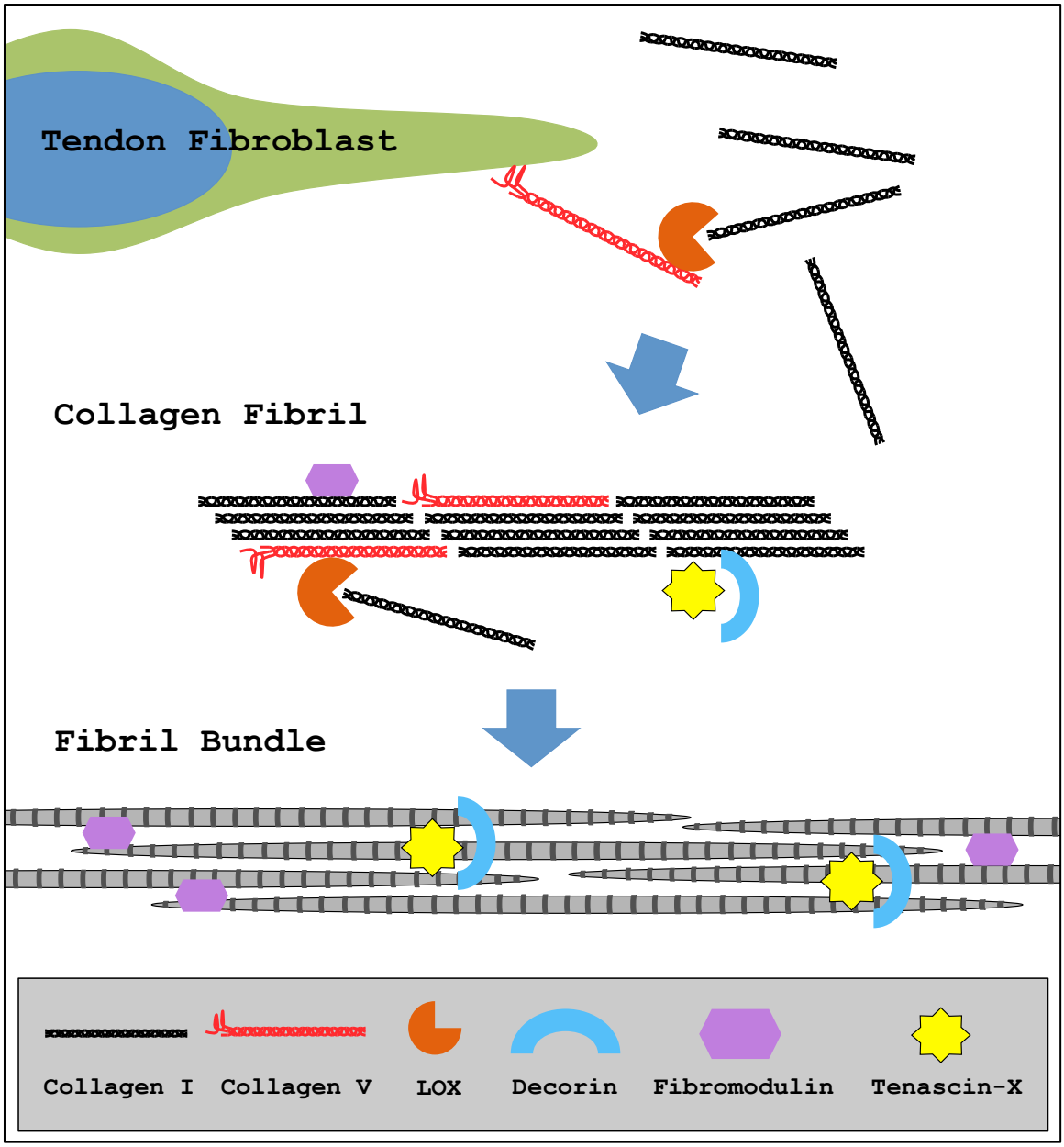

Figure 25. Collagen Fibrillogenesis Model. A schematic model was developed in order to combine the established fibrillogenesis regulators and combine these with the here-discovered role of LOX. Collagen type V is co-located with the cell membrane, ensuring thereby its incorporation into fibrils. Collagen V guides LOX to the proximity of the fibrils to facilitate cross-linking were necessary. Decorin and fibromodulin are meanwhile responsible for correct fibril spacing and thereby reduce LOX activity in finished fibrils by sterical hindrance. Tenascin-X co-aggregates with decorin to stabilise fibril spacing. (Sizing of symbols is not according to realistic scale)

Conclusions and Perspectives

The Tendon Construct

The tendon construct has been widely applied as a model to study tenocytes [14; 79; 88; 89; 109; 110; 115; 159]. In this study, a key aspect of tendon biology was added to the potential of the human tendon construct – development with time. This finding justifies using the tendon construct as an *in vitro* model to investigate tendon- and particularly collagen development. Adult human tenocytes are capable of driving processes that are not present in adult tendon, thus showing embryonic potential. Importantly, the presented collagen maturation is comparable with early tendon development *in vivo*.

In future studies the tendon construct can be a potent tool to uncover the scientific gaps in the mechanism of collagen fibrillogenesis. Moreover, effects of various stimuli on tenocytes can be evaluated and closely monitored over certain time frames. The briefly introduced tension stepper is a potential tool to study tendon cell mechanics in this context. In addition to investigating immediate cell-response, this allows to study the resulting changes in collagen production and -modification.

Growth Factor Supplementation of Tenocytes

IGF-I significantly increases collagen production in tenocytes, which is properly assimilated to the collagen network. Hence, the stimulus triggers the desired pathway to enhance tendon ECM production. FBS – despite being vital for tenocyte survival – reduces ECM production and therefore depicts a major problem with undefined cell supplements. Thus effects of different factors on ECM need to be studied carefully before attempting to apply these factors for tissue engineering or tendon healing, respectively.

The tendon construct is a valuable tool to monitor direct effects closely. However, *in vivo* studies need to complement this approach in order to evaluate the effect in the more complex *in vivo* environment. Since new tendon formation was increased in this study, the application of IGF-I on healing of ruptured tendons might bear potential to facilitate *de novo* tendon formation.

Collagen Cross-linking during Fibrillogenesis

Enzymatic cross-linking among collagen molecules is essential for the mechanical integrity of all collagenous tissues. The early development of the tendon construct is inhibited by LOX-inhibition. Interestingly, LOX also plays a major role in collagen fibril regulation, as proven by irregular fibril shapes when constructs are treated with BAPN. Another important finding of this study is that the cells seem to lack a control mechanism for proper collagen cross-linking. No compensatory mechanisms could be identified and the gene expression profile for various targets remained unaffected.

The role of LOX in fibrillogenesis regulation needs to be evaluated further in future studies. As shown by the means of a hypothetical model, the so far identified regulators certainly have a distinct interplay to guarantee functional collagen fibrils. Once this mechanism is uncovered, understanding tendon injuries might reach the next level and novel treatments can be developed. LOX was also recently discovered as a major factor driving metastasis development in cancer [9; 11]. Combining knowledge across different scientific focuses will help understanding the pathways controlling LOX function and activity in further detail.

References

1. Abrahamsson S-O, Lundborg G, Lohmander LS (1991) Recombinant Human Insulin-Like Growth Factor-I Stimulates In Vitro Matrix Synthesis and Cell Proliferation in Rabbit Flexor Tendon. *J Orthop Res* **9**:495-502.

2. Alexander RM (2002) Tendon elasticity and muscle function. *Comp Biochem Physiol A Mol Integr Physiol* **133**:1001-1011.

3. Anitua E, Sanchez M, Nurden AT, Zalduendo M, de la Fuente M, Azofra J, Andia I (2007) Reciprocal actions of platelet-secreted TGF-beta1 on the production of VEGF and HGF by human tendon cells. *Plast Reconstr Surg* **119**:950-959.

4. Arruda (2006) Regional variation of tibialis anterior tendon mechanics is lost following denervation. *Journal of Applied Physiology* **101**:1113-1117.

5. Avery NC, Bailey AJ (2005) Enzymic and non-enzymic cross-linking mechanisms in relation to turnover of collagen: relevance to aging and exercise. *Scand J Med Sci Sports* **15**:231-240.

6. Avery NC, Bailey AJ (2006) The effects of the Maillard reaction on the physical properties and cell interactions of collagen. *Pathol Biol (Paris)* **54**:387-395.

7. Bailey AJ (2001) Molecular mechanisms of ageing in connective tissues. *Mech Ageing Dev* **122**:735-755.

8. Bailey AJ, Paul RG, Knott L (1998) Mechanisms of maturation and ageing of collagen. *Mech Ageing Dev* **106**:1-56.

9. Baker AM, Bird D, Lang G, Cox TR, Erler JT (2013) Lysyl oxidase enzymatic function increases stiffness to drive colorectal cancer progression through FAK. *Oncogene* **32**:1863-1868.

10. Banes (1995) PGDF-BB, IGF-I and mechanical load stimulate DNA synthesis in avian tendon fibroblasts in vitro. *J Biomech* **28**:1505-1513.

11. Barker HE, Cox TR, Erler JT (2012) The rationale for targeting the LOX family in cancer. *Nat Rev Cancer* **12**:540-552.

12. Bayer ML, Schjerling P, Biskup E, Herchenhan A, Heinemeier KM, Doessing S, Krogsgaard M, Kjaer M (2012) No donor age effect of human serum on collagen synthesis signaling and cell proliferation of human tendon fibroblasts. *Mech Ageing Dev* **133**:246-254.

13. Bayer ML, Schjerling P, Herchenhan A, Zeltz C, Heinemeier KM, Christensen L, Krogsgaard M, Gullberg D, Kjaer M (2014) Release of tensile strain on engineered human tendon tissue disturbs cell adhesions, changes matrix architecture, and induces an inflammatory phenotype. *PLoS ONE* **9**:e86078.

14. Bayer ML, Yeung C-YC, Kadler KE, Qvortrup K, Baar K, Svensson RB, Peter Magnusson S, Krogsgaard M, Koch M et al. (2010) The initiation of embryonic-like collagen fibrillogenesis by adult human tendon fibroblasts when cultured under tension. *Biomater* **31**:4889-4897.

15. Beckham C, Dimond R, Greenlee TK (1977) The Role of Movement in the Development of a Digital Flexor Tendon. *American Journal of Anatomy* **150**:443-460.

16. Bennett MB, Ker RF, Imery NJ, Alexander RM (1986) Mechanical properties of various mammalian tendons. *Journal of Zoology* **209**:537-548.

17. Bensamoun SF, Tsubone T, Subramaniam M, Hawse JR, Boumediene E, Spelsberg TC, An K-N, Amadio PC (2006) Age-dependent changes in the mechanical properties of tail tendons in TGF- inducible early gene-1 knockout mice. *Journal of Applied Physiology* **101**:1419-1424.

18. Beynnon BD, Fleming BC (1998) Anterior cruciate ligament strain in-vivo: a review of previous work. *J Biomech* **31**:519-525.

19. Bi Y, Ehirchiou D, Kilts TM, Inkson CA, Embree MC, Sonoyama W, Li L, Leet AI, Seo BM et al. (2007) Identification of tendon stem/progenitor cells and the role of the extracellular matrix in their niche. *Nat Med* **13**:1219-1227.

20. Bierman EL (1978) The effect of donor age on the in vitro life span of cultured human arterial smooth-muscle cells. *In Vitro* **14**:951-955.

21. Biewener AA, Roberts TJ (2000) Muscle and tendon contributions to force, work, and elastic energy savings: a comparative perspective. *Exerc Sport Sci Rev* **28**:99-107.

22. Birk DE (2001) Type V collagen: heterotypic type I/V collagen interactions in the regulation of fibril assembly. *Micron* **32**:223-237.

23. Birk DE, Brückner P. 2011. Collagens, Suprastructures, and Collagen Fibril Assembly. In: Mecham, editor. The Extracellular Matrix: An Overview. Berlin Heidelberg: Springer-Verlag. pp 77-115.

24. Birk DE, Fitch JM, Babiarz JP, Linsenmayer TF (1988) Collagen type I and type V are present in the same fibril in the avian corneal stroma. *J Cell Biol* **106**:999-1008.

25. Birk DE, Trelstad RL (1986) Extracellular Compartments in Tendon Morphogenesis: Collagen Fibril, Bundle, and Macroaggregate Formation. *J Cell Biol* **103**:231-240.

26. Birk DE, Zycband EI, Woodruff S, Winkelmann DA, Trelstad RL (1997) Collagen fibrillogenesis in situ: fibril segments become long fibrils as the developing tendon matures. *Dev Dyn* **208**:291-298.

27. Boesen AP, Dideriksen K, Couppe C, Magnusson SP, Schjerling P, Boesen M, Aagaard P, Kjaer M, Langberg H (2014) Effect of growth hormone on aging connective tissue in muscle and tendon: gene expression, morphology, and function following immobilization and rehabilitation. *J Appl Physiol* **116**:192-203.

28. Boone CW, Mantel N, Caruso TD, Jr., Kazam E, Stevenson RE (1971) Quality control studies on fetal bovine serum used in tissue culture. *In Vitro* **7**:174-189.

29. Breidenbach AP, Dyment NA, Lu Y, Rao M, Shearn JTP, Rowe D, Kadler KE, Butler DL (2014) Fibrin gels exhibit improved biological, structural and mechanical properties compared to collagen gels in cell-based tendon tissue engineered constructs. *Tissue Eng Part A* 10.1089/ten.TEA.2013.0768.

30. Bristow J, Carey W, Egging D, Schalkwijk J (2005) Tenascin-X, collagen, elastin, and the Ehlers-Danlos syndrome. *Am J Med Genet C Semin Med Genet* **139C**:24-30.

31. Brown D, Wagner D, Li X, Richardson JA, Olson EN (1999) Dual role of the basic helix-loop-helix transcription factor scleraxis in mesoderm formation and chondrogenesis during mouse embryogenesis. *Development* **126**:4317-4329.

32. Butler DL, Gooch C, Kinneberg KRC, Boivin GP, Galloway MT, Nirmalanandhan VS, Shearn JT, Dyment NA, Juncosa-Melvin N (2010) The use of mesenchymal stem cells in collagen-based scaffolds for tissue-engineered repair of tendons. *Nature Protocols* **5**:849-863.

33. Cadby JA, Buehler E, Godbout C, van Weeren PR, Snedeker JG (2014) Differences between the cell populations from the peritenon and the tendon core with regard to their potential implication in tendon repair. *PLoS ONE* **9**:e92474.

34. Caliari SR, Harley BA (2011) The effect of anisotropic collagen-GAG scaffolds and growth factor supplementation on tendon cell recruitment, alignment, and metabolic activity. *Biomaterials* **32**:5330-5340.

35. Caliari SR, Harley BA (2013) Composite Growth Factor Supplementation Strategies to Enhance Tenocyte Bioactivity in Aligned Collagen-GAG Scaffolds. *Tissue Eng Part A* **19**:1100-1112.

36. Canty EG (2004) Coalignment of plasma membrane channels and protrusions (fibripositors) specifies the parallelism of tendon. *The Journal of Cell Biology* **165**:553-563.

37. Carroll CC, Dickinson JM, Haus JM, Lee GA, Hollon CJ, Aagaard P, Magnusson SP, Trappe TA (2008) Influence of aging on the in vivo properties of human patellar tendon. *J Appl Physiol (1985)* **105**:1907-1915.

38. Chakravarti S, Petroll WM, Hassell JR, Jester JV, Lass JH, Paul J, Birk DE (2000) Corneal opacity in lumican-null mice: defects in collagen fibril structure and packing in the posterior stroma. *Invest Ophthalmol Vis Sci* **41**:3365-3373.

39. Chaplin DM, Greenlee TK, Jr. (1975) The development of human digital tendons. *J Anat* **120**:253-274.

40. Chen JL, Yin Z, Shen WL, Chen X, Heng BC, Zou XH, Ouyang HW (2010) Efficacy of hESC-MSCs in knitted silk-collagen scaffold for tendon tissue engineering and their roles. *Biomaterials* **31**:9438-9451.

41. Chiquet M (1999) Regulation of extracellular matrix gene expression by mechanical stress. *Matrix Biology* **18**:417-426.

42. Clark JM, Harryman DT, 2nd (1992) Tendons, ligaments, and capsule of the rotator cuff. Gross and microscopic anatomy. *J Bone Joint Surg Am* **74**:713-725.

43. Costa MA, Wu C, Pham BV, Chong AK, Pham HM, Chang J (2006) Tissue engineering of flexor tendons: optimization of tenocyte proliferation using growth factor supplementation. *Tissue Eng* **12**:1937-1943.

44. Couppe´ C, Hansen P, Kongsgaard M, Kovanen V, Suetta C, Aagaard P, Kjær M, Magnusson SP (2009) Mechanical properties and collagen cross-linking of the patellar tendon in old and young men. *J Appl Physiol* **107**:880-886.

45. Craig AS, Birtles MJ, Conway JF, Parry DA (1989) An estimate of the mean length of collagen fibrils in rat tail-tendon as a function of age. *Connect Tissue Res* **19**:51-62.

46. Cronlund AL, Smith BD, Kagan HM (1985) Binding of lysyl oxidase to fibrils of type I collagen. *Connect Tissue Res* **14**:109-119.

47. Cserjesi P, Brown D, Ligon KL, Lyons GE, Copeland NG, Gilbert DJ, Jenkins NA, Olson EN (1995) Scleraxis: a basic helix-loop-helix protein that prefigures skeletal formation during mouse embryogenesis. *Development* **121**:1099-1110.

48. Daher RJ, Chahine NO, Razzano P, Patwa SA, Sgaglione NJ, Grande DA (2011) Tendon repair augmented with a novel circulating stem cell population. *Int J Clin Exp Med* **4**:214-219.

49. Dahlgren LA, Mohammed HO, Nixon AJ (2006) Expression of insulin-like growth factor binding proteins in healing tendon lesions. *J Orthop Res* **24**:183-192.

50. Danielson KG, Baribault H, Holmes DF, Graham H, Kadler KE, Iozzo RV (1997) Targeted disruption of decorin leads to abnormal collagen fibril morphology and skin fragility. *J Cell Biol* **136**:729-743.

51. de Vos RJ, Weir A, van Schie HTM, Bierma-Zeinstra SMA, Verhaar JAN, Weinans H, Tol JL (2010) Platelet-Rich Plasma Injection for Chronic Achilles Tendinopathy: A Randomized Controlled Trial. *JAMA: The Journal of the American Medical Association* **303**:144-149.

52. Derynck R, Zhang YE (2003) Smad-dependent and Smad-independent pathways in TGF-beta family signalling. *Nature* **425**:577-584.

53. Docheva D, Hunziker EB, Fassler R, Brandau O (2005) Tenomodulin is necessary for tenocyte proliferation and tendon maturation. *Mol Cell Biol* **25**:699-705.

54. Doessing S, Heinemeier KM, Holm L, Mackey AL, Schjerling P, Rennie M, Smith K, Reitelseder S, Kappelgaard AM et al. (2009) Growth hormone stimulates the collagen synthesis in human tendon and skeletal muscle without affecting myofibrillar protein synthesis. *J Physiol* **588**:341-351.

55. Dunkman AA, Buckley MR, Mienaltowski MJ, Adams SM, Thomas SJ, Satchell L, Kumar A, Pathmanathan L, Beason DP et al. (2013) Decorin expression is important for age-related changes in tendon structure and mechanical properties. *Matrix Biol* **32**:3-13.

56. Egerbacher M, Arnoczky SP, Caballero O, Lavagnino M, Gardner KL (2008) Loss of homeostatic tension induces apoptosis in tendon cells: an in vitro study. *Clin Orthop Relat Res* **466**:1562-1568.

57. Elbjeirami WM, Yonter EO, Starcher BC, West JL (2003) Enhancing mechanical properties of tissue-engineered constructs via lysyl oxidase crosslinking activity. *J Biomed Mater Res A* **66**:513-521.

58. Eliasson P, Fahlgren A, Pasternak B, Aspenberg P (2007) Unloaded rat Achilles tendons continue to grow, but lose viscoelasticity. *J Appl Physiol (1985)* **103**:459-463.

59. Eyre DR, Paz MA, Gallop PM (1984) Cross-linking in collagen and elastin. *Annu Rev Biochem* **53**:717-748.

60. Eyre DR, Weis M, Hudson DM, Wu JJ, Kim L (2011) A novel 3-hydroxyproline (3Hyp)-rich motif marks the triple-helical C terminus of tendon type I collagen. *J Biol Chem* **286**:7732-7736.

61. Ezura Y, Chakravarti S, Oldberg A, Chervoneva I, Birk DE (2000) Differential expression of lumican and fibromodulin regulate collagen fibrillogenesis in developing mouse tendons. *J Cell Biol* **151**:779-788.

62. Fallouh L, Nakagawa K, Sasho T, Arai M, Kitahara S, Wada Y, Moriya H, Takahashi K (2010) Effects of autologous platelet-rich plasma on cell viability and collagen synthesis in injured human anterior cruciate ligament. *J Bone Joint Surg Am* **92**:2909-2916.

63. Fan H, Liu H, Toh SL, Goh JC (2009) Anterior cruciate ligament regeneration using mesenchymal stem cells and silk scaffold in large animal model. *Biomaterials* **30**:4967-4977.

64. Fessel G, Snedeker JG (2009) Evidence against proteoglycan mediated collagen fibril load transmission and dynamic viscoelasticity in tendon. *Matrix Biol* **28**:503-510.

65. Filardo G, Kon E, Di Matteo B, Di Martino A, Tesei G, Pelotti P, Cenacchi A, Marcacci M (2014) Platelet-rich plasma injections for the treatment of refractory Achilles tendinopathy: results at 4 years. *Blood Transfus* 10.2450/2014.0289-13:1-8.

66. Fleischmajer R, Fisher LW, MacDonald ED, Jacobs L, Jr., Perlish JS, Termine JD (1991) Decorin interacts with fibrillar collagen of embryonic and adult human skin. *J Struct Biol* **106**:82-90.

67. Franchi M, Quaranta M, Macciocca M, De Pasquale V, Ottani V, Ruggeri A (2009) Structure relates to elastic recoil and functional role in quadriceps tendon and patellar ligament. *Micron* **40**:370-377.

68. Fratzl P (2008) Collagen Structure and Mechanics. New York: Springer US.

69. Fratzl P, Misof K, Zizak I, Rapp G, Amenitsch H, Bernstorff S (1998) Fibrillar structure and mechanical properties of collagen. *J Struct Biol* **122**:119-122.

70. Gardner K, Arnoczky SP, Caballero O, Lavagnino M (2008) The effect of stress-deprivation and cyclic loading on the TIMP/MMP ratio in tendon cells: an in vitro experimental study. *Disabil Rehabil* **30**:1523-1529.

71. Gere JM, Goodno BJ (2009) Mechanics of materials. Toronto, ON ; Clifton Park, NY: Cengage Learning. xviii, 1022 p. pp.

72. Gimble JM, Katz AJ, Bunnell BA (2007) Adipose-Derived Stem Cells for Regenerative Medicine. *Circulation Research* **100**:1249-1260.

73. Goh K, Hiller J, Haston J, Holmes D, Kadler K, Murdoch A, Meakin J, Wess T (2005) Analysis of collagen fibril diameter distribution in connective tissues using small-angle X-ray scattering. *Biochimica et Biophysica Acta (BBA) - General Subjects* **1722**:183-188.

74. Goh KL, Holmes DF, Lu Y, Purslow PP, Kadler KE, Bechet D, Wess TJ (2012) Bimodal collagen fibril diameter distributions direct age-related variations in tendon resilience and resistance to rupture. *J Appl Physiol* **113**:878-888.

75. Graham HK, Holmes DF, Watson RB, Kadler KE (2000) Identification of collagen fibril fusion during vertebrate tendon morphogenesis. The process relies on unipolar fibrils and is regulated by collagen-proteoglycan interaction. *J Mol Biol* **295**:891-902.

76. Gray H, Clemente CD (1985) Anatomy of the human body. Philadelphia: Lea & Febiger. xvii, 1676 p. pp.

77. Greenspan D. 2005. Biosynthetic Processing of Collagen Molecules. In: Brinckmann, Notbohm, Müller, editors. Collagen. Springer Berlin Heidelberg. pp 149-183.

78. Gross J, Kirk D (1958) The heat precipitation of collagen from neutral salt solutions: some rate-regulating factors. *J Biol Chem* **233**:355-360.

79. Hagerty P, Lee A, Calve S, Lee CA, Vidal M, Baar K (2012) The effect of growth factors on both collagen synthesis and tensile strength of engineered human ligaments. *Biomaterials* **33**:6355-6361.
80. Hammer N, Huster D, Fritsch S, Hadrich C, Koch H, Schmidt P, Sichting F, Wagner MF, Boldt A (2014) Do cells contribute to tendon and ligament biomechanics? *PLoS ONE* **9**:e105037.
81. Hansen M, Boesen A, Holm L, Flyvbjerg A, Langberg H, Kjaer M (2013) Local administration of insulin-like growth factor-I (IGF-I) stimulates tendon collagen synthesis in humans. *Scand J Med Sci Sports* **23**:614-619.
82. Hanson DA, Eyre DR (1996) Molecular site specificity of pyridinoline and pyrrole cross-links in type I collagen of human bone. *J Biol Chem* **271**:26508-26516.
83. Haraldsson BT, Aagaard P, Krogsgaard M, Alkjaer T, Kjaer M, Magnusson SP (2005) Region-specific mechanical properties of the human patella tendon. *J Appl Physiol* **98**:1006-1012.
84. Hedbom E, Heinegard D (1993) Binding of fibromodulin and decorin to separate sites on fibrillar collagens. *J Biol Chem* **268**:27307-27312.
85. Heinemeier KM, Olesen JL, Haddad F, Schjerling P, Baldwin KM, Kjaer M (2009) Effect of unloading followed by reloading on expression of collagen and related growth factors in rat tendon and muscle. *J Appl Physiol* **106**:178-186.
86. Heinemeier KM, Schjerling P, Heinemeier J, Magnusson SP, Kjaer M (2013) Lack of tissue renewal in human adult Achilles tendon is revealed by nuclear bomb (14)C. *FASEB J* **27**:2074-2079.
87. Heisterbach PE, Todorov A, Fluckiger R, Evans CH, Majewski M (2011) Effect of BMP-12, TGF-beta1 and autologous conditioned serum on growth factor expression in Achilles tendon healing. *Knee Surg Sports Traumatol Arthrosc* **20**:1907-1914.
88. Herchenhan A. 2010. Crimp Formation in Chick Embryonic Tendon: A Finite Element Analysis. In: Faculty of Life Sciences. Manchester: University of Manchester.
89. Herchenhan A, Kalson NS, Holmes DF, Hill P, Kadler KE, Margetts L (2011) Tenocyte contraction induces crimp formation in tendon-like tissue. *Biomech Model Mechanobiol* **11**:449-459.
90. Hinz B, Phan SH, Thannickal VJ, Galli A, Bochaton-Piallat ML, Gabbiani G (2007) The myofibroblast: one function, multiple origins. *Am J Pathol* **170**:1807-1816.
91. Hiraki Y, Shukunami C (2005) Angiogenesis inhibitors localized in hypovascular mesenchymal tissues: chondromodulin-I and tenomodulin. *Connect Tissue Res* **46**:3-11.
92. Holmes DF, Graham HK, Trotter JA, Kadler KE (2001) STEM/TEM studies of collagen fibril assembly. *Micron* **32**:273-285.
93. Holmes DF, Kadler KE (2005) The Precision of Lateral Size Control in the Assembly of Corneal Collagen Fibrils. *Journal of Molecular Biology* **345**:773-784.
94. Holmes DF, Tait A, Hodson NW, Sherratt MJ, Kadler KE (2010) Growth of collagen fibril seeds from embryonic tendon: fractured fibril ends nucleate new tip growth. *J Mol Biol* **399**:9-16.
95. Honegger A, Humbel RE (1986) Insulin-like growth factors I and II in fetal and adult bovine serum. Purification, primary structures, and immunological cross-reactivities. *J Biol Chem* **261**:569-575.
96. Hynes RO (1992) Integrins: versatility, modulation, and signaling in cell adhesion. *Cell* **69**:11-25.
97. James R, Kumbar SG, Laurencin CT, Balian G, Chhabra AB (2011) Tendon tissue engineering: adipose-derived stem cell and GDF-5 mediated regeneration using electrospun matrix systems. *Biomed Mater* **6**:025011.
98. Johnson GA, Tramaglini DM, Levine RE, Ohno K, Choi NY, Woo SL (1994) Tensile and viscoelastic properties of human patellar tendon. *J Orthop Res* **12**:796-803.
99. Juncosa-Melvin N, Boivin GP, Gooch C, Galloway MT, West JR, Dunn MG, Butler DL (2006) The Effect of Autologous Mesenchymal Stem Cells on the Biomechanics and

Histology of Gel-Collagen Sponge Constructs Used for Rabbit Patellar Tendon Repair. *Tissue Engineering* **12**:369-379.

100. Juncosa-Melvin N, Matlin KS, Holdcraft RW, Nirmalanandhan VS, Butler DL (2007) Mechanical Stimulation Increases Collagen Type I and Collagen Type III Gene Expression of Stem Cell?Collagen Sponge Constructs for Patellar Tendon Repair. *Tissue Engineering* **13**:1219-1226.

101. Kadler KE, Hill A, Canty-Laird EG (2008) Collagen fibrillogenesis: fibronectin, integrins, and minor collagens as organizers and nucleators. *Curr Opin Cell Biol* **20**:495-501.

102. Kadler KE, Hojima Y, Prockop DJ (1987) Assembly of collagen fibrils de novo by cleavage of the type I pC-collagen with procollagen C-proteinase. Assay of critical concentration demonstrates that collagen self-assembly is a classical example of an entropy-driven process. *J Biol Chem* **262**:15696-15701.

103. Kadler KE, Holmes DF, Graham H, Starborg T (2000) Tip-mediated fusion involving unipolar collagen fibrils accounts for rapid fibril elongation, the occurrence of fibrillar branched networks in skin and the paucity of collagen fibril ends in vertebrates. *Matrix Biol* **19**:359-365.

104. Kadler KE, Holmes DF, Trotter JA, Chapman JA (1996) Collagen fibril formation. *Biochemical Journal* **316**:1-11.

105. Kagan HM, Li W (2003) Lysyl oxidase: properties, specificity, and biological roles inside and outside of the cell. *J Cell Biochem* **88**:660-672.

106. Kalamajski S, Liu C, Tillgren V, Rubin K, Oldberg A, Rai J, Weis M, Eyre DR (2014) Increased C-telopeptide Cross-linking of Tendon Type I Collagen in Fibromodulin-deficient Mice. *J Biol Chem* **289**:18873-18879.

107. Kalamajski S, Oldberg A (2009) Homologous sequence in lumican and fibromodulin leucine-rich repeat 5-7 competes for collagen binding. *J Biol Chem* **284**:534-539.

108. Kalamajski S, Oldberg A (2010) The role of small leucine-rich proteoglycans in collagen fibrillogenesis. *Matrix Biol* **29**:248-253.

109. Kalson NS, Holmes DF, Herchenhan A, Lu Y, Starborg T, Kadler KE (2011) Slow stretching that mimics embryonic growth rate stimulates structural and mechanical development of tendon-like tissue in vitro. *Dev Dyn* **240**:2520-2528.

110. Kalson NS, Holmes DF, Kapacee Z, Otermin I, Lu Y, Ennos RA, Canty-Laird EG, Kadler KE (2010) An experimental model for studying the biomechanics of embryonic tendon: Evidence that the development of mechanical properties depends on the actinomyosin machinery. *Matrix Biol* **29**:678-689.

111. Kalson NS, Starborg T, Lu Y, Mironov A, Humphries SM, Holmes DF, Kadler KE (2013) Nonmuscle myosin II powered transport of newly formed collagen fibrils at the plasma membrane. *Proc Natl Acad Sci U S A* **110**:E4743-4752.

112. Kang HJ, Kang ES (1999) Ideal concentration of growth factors in rabbit's flexor tendon culture. *Yonsei Med J* **40**:26-29.

113. Kaniki N, Willits K, Mohtadi NG, Fung V, Bryant D (2014) A retrospective comparative study with historical control to determine the effectiveness of platelet-rich plasma as part of nonoperative treatment of acute achilles tendon rupture. *Arthroscopy* **30**:1139-1145.

114. Kannus P (2000) Structure of the tendon connective tissue. *Scand J Med Sci Sports* **10**:312-320.

115. Kapacee Z, Richardson S, Lu Y, Starborg T, Holmes D, Baar K, Kadler K (2008) Tension is required for fibripositor formation. *Matrix Biol* **27**:371-375.

116. Kapacee Z, Yeung C-YC, Lu Y, Crabtree D, Holmes DF, Kadler KE (2010) Synthesis of embryonic tendon-like tissue by human marrow stromal/mesenchymal stem cells requires a three-dimensional environment and transforming growth factor β3. *Matrix Biology* **29**:668-677.

117. Kastelic J, A. G, E. B (1978) The Multicomposite Structure of Tendon. *Connect Tissue Res* **6**:11-23.

118. Ker RF, Dimery NJ, Alexander RM (1986) The role of tendon elasticity in hopping in a wallaby (Macropus rufogriseus). *Journal of Zoology* **208**:417-428.
119. Kindy MS, Chang CJ, Sonenshein GE (1988) Serum deprivation of vascular smooth muscle cells enhances collagen gene expression. *J Biol Chem* **263**:11426-11430.
120. Kjær M (2004) Role of Extracellular Matrix in Adaptation of Tendon and Skeletal Muscle to Mechanical Loading. *PHYSIOLOGICAL REVIEWS* **84**:649-698.
121. Klass BR, Grobbelaar AO, Rolfe KJ (2009) Transforming growth factor beta1 signalling, wound healing and repair: a multifunctional cytokine with clinical implications for wound repair, a delicate balance. *Postgrad Med J* **85**:9-14.
122. Kongsgaard M, Kovanen V, Aagaard P, Doessing S, Hansen P, Laursen AH, Kaldau NC, Kjaer M, Magnusson SP (2009) Corticosteroid injections, eccentric decline squat training and heavy slow resistance training in patellar tendinopathy. *Scand J Med Sci Sports* **19**:790-802.
123. Kurtz CA, Loebig TG, Anderson DD, DeMeo PJ, Campbell PG (1999) Insulin-like growth factor I accelerates functional recovery from Achilles tendon injury in a rat model. *Am J Sports Med* **27**:363-369.
124. Laemmli UK (1970) Cleavage of structural proteins during the assembly of the head of bacteriophage T4. *Nature* **227**:680-685.
125. Lau YK, Gobin AM, West JL (2006) Overexpression of lysyl oxidase to increase matrix crosslinking and improve tissue strength in dermal wound healing. *Ann Biomed Eng* **34**:1239-1246.
126. Leicht M, Briest W, Holzl A, Zimmer HG (2001) Serum depletion induces cell loss of rat cardiac fibroblasts and increased expression of extracellular matrix proteins in surviving cells. *Cardiovasc Res* **52**:429-437.
127. Levene CI, Gross J (1959) Alterations in state of molecular aggregation of collagen induced in chick embryos by beta-aminopropionitrile (lathyrus factor). *J Exp Med* **110**:771-790.
128. Lichtwark GA, Wilson AM (2005) In vivo mechanical properties of the human Achilles tendon during one-legged hopping. *J Exp Biol* **208**:4715-4725.
129. Lindner D, Zietsch C, Becher PM, Schulze K, Schultheiss HP, Tschope C, Westermann D (2012) Differential expression of matrix metalloproteases in human fibroblasts with different origins. *Biochem Res Int* **2012**:875742.
130. Linsenmayer TF, Gibney E, Igoe F, Gordon MK, Fitch JM, Fessler LI, Birk DE (1993) Type V collagen: molecular structure and fibrillar organization of the chicken alpha 1(V) NH2-terminal domain, a putative regulator of corneal fibrillogenesis. *J Cell Biol* **121**:1181-1189.
131. Liu CF, Aschbacher-Smith L, Barthelery N, Dyment N, Butler DL, Wylie C (2011) What we should know before using tissue engineering techniques to repair injured tendons: A developmental biology perspective. *Tissue Eng Part B Rev* **17**:165-176.
132. Liu W, Watson SS, Lan Y, Keene DR, Ovitt CE, Liu H, Schweitzer R, Jiang R (2010) The atypical homeodomain transcription factor Mohawk controls tendon morphogenesis. *Mol Cell Biol* **30**:4797-4807.
133. Magarian EM, Vavken P, Murray MM (2010) Human anterior cruciate ligament fibroblasts from immature patients have a stronger in vitro response to platelet concentrates than those from mature individuals. *Knee* **18**:247-251.
134. Magnusson SP, Langberg H, Kjaer M (2010) The pathogenesis of tendinopathy: balancing the response to loading. *Nature Reviews Rheumatology* **6**:262-268.
135. Magnusson SP, Qvortrup K, Larsen JO, Rosager S, Hanson P, Aagaard P, Krogsgaard M, Kjaer M (2002) Collagen fibril size and crimp morphology in ruptured and intact Achilles tendons. *Matrix Biol* **21**:369-377.
136. Malfait F, Coucke P, Symoens S, Loeys B, Nuytinck L, De Paepe A (2005) The molecular basis of classic Ehlers-Danlos syndrome: a comprehensive study of biochemical and molecular findings in 48 unrelated patients. *Hum Mutat* **25**:28-37.

137. Mao JR, Taylor G, Dean WB, Wagner DR, Afzal V, Lotz JC, Rubin EM, Bristow J (2002) Tenascin-X deficiency mimics Ehlers-Danlos syndrome in mice through alteration of collagen deposition. *Nat Genet* **30**:421-425.
138. Marturano JE, Arena JD, Schiller ZA, Georgakoudi I, Kuo CK (2013) Characterization of mechanical and biochemical properties of developing embryonic tendon. *Proc Natl Acad Sci U S A* **110**:6370-6375.
139. Mathew SJ, Hansen JM, Merrell AJ, Murphy MM, Lawson JA, Hutcheson DA, Hansen MS, Angus-Hill M, Kardon G (2011) Connective tissue fibroblasts and Tcf4 regulate myogenesis. *Development* **138**:371-384.
140. McBride DJ, Trelstad RL, Silver FH (1988) Structural and mechanical assessment of developing chick tendon. *International Journal of Biological Macromolecules* **10**:194-200.
141. McNeilly CM, Banes AJ, Benjamin M, Ralphs JR (1996) Tendon cells in vivo form a three dimensional network of cell processes linked by gap junctions. *J Anat* **189 (Pt 3)**:593-600.
142. Mendias CL, Gumucio JP, Lynch EB (2012) Mechanical loading and TGF-beta change the expression of multiple miRNAs in tendon fibroblasts. *J Appl Physiol* **113**:56-62.
143. Molloy T, Wang Y, Murrell G (2003) The roles of growth factors in tendon and ligament healing. *Sports Med* **33**:381-394.
144. Molnar J, Fong KS, He QP, Hayashi K, Kim Y, Fong SF, Fogelgren B, Szauter KM, Mink M et al. (2003) Structural and functional diversity of lysyl oxidase and the LOX-like proteins. *Biochim Biophys Acta* **1647**:220-224.
145. Murchison ND, Price BA, Conner DA, Keene DR, Olson EN, Tabin CJ, Schweitzer R (2007) Regulation of tendon differentiation by scleraxis distinguishes force-transmitting tendons from muscle-anchoring tendons. *Development* **134**:2697-2708.
146. Myllyharju J. 2005. Intracellular Post-Translational Modifications of Collagens. In: Brinckmann, Notbohm, Müller, editors. Collagen. Springer Berlin Heidelberg. pp 115-147.
147. Myllyharju J, Kivirikko KI (2004) Collagens, modifying enzymes and their mutations in humans, flies and worms. *Trends Genet* **20**:33-43.
148. Nagase H, Visse R, Murphy G (2006) Structure and function of matrix metalloproteinases and TIMPs. *Cardiovasc Res* **69**:562-573.
149. Nagase H, Woessner JF, Jr. (1999) Matrix metalloproteinases. *J Biol Chem* **274**:21491-21494.
150. Nielsen RH, Couppe C, Jensen JK, Olsen MR, Heinemeier KM, Malfait F, Symoens S, Paepe AD, Schjerling P et al. (2014) Low tendon stiffness and abnormal ultrastructure distinguish classic Ehlers-Danlos syndrome from benign joint hypermobility syndrome in patients. *FASEB J* 10.1096/fj.14-249656.
151. Nielsen RH, Holm L, Malmgaard-Clausen NM, Reitelseder S, Heinemeier KM, Kjaer M (2014) Increase in tendon protein synthesis in response to insulin-like growth factor-I is preserved in elderly men. *J Appl Physiol (1985)* **116**:42-46.
152. Nirmalanandhan V, Rao M, Shearn J, Juncosamelvin N, Gooch C, Butler D (2008) Effect of scaffold material, construct length and mechanical stimulation on the in vitro stiffness of the engineered tendon construct. *J Biomech* **41**:822-828.
153. Niyibizi C, Eyre DR (1994) Structural characteristics of cross-linking sites in type V collagen of bone. Chain specificities and heterotypic links to type I collagen. *Eur J Biochem* **224**:943-950.
154. Noyes FR, Grood ES (1976) The Strength of the Anterior Cruciate Ligament in Humans and Rhesus Monkeys. *Journal of Bone and Joint Surgery* **58**.
155. Orgel JP, Eid A, Antipova O, Bella J, Scott JE (2009) Decorin core protein (decoron) shape complements collagen fibril surface structure and mediates its binding. *PLoS ONE* **4**:e7028.
156. Park A, Hogan MV, Kesturu GS, James R, Balian G, Chhabra AB (2010) Adipose-derived mesenchymal stem cells treated with growth differentiation factor-5 express tendon-specific markers. *Tissue Eng Part A* **16**:2941-2951.

157. Parry DA, Barnes GR, Craig AS (1978) A comparison of the size distribution of collagen fibrils in connective tissues as a function of age and a possible relation between fibril size distribution and mechanical properties. *Proc R Soc Lond B Biol Sci* **203**:305-321.
158. Paxton JZ, Baar K (2007) Tendon mechanics: the argument heats up. *Journal of Applied Physiology* **103**:423-424.
159. Paxton JZ, Hagerty P, Andrick JJ, Baar K (2011) Optimizing an intermittent stretch paradigm using ERK1/2 phosphorylation results in increased collagen synthesis in engineered ligaments. *Tissue Eng Part A* **18**:277-284.
160. Phillips CL, Combs SB, Pinnell SR (1994) Effects of ascorbic acid on proliferation and collagen synthesis in relation to the donor age of human dermal fibroblasts. *J Invest Dermatol* **103**:228-232.
161. Pierard GE, Le T, Pierard-Franchimont C, Lapiere CM (1988) Morphometric study of cauliflower collagen fibrils in Ehlers-Danlos syndrome type I. *Coll Relat Res* **8**:453-457.
162. Pinnell SR, Martin GR (1968) The cross-linking of collagen and elastin: enzymatic conversion of lysine in peptide linkage to alpha-aminoadipic-delta-semialdehyde (allysine) by an extract from bone. *Proc Natl Acad Sci U S A* **61**:708-716.
163. Pittenger MF, Mackay AM, Beck SC, Jaiswal RK, Douglas R, Mosca JD, Moorman MA, Simonetti DW, Craig S et al. (1999) Multilineage potential of adult human mesenchymal stem cells. *Science* **284**:143-147.
164. Pridgen BC, Woon CY, Kim M, Thorfinn J, Lindsey D, Pham H, Chang J (2011) Flexor Tendon Tissue Engineering: Acellularization of Human Flexor Tendons with Preservation of Biomechanical Properties and Biocompatibility. *Tissue Eng Part C Methods* **17**:819-828.
165. Pringle GA, Dodd CM (1990) Immunoelectron microscopic localization of the core protein of decorin near the d and e bands of tendon collagen fibrils by use of monoclonal antibodies. *J Histochem Cytochem* **38**:1405-1411.
166. Provenzano PP, Vanderby R, Jr. (2006) Collagen fibril morphology and organization: implications for force transmission in ligament and tendon. *Matrix Biol* **25**:71-84.
167. Pryce BA, Watson SS, Murchison ND, Staverosky JA, Dunker N, Schweitzer R (2009) Recruitment and maintenance of tendon progenitors by TGF signaling are essential for tendon formation. *Development* **136**:1351-1361.
168. Puxkandl R, Zizak I, Paris O, Keckes J, Tesch W, Bernstorff S, Purslow P, Fratzl P (2002) Viscoelastic properties of collagen: synchrotron radiation investigations and structural model. *Philosophical Transactions of the Royal Society B: Biological Sciences* **357**:191-197.
169. Qi J, Dmochowski JM, Banes AN, Tsuzaki M, Bynum D, Patterson M, Creighton A, Gomez S, Tech K et al. (2012) Differential expression and cellular localization of novel isoforms of the tendon biomarker tenomodulin. *J Appl Physiol (1985)* **113**:861-871.
170. Qin TW, Chen Q, Sun YL, Steinmann SP, Amadio PC, An KN, Zhao C (2012) Mechanical characteristics of native tendon slices for tissue engineering scaffold. *J Biomed Mater Res B Appl Biomater* **100**:752-758.
171. Ralphs JR, Waggett AD, Benjamin M (2002) Actin stress fibres and cell-cell adhesion molecules in tendons: organisation in vivo and response to mechanical loading of tendon cells in vitro. *Matrix Biol* **21**:67-74.
172. Redaelli A, Vesentini S, Soncini M, Vena P, Mantero S, Montevecchi FM (2003) Possible role of decorin glycosaminoglycans in fibril to fibril force transfer in relative mature tendons--a computational study from molecular to microstructural level. *J Biomech* **36**:1555-1569.
173. Riley GP, Curry V, DeGroot J, van El B, Verzijl N, Hazleman BL, Bank RA (2002) Matrix metalloproteinase activities and their relationship with collagen remodelling in tendon pathology. *Matrix Biol* **21**:185-195.
174. Rizzuto E, Catizone A, Musaro A, Del Prete Z (2012) Dystrophic tendon functionality is recovered by muscle-specific expression of insulin-like growth factor in mdx mice. *J Biomech* **46**:604-607.

175. Rumian AP, Wallace AL, Birch HL (2007) Tendons and ligaments are anatomically distinct but overlap in molecular and morphological features--a comparative study in an ovine model. *J Orthop Res* **25**:458-464.
176. Saber S, Zhang AY, Ki SH, Lindsey DP, Smith RL, Riboh J, Pham H, Chang J (2010) Flexor tendon tissue engineering: bioreactor cyclic strain increases construct strength. *Tissue Eng Part A* **16**:2085-2090.
177. Schalkwijk J, Zweers MC, Steijlen PM, Dean WB, Taylor G, van Vlijmen IM, van Haren B, Miller WL, Bristow J (2001) A recessive form of the Ehlers-Danlos syndrome caused by tenascin-X deficiency. *N Engl J Med* **345**:1167-1175.
178. Schonherr E, Witsch-Prehm P, Harrach B, Robenek H, Rauterberg J, Kresse H (1995) Interaction of biglycan with type I collagen. *J Biol Chem* **270**:2776-2783.
179. Schweitzer R, Chyung JH, Murtaugh LC, Brent AE, Rosen V, Olson EN, Lassar A, Tabin CJ (2001) Analysis of the tendon cell fate using Scleraxis, a specific marker for tendons and ligaments. *Development* **128**:3855-3866.
180. Scott A, Khan KM, Duronio V (2005) IGF-I activates PKB and prevents anoxic apoptosis in Achilles tendon cells. *J Orthop Res* **23**:1219-1225.
181. Scott JE (1996) Proteodermatan and proteokeratan sulfate (decorin, lumican/fibromodulin) proteins are horseshoe shaped. Implications for their interactions with collagen. *Biochemistry* **35**:8795-8799.
182. Shukunami C, Oshima Y, Hiraki Y (2001) Molecular cloning of tenomodulin, a novel chondromodulin-I related gene. *Biochem Biophys Res Commun* **280**:1323-1327.
183. Shukunami C, Takimoto A, Oro M, Hiraki Y (2006) Scleraxis positively regulates the expression of tenomodulin, a differentiation marker of tenocytes. *Dev Biol* **298**:234-247.
184. Siddappa R, Licht R, van Blitterswijk C, de Boer J (2007) Donor variation and loss of multipotency during in vitro expansion of human mesenchymal stem cells for bone tissue engineering. *J Orthop Res* **25**:1029-1041.
185. Silver D, Miller J, Harrison R, Prockop DJ (1992) Helical model of nucleation and propagation to account for the growth of type I collagen fibrils from symmetrical pointed tips: a special example of self-assembly of rod-like monomers. *Proc Natl Acad Sci U S A* **89**:9860-9864.
186. Silver FH, Freeman JW, DeVore D (2001) Viscoelastic properties of human skin and processed dermis. *Skin Res Technol* **7**:18-23.
187. Smith SM, Zhang G, Birk DE (2014) Collagen V localizes to pericellular sites during tendon collagen fibrillogenesis. *Matrix Biol* **33**:47-53.
188. Starborg T, Kalson NS, Lu Y, Mironov A, Cootes TF, Holmes DF, Kadler KE (2013) Using transmission electron microscopy and 3View to determine collagen fibril size and three-dimensional organization. *Nat Protoc* **8**:1433-1448.
189. Strocchi R, de Pasquale V, Gubellini P, Facchini A, Marcacci M, Buda R, Zaffagnini S, Ruggeri A (1992) The human anterior cruciate ligament: histological and ultrastructural observations. *J Anat* **180 (Pt 3)**:515-519.
190. Svensson L, Aszodi A, Reinholt FP, Fassler R, Heinegard D, Oldberg A (1999) Fibromodulin-null mice have abnormal collagen fibrils, tissue organization, and altered lumican deposition in tendon. *J Biol Chem* **274**:9636-9647.
191. Svensson RB, Hassenkam T, Hansen P, Kjaer M, Magnusson SP (2011) Tensile force transmission in human patellar tendon fascicles is not mediated by glycosaminoglycans. *Connect Tissue Res* **52**:415-421.
192. Svensson RB, Hassenkam T, Hansen P, Peter Magnusson S (2010) Viscoelastic behavior of discrete human collagen fibrils. *Journal of the Mechanical Behavior of Biomedical Materials* **3**:112-115.
193. Svensson RB, Mulder H, Kovanen V, Magnusson SP (2013) Fracture mechanics of collagen fibrils: influence of natural cross-links. *Biophys J* **104**:2476-2484.

194. Syedain ZH, Weinberg JS, Tranquillo RT (2008) Cyclic distension of fibrin-based tissue constructs: evidence of adaptation during growth of engineered connective tissue. *Proc Natl Acad Sci U S A* **105**:6537-6542.
195. Szczesny SE, Elliott DM (2014) Interfibrillar shear stress is the loading mechanism of collagen fibrils in tendon. *Acta Biomater* **10**:2582-2590.
196. Tang QO, Shakib K, Heliotis M, Tsiridis E, Mantalaris A, Ripamonti U, Tsiridis E (2009) TGF-beta3: A potential biological therapy for enhancing chondrogenesis. *Expert Opinion on Biological Therapy* **9**:689-701.
197. Tang SS, Trackman PC, Kagan HM (1983) Reaction of aortic lysyl oxidase with beta-aminopropionitrile. *J Biol Chem* **258**:4331-4338.
198. Thomopoulos S, Kim HM, Das R, Silva MJ, Sakiyama-Elbert S, Amiel D, Gelberman RH (2010) The effects of exogenous basic fibroblast growth factor on intrasynovial flexor tendon healing in a canine model. *J Bone Joint Surg Am* **92**:2285-2293.
199. Thorpe CT, Streeter I, Pinchbeck GL, Goodship AE, Clegg PD, Birch HL (2010) Aspartic Acid Racemization and Collagen Degradation Markers Reveal an Accumulation of Damage in Tendon Collagen That Is Enhanced with Aging. *Journal of Biological Chemistry* **285**:15674-15681.
200. Trackman PC, Bedell-Hogan D, Tang J, Kagan HM (1992) Post-translational glycosylation and proteolytic processing of a lysyl oxidase precursor. *J Biol Chem* **267**:8666-8671.
201. Uzel MI, Scott IC, Babakhanlou-Chase H, Palamakumbura AH, Pappano WN, Hong HH, Greenspan DS, Trackman PC (2001) Multiple bone morphogenetic protein 1-related mammalian metalloproteinases process pro-lysyl oxidase at the correct physiological site and control lysyl oxidase activation in mouse embryo fibroblast cultures. *J Biol Chem* **276**:22537-22543.
202. van der Valk J, Brunner D, De Smet K, Fex Svenningsen A, Honegger P, Knudsen LE, Lindl T, Noraberg J, Price A et al. (2010) Optimization of chemically defined cell culture media--replacing fetal bovine serum in mammalian in vitro methods. *Toxicol In Vitro* **24**:1053-1063.
203. Verrecchia F, Mauviel A (2007) Transforming growth factor-beta and fibrosis. *World J Gastroenterol* **13**:3056-3062.
204. Vicente-Manzanares M, Choi CK, Horwitz AR (2009) Integrins in cell migration--the actin connection. *J Cell Sci* **122**:199-206.
205. Vogel KG, Paulsson M, Heinegard D (1984) Specific inhibition of type I and type II collagen fibrillogenesis by the small proteoglycan of tendon. *Biochem J* **223**:587-597.
206. Voloshenyuk TG, Landesman ES, Khoutorova E, Hart AD, Gardner JD (2011) Induction of cardiac fibroblast lysyl oxidase by TGF-beta1 requires PI3K/Akt, Smad3, and MAPK signaling. *Cytokine* **55**:90-97.
207. Wall ME, Banes AJ (2005) Early responses to mechanical load in tendon: Role for calcium signaling, gap junctions and intercellular communication. *Journal of Musculoskeletal and Neuronal Interaction* **5**:70-84.
208. Wang JH (2006) Mechanobiology of tendon. *J Biomech* **39**:1563-1582.
209. Wang L, Uhlig PC, Eikenberry EF, Robenek H, Bruckner P, Hansen U (2014) Lateral growth limitation of corneal fibrils and their lamellar stacking depend on covalent collagen cross-linking by transglutaminase-2 and lysyl oxidases, respectively. *J Biol Chem* **289**:921-929.
210. Wang R, Brewster LP, Gleason RL, Jr. (2013) In-situ characterization of the uncrimping process of arterial collagen fibers using two-photon confocal microscopy and digital image correlation. *J Biomech* **46**:2726-2729.
211. Ward NP, Hulmes DJ, Chapman JA (1986) Collagen self-assembly in vitro: electron microscopy of initial aggregates formed during the lag phase. *J Mol Biol* **190**:107-112.
212. Wenstrup RJ, Florer JB, Brunskill EW, Bell SM, Chervoneva I, Birk DE (2004) Type V collagen controls the initiation of collagen fibril assembly. *J Biol Chem* **279**:53331-53337.

213. Wenstrup RJ, Florer JB, Cole WG, Willing MC, Birk DE (2004) Reduced type I collagen utilization: a pathogenic mechanism in COL5A1 haplo-insufficient Ehlers-Danlos syndrome. *J Cell Biochem* **92**:113-124.
214. Wenstrup RJ, Florer JB, Davidson JM, Phillips CL, Pfeiffer BJ, Menezes DW, Chervoneva I, Birk DE (2006) Murine model of the Ehlers-Danlos syndrome. col5a1 haploinsufficiency disrupts collagen fibril assembly at multiple stages. *J Biol Chem* **281**:12888-12895.
215. Wenstrup RJ, Smith SM, Florer JB, Zhang G, Beason DP, Seegmiller RE, Soslowsky LJ, Birk DE (2011) Regulation of collagen fibril nucleation and initial fibril assembly involves coordinate interactions with collagens V and XI In developing tendon. *J Biol Chem* **286**:20455-20465.
216. Winston BW, Krein PM, Mowat C, Huang Y (1999) Cytokine-induced macrophage differentiation: a tale of 2 genes. *Clin Invest Med* **22**:236-255.
217. Wren TA, Yerby SA, Beaupre GS, Carter DR (2001) Mechanical properties of the human achilles tendon. *Clin Biomech (Bristol, Avon)* **16**:245-251.
218. Xu T, Bianco P, Fisher LW, Longenecker G, Smith E, Goldstein S, Bonadio J, Boskey A, Heegaard AM et al. (1998) Targeted disruption of the biglycan gene leads to an osteoporosis-like phenotype in mice. *Nat Genet* **20**:78-82.
219. Yoon JH, Halper J (2005) Tendon proteoglycans: biochemistry and function. *J Musculoskelet Neuronal Interact* **5**:22-34.
220. Zhang G, Ezura Y, Chervoneva I, Robinson PS, Beason DP, Carine ET, Soslowsky LJ, Iozzo RV, Birk DE (2006) Decorin regulates assembly of collagen fibrils and acquisition of biomechanical properties during tendon development. *Journal of Cellular Biochemistry* **98**:1436-1449.
221. Zhang J, Wang J (2010) Characterization of differential properties of rabbit tendon stem cells and tenocytes. *BMC Musculoskeletal Disorders* **11**:10.
222. Zheng X, Baker H, Hancock WS, Fawaz F, McCaman M, Pungor E, Jr. (2006) Proteomic analysis for the assessment of different lots of fetal bovine serum as a raw material for cell culture. Part IV. Application of proteomics to the manufacture of biological drugs. *Biotechnol Prog* **22**:1294-1300.
223. Zhu J, Zhang X, Ma Y, Zhou C, Ao Y (2012) Ultrastructural and Morphological Characteristics of Human Anterior Cruciate Ligament and Hamstring Tendons. *Anat Rec (Hoboken)* **295**:1430-1436.

Manuscript I

In Vitro Tendon Tissue Development From Human Fibroblasts Demonstrates Collagen Fibril Diameter Growth Associated With a Rise in Mechanical Strength.

For supplementary videos please follow this link:
https://www.dropbox.com/sh/oy76udf1sc5rioy/AABJP9CZhsQ-Lyz3lWKfei9Ra?dl=0

DEVELOPMENTAL DYNAMICS 242:2–8, 2013

RESEARCH ARTICLE

In Vitro Tendon Tissue Development From Human Fibroblasts Demonstrates Collagen Fibril Diameter Growth Associated With a Rise in Mechanical Strength

Andreas Herchenhan,* Monika L. Bayer, René B. Svensson, S. Peter Magnusson, and Michael Kjær

Background: Collagen-rich tendons and ligaments are important for joint stability and force transmission, but the capacity to form new tendon is poorly understood. In the present study, we investigated mechanical strength, fibril size, and structure during development of tendon-like tissue from adult human tenocytes (termed tendon constructs) in vitro over 5 weeks in 3D tissue culture. Results: The constructs displayed large elongated tendon cells aligned along the tendon axis together with collagen fibrils that increased in diameter by 50% from day 14 to 35, which approaches that observed in adult human tendon in vivo. The increase in diameter was accompanied by a 5-fold increase in mechanical strength (0.9±0.1 MPa to 4.9±0.6 MPa) and Young's modulus (5.8±0.9 MPa to 32.3±4.2 MPa), while the maximal strain at failure (16%) remained constant throughout the 5-week culture period. Conclusions: The present study demonstrates that 3D tendon constructs can be formed by isolated human tendon fibroblasts, and when these constructs are subjected to static self-generated tension, the fibrils will grow in size and strength approaching that of adult human tendon in vivo. *Developmental Dynamics 242:2–8, 2013.* © 2012 Wiley Periodicals, Inc.

Key words: tendon construct; tendon engineering; TEM; fibrin; FIB/SEM

Key Findings:

- Tendon constructs from human adult tendon cells develop a similar ultrastructure to similarly aged human embryonic tendon.
- The collagen fibrils of adult human tendon cell derived constructs increase in diameter and packing density over 5 weeks.
- The construct increases its mechanical strength and stiffness significantly over 5 weeks.
- The tendon cells elongate similar to their natural configuration, however with considerably higher volume.

Accepted 15 October 2012

INTRODUCTION

Tensile, collagen-rich fibril structures, like tendon and ligaments, are important for force transmission to produce movement and joint stability in the body and thus it is important to understand the formation of collagen fibrils in human tissue both during normal development and regenerative conditions. The arrangement of collagen and tropocollagen in tendon has been well described (Birk and Brückner, 2011). It has been shown that embryonic and newly developed fibrils in animal models are uniform in

Additional supporting information may be found in the online version of this article.

Institute of Sports Medicine, Department of Orthopedic Surgery M, Bispebjerg Hospital and Center for Healthy Aging, Faculty of Health Sciences, University of Copenhagen, Copenhagen, Denmark

Grant sponsor: Nordea Foundation, Center for Healthy Aging; Grant sponsor: Department of Health Sciences, University of Copenhagen; Grant sponsor: Academy of Muscle Biology, Exercise and Health Research.

***Correspondence to: Andreas Herchenhan, Bispebjerg Hospital (M81), Bispebjerg Bakke 23, 2400 Copenhagen NV, Denmark. E-mail: andreashe@sund.ku.dk**

DOI 10.1002/dvdy.23896
Published online 26 October 2012 in Wiley Online Library (wileyonlinelibrary.com).

diameter and possess a relatively short length (Birk et al., 1997; Canty and Kadler, 2002). However, the exact mechanism of fibril maturation is still debated. It has been suggested that small collagen fibrils merge laterally and a re-arrangement of the structure results in cylindrical collagen fibrils with large diameters between 150 and 300 nm (Birk and Brückner, 2011). Others have suggested that collagen fibrils "grow" by the addition of new collagen molecules to the existing fibrils (Holmes et al., 2001, 2010). It is generally agreed upon that the mechanism results in thicker and longer collagen fibrils, which improve the mechanical stability of the tendon (Birk and Brückner, 2011).

Embryonic tissue harvesting has been used in animal models to investigate early fibril formation and development, but this approach is not applicable to a human model. Thus, in vitro approaches like tendon engineering using tenocytes embedded in a fibrin gel provide an alternative possibility (Kapacee et al., 2008). Such a system, using chick embryonic tenocytes, has demonstrated the capability to form tendon constructs, and after 10 days in static culture the constructs yield collagen fibrils arranged in a crimp pattern with mechanical properties similar to 14-day-old chick embryonic tendon (Kalson et al., 2010; Herchenhan et al., 2011). This approach has been extended to human tendon fibroblasts where the cells revealed the potential to produce a tendon like-structure in vitro with aligned collagen fibrils along the axis of tension (Bayer et al., 2010). However, it remains unknown to what extent these tendon constructs that possess structural similarities to intact tendons can develop into strong tendon-like structures (Bayer et al., 2010). The aim of the present study was to investigate the collagen fibril diameter, fibroblast configuration, and mechanical properties of an in vitro human tendon construct during 5 weeks of static tension.

RESULTS

Collagen Fibril Diameter

Ultrathin transverse sections of the tendon constructs were obtained after 14, 21, 28, and 35 days. Figure 1 shows representative electron micrographs from one cell line for each time point with focus on the extra-cellular space where collagen fibrils can be found. There seems to be an equal distribution of circular-shaped fibrils, which indicates that they are aligned longitudinally with the axis of tension, comparable to tendon in vivo. Figure 1A shows the tendon construct at 14 days with a limited number of narrow diameter fibrils. The number of fibrils increased up to approximately 28 days over time (Fig. 1C), and comparable packing to normal tendon density was observed at 35 days (Fig. 1D). An electron micrograph of adult human tendon for that comparison is shown in Figure 1E. In the normal human tendon, the individual fibroblast is tightly arranged in between the collagen fibrils, which have varying diameters to achieve an optimal packing density. Clearly, the collagen fibrils reach higher diameters in adult human tendon (Fig. 1E) compared to 35-day-old tendon constructs (Fig. 1D). Figure 1F presents the average mean fibril diameter for constructs derived from the 6 donor-cell lines at the different time points. The average collagen fibril diameter increased significantly from 37.9±1.9 nm at 14 days post-seeding to 42.7±2.7 nm at 21 days, 49.5±1.8 nm at 28 days, and finally to 59.7±3.9 nm at 35 days post-seeding ($P < 0.001$).

Mechanical Properties

The mechanical properties of the tendon constructs were tested after 14, 21, 28, and 35 days. The ultimate tensile strength at 14 days was 0.9±0.1 MPa. The strength increased significantly over time to 2.4±0.4 MPa at 21 days, 4.2±0.5 MPa at 28 days, and up to 4.9±0.6 MPa at 35 days post-seeding (Fig. 2A). The tensile strain did not show any significant difference over time, displaying a constant value of approximately 16% (Fig. 2B). The Young's modulus increased similar to the increase in strength over time. Shortly after formation at 14 days, the modulus was 5.8±0.9 MPa and it increased to 16.7±2.4 MPa at 21 days, further to 26.8±2.7 at 28 days, and reached 32.3±4.2 MPa at 35 days post-seeding (Fig. 2C). The result at 35 days was significantly higher than at 14 and 21 days, respectively ($P < 0.05$).

Cell Configuration

Cell morphology was investigated in the constructs and in native tendon. The outline of a cell (presumably fibroblast) from a hamstring tendon in a healthy human was elongated in its form with the cell tightly enclosed by a dense collagen network (Fig. 3A,C; see Supp. Video S1, which is available online). Only the outline of the cell is shown because of the dense surrounding collagen fibril network and limitations in image resolution that precluded getting acceptable recordings of the nucleus. The length of the cell is around 37 μm and the total volume was about 28.5 μm^3. The 3D reconstruction in Figure 3B and D (and Supp. Video S2, respectively) shows an example of a cell (presumably fibroblast) in a tendon construct that is 35 days old. The cell is elongated and arranged along the longitudinal axis of the construct structure. From the pictures, it is clear that the cell is more than 60 μm long with a diameter of around 8 μm near the nucleus, and it can be calculated from the obtained data that the total cell volume is around 700 μm^3.

DISCUSSION

The present study confirmed that 3D tendon constructs can be formed by using isolated human tendon fibroblasts: When constructs are subjected to static tension, collagen fibrils are formed that align along the axis of tension. A new finding in this study was that these fibrils grow in diameter over a 5-week period (Fig. 1) up to a size approaching that typically seen, at the lower end, in adult human tendon in vivo. Importantly, these observations were associated with increased ultimate tensile strength of the construct over time. The ultimate tensile stress of the construct rose 5-fold from week 2 to week 5 (Fig. 2A), while the failure strain remained around 16% throughout the experiment (Fig. 2B). Finally, tendon stiffness expressed as Young's modulus increased markedly throughout the 5-week period of static tensile

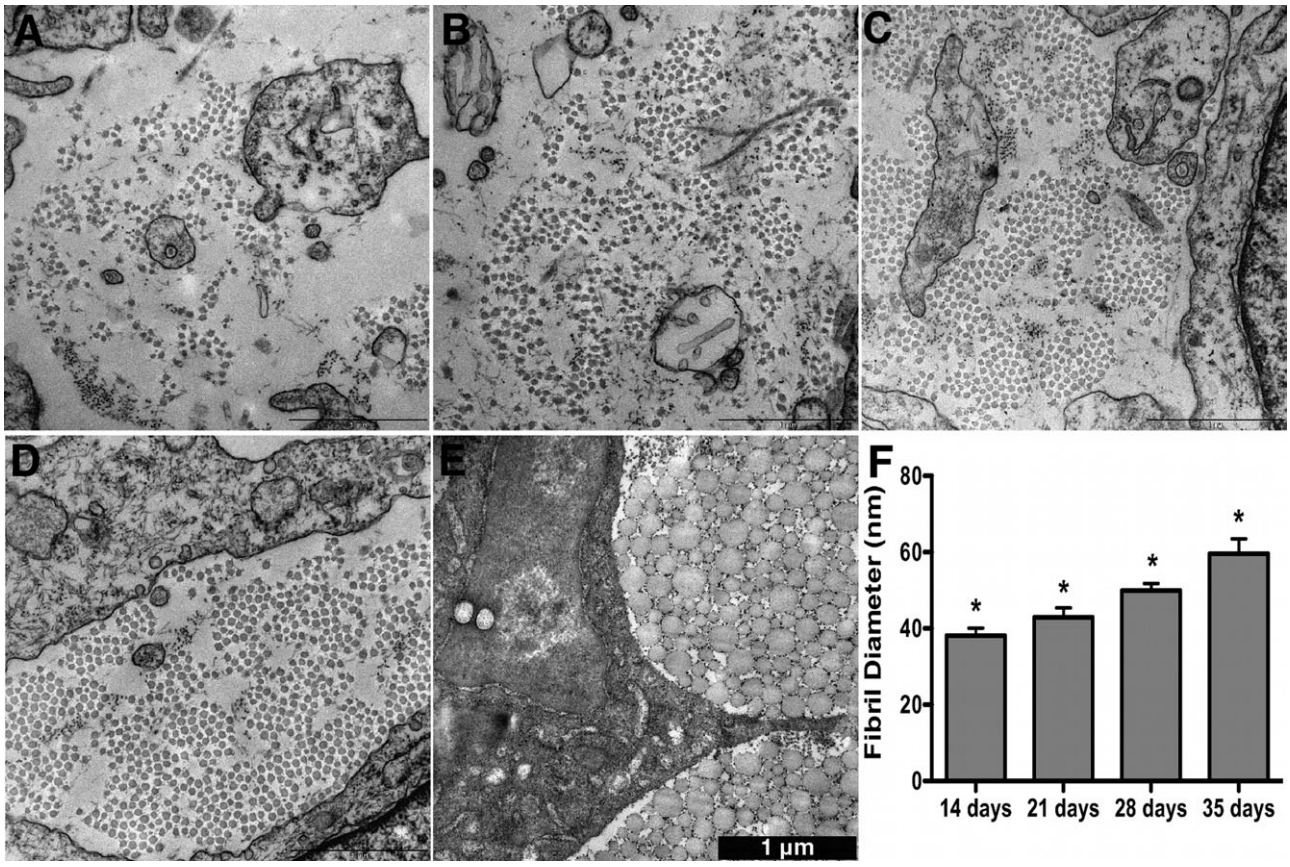

Fig. 1. Electron micrographs from human tenocyte-derived tendon constructs at 14 (**A**), 21 (**B**), 28 (**C**), and 35 (**D**) days post-seeding. An increase in collagen diameter and packing density can be seen over time. As comparison, an electron micrograph of adult human tendon (**E**) shows the densely packed collagen fibrils with their typical bimodal diameter distribution. The cell is fitted tightly in between the ECM. A–E: 46,000-fold magnification. Scale bar = 1 μm. **F**: Quantitative assessment of mean collagen fibril diameters in the tendon construct at 14, 21, 28, and 35 days post-seeding. The mean diameter increases significantly ($P < 0.001$) from 37.9±1.9 nm (mean±SEM) at 14 days in a linear manner to 59.7±3.9 nm after 35 days. Five hundred fibrils were measured per time point and each of the six cell donors. *$P < 0.001$ compared to the other time points.

tension on the tendon construct made from adult human tendon fibroblasts in 3D cell culture.

Interestingly, human tendon develops in this model by an increase in individual collagen fibril diameter in the early weeks of construct development. Moreover, the individual fibril can already after 5 weeks reach a diameter (average around 60 nm, max values of over 90 nm) similar to that in the low end of adult human tendon (Magnusson et al., 2002; Kongsgaard et al., 2010). In the present study, the range of fibril diameters was relatively small and indicate a unimodal distribution, while human adult tendons have a smaller number of large fibrils (>100 nm) that are often surrounded by larger amounts of small-diameter fibrils (40–100 nm) (Magnusson et al., 2002; Kongsgaard et al., 2010). The diameter of collagen fibrils varies among different tissue types and develops in load-bearing structures, such as tendon, from a unimodal distribution during the fetal stage to a bimodal distribution at maturity (Parry et al., 1978). On this basis, the present findings indicate that the tendon constructs are similar to that of developing tendon.

Moreover, Strocchi et al. (1992) have shown that the collagen fibril diameter in the anterior cruciate ligament is somewhat smaller than that in tendons, ranging from 20 to 90 nm. Fibril bundles run in several directions and the mean diameter can be unimodal at 45 nm, or multimodal with peaks at 35, 50, and 75 nm (Strocchi et al., 1992). These values are comparable to the values obtained of the tendon construct in the present study. Further, data on constructs derived from chick embryonic tenocytes showed a mean collagen fibril diameter of approximately 30 nm at formation and up to 40 nm after 4 days of mechanical stretching (Kalson et al., 2011).

Interestingly, tendon-like constructs derived from chick embryonic tendon cells reached 2 MPa in mechanical strength and a Young's modulus of 13 MPa after 10 days, but did not improve further with time (Kalson et al., 2010). Another study using a similar system with chick embryonic tenocytes showed a Young's modulus of 5.5 MPa 14 days after seeding when treated with additional Transforming Growth Factor-β (Paxton et al., 2010). In comparison to these values, the human tendon construct in the present study reached a 2.5-fold higher ultimate tensile stress and a 6-fold higher Young's modulus after 5 weeks under static tension.

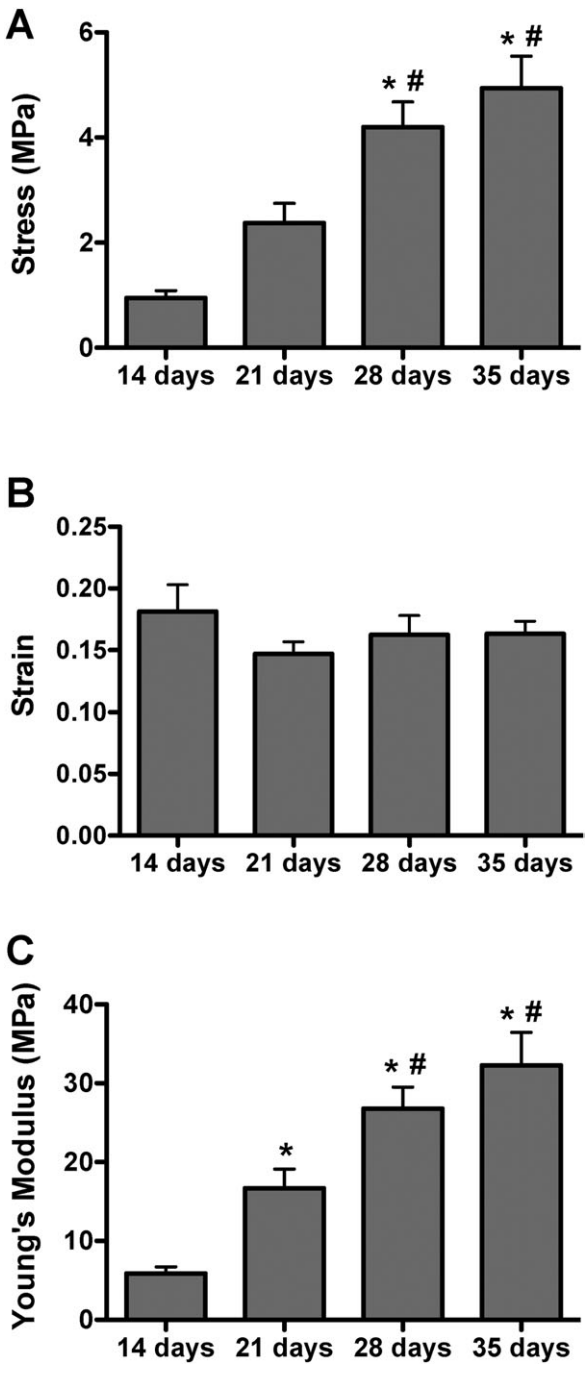

Fig. 2. Mechanical data at failure of the human tendon construct over time. **A**: Mechanical stress increases significantly from 14 days to after 28 days in static culture. Between 28 and 35 days, no statistical significance could be detected. **B**: Failure strain of the constructs remains constant at approximately 16% over 35 days. **C**: The Young's Modulus develops significantly from 14 days to 28 days. A further increase from 28 to 35 days is visible, but could not be statistically detected. Triplicates per cell donor and time point, respectively, were measured. *$P < 0.05$ compared to day 14; #$P < 0.05$ compared to day 21.

Furthermore, the human tendon construct did not cease to develop or deteriorate as described in the chick tendon construct after 10 days (Kalson et al., 2010). We observed the development of the human tendon constructs until 35 days after seeding, and the tenocytes increased the collagen fibril diameter and thereby modified the mechanical integrity of the system over the entire time range. This proposes a higher capacity of human tenocytes over chick embryonic tenocytes to form new tendon tissue in vivo.

In the present study, the constructs were under a cell-generated static strain, but the magnitude of this could not be quantified. In another study using constructs from chick embryo, the application of a constant strain resulted in increased collagen type I expression, a faster increase of collagen fibril diameter and collagen volume fraction, and ultimately increased mechanical properties of the construct (Kalson et al., 2011). It is thus likely that the mechanical stretching acted as a stimulus upon fibril growth in the present study. Furthermore, variations within the strain paradigm can of course also be considered in future studies, such as short cyclical loading with diverse strain rates and amplitudes (Paxton et al., 2011).

Chaplin and Greenlee (1975) conducted a microscopy study on human embryonic digital tendon aged 40 to 112 weeks where they compared light and electron micrographs (Chaplin and Greenlee, 1975). They could show that human embryonic tendons start developing as highly cellular structures with very few and small-diameter collagen fibrils. After 6 weeks, collagen fibrils have developed in close proximity to the cells. It is interesting that an identical development could be observed within the human tendon construct in this study at 14 days after seeding. At 95 days of embryonic development, most of the extracellular space is filled with longitudinally aligned collagen fibrils of small unimodal diameter, as described by Chaplin and Greenlee (1975). Yet the cell volume fraction was still relatively high and the collagen packing density remained loose (Chaplin and Greenlee, 1975). Comparing these electron micrographs with our human tendon construct 35 days post-seeding reveals a strong similarity between the structures. The longer time period within the embryonic tendon for this development can be explained by the fact that the cells still need to differentiate, whereas in the tendon construct the cells are derived from adults and therefore ready to produce new ECM (Chaplin and Greenlee, 1975).

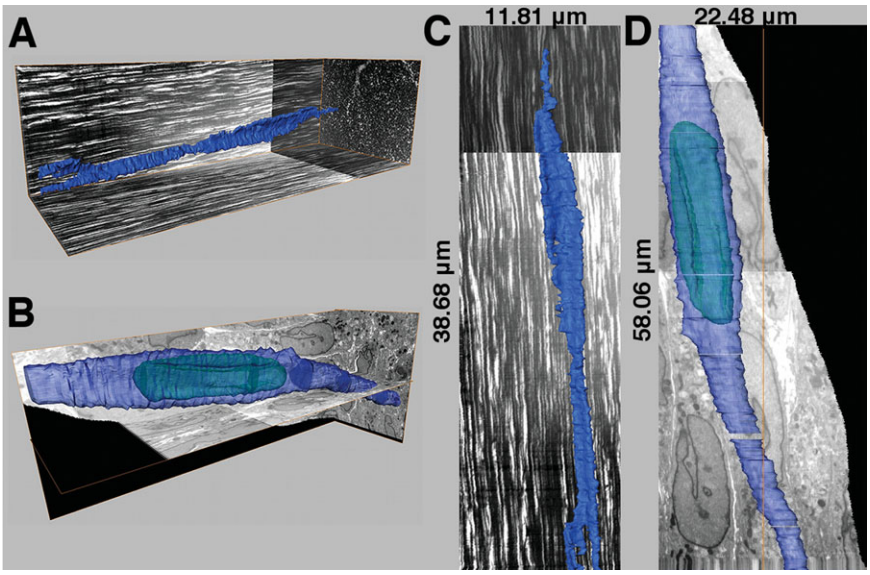

Fig. 3. Three-dimensional reconstructions of single cells within human adult tendon (**A**) and 35-day-old human tendon construct (**B**). The cell in adult tendon is highly elongated and tightly enclosed by a dense collagen network, which can be seen in the surrounding images. In the tendon construct (**B**), the cell is larger but still elongated and arranged along the longitudinal axis of the structure. **C, D**: Measurements provided to show that the cell within the tendon construct is significantly larger than in adult human tendon. Compare Supp. Videos S1 and S2.

Since the tendon constructs can be considered similar to human embryonic tendon, it is not surprising that their mechanical properties were significantly lower compared to adult human tendon. Embryonic tendon has a low collagen fibril volume fraction that makes up most of the mechanical integrity. In contrast, adult human tendon has a densely packed collagen fibril network throughout the entire structure that reaches optimal mechanical strength over its cross-sectional area (Kastelic et al., 1978). Couppé et al. (2009) measured the mechanical properties of human patellar tendon in young and old men, in vivo, and showed a tendon strength exceeding 51±8 and 65±24 MPa, respectively, during maximal isometric knee activation. This is approximately 10-fold higher than the values obtained in the strongest tendon constructs within this study. So despite the fact that tendon construct fibrils reached close to physiological levels of fibril diameter, the stress that the construct can tolerate is still by far lower than in vivo human tendon. Significant differences in the collagen content and collagen fibril length are presumably key factors to explain this discrepancy.

The strain in the tendon constructs is around 16% and, therefore, approximately 3-fold higher than what is seen during maximal muscle loading of the human patella tendon in vivo with values around 6–7 (Couppé et al., 2009). With regards to the Achilles tendon, strain levels of around 6% were reached in humans in vivo during maximal calf muscle contraction (Magnusson et al., 2001). Naturally in the human in vivo models, ultimate breaking stress was not determined, so most likely the strain at maximal muscle contraction displays values several percent lower than the ultimate tensile strain. Absolute mechanical properties of human ligaments were estimated by Woo et al. who found an ultimate tensile strength of 72 MPa, tensile strain of 9%, and a Young's modulus of approximately 1 GPa (Woo et al., 1999). Still, the strain range of the construct is not markedly higher than values realistic for physiological breakage of tendons. A study conducted on young and old cadaveric human patellar tendon showed failure strain values of approximately 15% and another study showed failure strain levels in different human patellar tendon regions between 10 and 20% (Johnson et al., 1994; Chun and Butler, 2006). Furthermore, Haraldsson and colleagues reported strain values for individual human patellar tendon collagen fascicles of approximately 13%, which is also close to the results in the present study (Haraldsson et al., 2005).

Cells within adult human tendon are elongated with very small diameters to fit optimally in between the densely packed collagen fibril network. We utilized three-dimensional electron microscopy to visualize single cells from adult human tendon and from the tendon construct and found that within 5 weeks the cells in constructs are elongated and aligned in the direction of tension, but display a very large volume. Earlier studies showed that cells in the chick construct reached an average length of approximately 50 µm under static culturing conditions and more than 100 µm in stretched constructs (Kalson et al., 2011), which is within the same order of magnitude as the cells within the human tendon construct.

The in vitro tendon constructs developed considerably within this short time range and displayed collagen fibrils that reached diameters that were within the physiological range of human ligaments and tendons. The main difference to functional tendon is the very low collagen content combined with a high cellular fraction, which leads to inferior mechanical properties. However, the structural characteristics of the constructs are similar to developing embryonic human tendons.

EXPERIMENTAL PROCEDURES

Cell Culture

Tendon fibroblasts were isolated from human semitendinosis and gracilis tendon as previously described in detail (Bayer et al., 2010). Briefly, 6 patients (18–32 years old) undergoing reconstructive surgery after anterior cruciate ligament (ACL) rupture gave their informed consent to donate excess tendon tissue. Tissue was transported to a cell culture laboratory immediately following harvest, and a small portion of each sample was immediately fixed in 2% Glutaraldehyde for EM analysis. Under aseptic conditions, the tissue was

minced in pieces of ~2 mm^3 and digested overnight in DMEM/F12 (Gibco, Gaithersburg, MD; Invitrogen, Carlsbad, CA) supplemented with 0.1% collagenase type II (Worthington, Lakewood, NJ) and 20% fetal bovine serum (FBS) (Gibco, Invitrogen). Following repeated washes in culture medium (DMEM/F12, 10% FBS), cells were seeded into flasks and cultured until the next passage. Cells in the 3rd to 6th passage were used for experiments. The present experiment was approved by the local ethical committee (ref. H-3-2010-070).

Tendon Construct Formation

Tendon constructs from human tenocytes were assembled as described previously with minor modifications (Bayer et al., 2010). Briefly, each well of a six-well plate was coated with ~1.5 ml SYLGARD (Dow-Chemicals, Midland, MI) and allowed to set at 55°C for 48 hr. Next, two short silk sutures (0.5 cm, Ethicon) were pinned onto the coated plates with minutien insect pins (0.1-mm diameter) (Fine Science Tools GmbH, Foster City, CA) with a distance of 1.5 cm in between sutures. The plates were sterilized by immersion in 70% ethanol for 45 min. Human tendon fibroblasts were suspended in culture medium containing 4 mg human fibrinogen and 1 U of human thrombin (Sigma Aldrich, St. Louis, MO) to a final concentration of 2.5×10^5 per 800 μl and rapidly spread over the complete surface of the coated wells. The cell-embedded fibrin gel was allowed to set for 30 min at 37°C, and cultured until the matrix was fully contracted between the anchor points. Every other day, culture medium supplemented with 0.2 mM L-ascorbic acid 2-phosphate and 0.05 mM L-Proline (Sigma Aldrich) was replaced and adhesions to the side of the well were detached using a fine pipette tip to allow gel contraction. All constructs in this study formed a continuous tendon-like tissue between the anchor points after 10–12 days and were analysed at 14, 21, 28, and 35 days post-seeding.

Mechanical Testing

Tensile testing of the tendon constructs at the different time points was performed in a PC-driven micromechanical rig with liquid chamber (20 N loadcell, sampling rate 10 Hz; Deben, Suffolk, UK). A stereoscopic microscope (SMZ1000, Nikon, Tokyo, Japan) with C-mount lens (×8), equipped with a 15-Hz digital camera (DFWX700, Sony, Tokyo, Japan; 640×480 Pixel) was used for imaging during the test to verify clamping length and monitor the rupture site of the construct.

The tendon constructs were glued on specimen plates with a mounting distance of 10 mm, so that only the mid-portion of the constructs was investigated. The glue was left to dry for 15 min while the mid-portion was wrapped in PBS-soaked gauze. Subsequently, the specimen was transferred to a PBS-bath and after a short adaptation period, the test was started. The samples were stretched at 2 mm/min until the onset of force. After a short relaxation period, the constructs were further stretched until failure. The resulting force-elongation curves were low-pass filtered by a moving average.

The data analysis was based on the assumption that the construct had a circular cross-section. Construct diameters and mounting length were measured at the onset of force. For ultimate tensile stress calculation, the minimal diameter was used and the strain was determined from the onset of force until failure. Young's modulus was calculated based on stress and strain from the onset of force up to the point of failure.

Transmission Electron Microscopy

After discarding culture medium and rinsing in PBS, constructs were fixed in 2% Glutaraldehyde in 0.05 M phosphate buffer for 30 min at RT. The constructs were then cut in three equal pieces and fixed in fresh fixative for at least 2 hr at 4°C. After washing in 0.15 M phosphate buffer, the samples were post-fixed with 1% OsO_4 in 0.12 M Sodium Cacodylate buffer for 2 hr at RT. Following another washing in dH_2O, the samples were stained en bloc with 1% aqueous uranyl for 16 hr at 4°C, dehydrated in a graded serious of ethanol, and embedded in Epon (Hexicon, Houston, TX).

Ultrathin cross-sections were cut with a Reichert-Jung Ultracut E microtome using a diamond knife and were collected on one-hole copper grids with Formvar supporting membranes. Images were acquired in a Philips TM 100 transmission electron microscope, operated at an accelerating voltage of 80 kV, with a Megaview 2 camera, and processed with the iTEM AnalySIS software package (ResAlta Research Technologies, Golden, CO). The NIH-based image-processing program, Image J, was used for measurement of collagen fibril diameter. On randomly selected micrographs, 250 fibrils were analysed per specimen, cell line, and time point, respectively.

Focussed Ion Beam/ Scanning Electron Microscopy (FIB/ SEM)

FIB/SEM was used to qualitatively assess the configuration of the cells within the tendon construct system compared to their original cell configuration in adult human tendon. Specimens were fixed as described above and post-fixed in a solution of 1% OsO_4, 1.5% $K_4[Fe_6]$ in 0.12 M sodium cacodylate buffer for 1 hr. After extensive washing in water, the samples were treated with 1% tannic acid in 0.12 M sodium cacodylate buffer for 1 hr, washed and post-fixed in 1% OsO_4 in 0.12 M sodium cacodylate buffer. After extensive washing in water, the samples were counterstained in 1% aqueous uranyl for 16 hr at 4°C. Following dehydration in a series of graded ethanol, the samples were embedded in Epon according to standard procedures.

Ultrathin sections of the samples were observed in TEM to confirm the quality of the sample. Subsequently, the blocks were cleaned in absolute ethanol, mounted on aluminium stubs using carbon cement, and gold coated.

Specimens were investigated using a Quanta FEG 3D dual beam Focussed Ion Beam/Scanning Electron Microscope (FEI, Eindhoven, The Netherlands). Imaging was accomplished at an accelerating voltage of 5 kV, and further adjustments were made according to standard procedures (Bushby et al., 2011). Due to

the dimensions of the field of view, the samples could be tracked for no longer than 60 μm with a section thickness of 30 nm.

Statistical Analysis

Results are presented as mean±SEM. All data were analysed using a one-way analysis of variance with Bonferroni corrected post-hoc *t*-tests. The level of significance was set at $P < 0.05$.

ACKNOWLEDGMENTS

The authors gratefully acknowledge the help with tissue acquisition from the Department of Orthopaedic Surgery at Bispebjerg Hospital. The Core Facility for Integrated Microscopy at the University of Copenhagen is thankfully acknowledged for support and access to electron microscopes. Funding is gratefully acknowledged from the Nordea Foundation (Healthy Aging grant), the University of Copenhagen, Department of Health Sciences, and the Academy of Muscle Biology, Exercise and Health Research.

REFERENCES

Bayer ML, Yeung C-YC, Kadler KE, Qvortrup K, Baar K, Svensson RB, Peter Magnusson S, Krogsgaard M, Koch M, Kjaer M. 2010. The initiation of embryonic-like collagen fibrillogenesis by adult human tendon fibroblasts when cultured under tension. Biomater 31: 4889–4897.

Birk DE, Brückner P. 2011. Collagens, suprastructures, and collagen fibril assembly. In: Mecham RP, editor. The extracellular matrix: an overview. Berlin Heidelberg: Springer-Verlag. p 77–115.

Birk DE, Zycband EI, Woodruff S, Winkelmann DA, Trelstad RL. 1997. Collagen fibrillogenesis in situ: fibril segments become long fibrils as the developing tendon matures. Dev Dyn 208:291–298.

Bushby AJ, P'Ng K M, Young RD, Pinali C, Knupp C, Quantock AJ. 2011. Imaging three-dimensional tissue architectures by focused ion beam scanning electron microscopy. Nat Protoc 6: 845–858.

Canty EG, Kadler KE. 2002. Collagen fibril biosynthesis in tendon: a review and recent insights. Comp Biochem Physiol A Mol Integr Physiol 133: 979–985.

Chaplin DM, Greenlee TK Jr. 1975. The development of human digital tendons. J Anat 120:253–274.

Chun KJ, Butler DL. 2006. Spatial variation in material properties in fasciclebone units from human patellar tendon. Key Eng Mater 326–328:797–802.

Couppé C, Hansen P, Kongsgaard M, Kovanen V, Suetta C, Aagaard P, Kjær M, Magnusson SP. 2009. Mechanical properties and collagen cross-linking of the patellar tendon in old and young men. J Appl Physiol 107:880–886.

Haraldsson BT, Aagaard P, Krogsgaard M, Alkjaer T, Kjaer M, Magnusson SP. 2005. Region-specific mechanical properties of the human patella tendon. J Appl Physiol 98:1006–1012.

Herchenhan A, Kalson NS, Holmes DF, Hill P, Kadler KE, Margetts L. 2011. Tenocyte contraction induces crimp formation in tendon-like tissue. Biomech Model Mechanobiol 11:449–459.

Holmes DF, Graham HK, Trotter JA, Kadler KE. 2001. STEM/TEM studies of collagen fibril assembly. Micron 32: 273–285.

Holmes DF, Tait A, Hodson NW, Sherratt MJ, Kadler KE. 2010. Growth of collagen fibril seeds from embryonic tendon: fractured fibril ends nucleate new tip growth. J Mol Biol 399:9–16.

Johnson GA, Tramaglini DM, Levine RE, Ohno K, Choi NY, Woo SL. 1994. Tensile and viscoelastic properties of human patellar tendon. J Orthop Res 12:796–803.

Kalson NS, Holmes DF, Kapacee Z, Otermin I, Lu Y, Ennos RA, Canty-Laird EG, Kadler KE. 2010. An experimental model for studying the biomechanics of embryonic tendon: Evidence that the development of mechanical properties depends on the actinomyosin machinery. Matrix Biol 29:678–689.

Kalson NS, Holmes DF, Herchenhan A, Lu Y, Starborg T, Kadler KE. 2011. Slow stretching that mimics embryonic growth rate stimulates structural and mechanical development of tendon-like tissue in vitro. Dev Dyn 240:2520–2528.

Kapacee Z, Richardson S, Lu Y, Starborg T, Holmes D, Baar K, Kadler K. 2008. Tension is required for fibripositor formation. Matrix Biol 27:371–375.

Kastelic J, Galeski A, Baer E. 1978. The multicomposite structure of tendon. Connect Tissue Res 6:11–23.

Kongsgaard M, Qvortrup K, Larsen J, Aagaard P, Doessing S, Hansen P, Kjaer M, Magnusson SP. 2010. Fibril morphology and tendon mechanical properties in patellar tendinopathy: effects of heavy slow resistance training. Am J Sports Med 38:749–756.

Magnusson SP, Aagaard P, Dyhre-Poulsen P, Kjaer M. 2001. Load-displacement properties of the human triceps surae aponeurosis in vivo. J Physiol 531: 277–288.

Magnusson SP, Qvortrup K, Larsen JO, Rosager S, Hanson P, Aagaard P, Krogsgaard M, Kjaer M. 2002. Collagen fibril size and crimp morphology in ruptured and intact Achilles tendons. Matrix Biol 21:369–377.

Parry DA, Barnes GR, Craig AS. 1978. A comparison of the size distribution of collagen fibrils in connective tissues as a function of age and a possible relation between fibril size distribution and mechanical properties. Proc R Soc Lond B Biol Sci 203:305–321.

Paxton JZ, Grover LM, Baar K. 2010. Engineering an in VitroModel of a Functional Ligament from Bone to Bone. Tissue Eng Part A 16:3515–3525.

Paxton JZ, Hagerty P, Andrick JJ, Baar K. 2011. Optimizing an intermittent stretch paradigm using ERK1/2 phosphorylation results in increased collagen synthesis in engineered ligaments. Tissue Eng Part A 18:277–284.

Strocchi R, de Pasquale V, Gubellini P, Facchini A, Marcacci M, Buda R, Zaffagnini S, Ruggeri A. 1992. The human anterior cruciate ligament: histological and ultrastructural observations. J Anat 180:515–519.

Woo SL, Debski RE, Withrow JD, Janaushek MA. 1999. Biomechanics of knee ligaments. Am J Sports Med 27: 533–543.

Manuscript II

Insulin-like growth factor I enhances collagen synthesis in engineered human tendon tissue.

Growth Hormone & IGF Research xxx (2014) xxx–xxx

Contents lists available at ScienceDirect

Growth Hormone & IGF Research

journal homepage: www.elsevier.com/locate/ghir

Insulin-like growth factor I enhances collagen synthesis in engineered human tendon tissue

Andreas Herchenhan *, Monika L. Bayer, Pernilla Eliasson, S. Peter Magnusson, Michael Kjaer

Institute of Sports Medicine Copenhagen, Bispebjerg Hospital, Bispebjerg Bakke 23, Building 8, 2nd floor, 2400 Copenhagen, Denmark
Centre for Healthy Aging, Faculty of Health and Medical Sciences, University of Copenhagen, Denmark

ARTICLE INFO

Article history:
Received 9 May 2014
Received in revised form 6 August 2014
Accepted 11 September 2014
Available online xxxx

Keywords:
Tendon formation
Fetal bovine serum
Fibrillogenesis
Tenomodulin
Scleraxis
Collagen content
3D cell culture

ABSTRACT

Objective: Isolated human tendon cells form 3D tendon constructs that demonstrate collagen fibrillogenesis and feature structural similarities to tendon when cultured under tensile load. The exact role of circulating growth factors for collagen formation in tendon is sparsely examined. We investigated the influence of insulin-like growth factor I (IGF-I) on tendon construct formation in 3D cell culture.
Design: Tendon constructs were grown in 0.5 or 10% FBS with or without IGF-I (250 mg/ml) supplementation. Collagen content (fluorometric), mRNA levels (PCR) and fibril diameter (transmission electron microscopy) were determined at 7, 10, 14, 21 and 28 days.
Results: IGF-I revealed a stimulating effect on fibril diameter (up to day 21), mRNA for collagen (to day 28), tenomodulin (to day 28) and scleraxis (at days 10 and 14), and on overall collagen content. 10% FBS diminished the development of fibril diameter (day 14), collagen content (at days 21 and 28) and mRNA expression for collagen, tenomodulin and scleraxis.
Conclusion: IGF-I supplementation promotes early onset of tensile load induced collagen formation and tendon structural arrangement, whereas the FBS concentration routinely used in cultures diminishes collagen expression, collagen content and fibril formation.

1. Introduction

The connective tissue of tendon is responsible for efficient force transmission between muscle and bone and has therefore exceptional mechanical properties. Tendon is structurally arranged in a highly hierarchical manner ranging from single collagen molecules to the entire tendon unit [1]. Collagen is the most abundant protein in tendon, and it provides the basis for the structural and mechanical integrity of the tissue. Collagen development and structural organization are crucial processes during embryogenesis and are essential given the relatively low turnover of tendon collagen tissue in adult life [2].

The *in vivo* environment of cells is a three-dimensional (3D) extracellular matrix (ECM); however, most *in vitro* studies to date utilize cells in 2D monolayers [3,4]. More recently, 3D cell culture approaches have shown considerable advantages over 2D cell monolayers. Fibroblast adhesion to substrate was shown in 3D to be improved six-fold over 2D; cell migration is significantly increased and 3D-specific cell adhesions are established [5]. The 3D cell shape and the available space can even decide upon cell fate, while cells in 2D are limited to a flat arrangement [6].

Fibrin gels are suggested to serve as a biocompatible, stable and bioactive microenvironment for successful 3D cell culture [7,8]. We recently introduced a 3D tendon construct system from adult human tendon fibroblasts [9,10]. Driven by their actin-myosin machinery, the fibroblasts contract a fibrin gel, which is constrained by two opposed anchor points, leading to a rod-shaped structure [11]. The cells are thereby aligned along the longitudinal axis, similar to their in vivo state [10,11]. Embryonic-like cell protrusions—earlier termed fibripositors—are established as a link between the cells and the collagen network, and the construct shows has viscoelastic mechanical properties under tensile testing [9,11]. Finally, the tendon constructs develop larger collagen fibrils with increasing diameter during 5 weeks that result in increasing resistance toward tensile mechanical forces [10]. Taken together, these characteristics prove that the tendon construct is a valid model for studying tendon development. Further studies have shown that the system is sensitive to stretching stimuli, which leads to increased collagen expression and fibril diameter [12,13].

The mean collagen fibril diameter and the diameter distribution are characteristics that vary considerably between tissues depending on their function. Ligaments such as the anterior cruciate ligament have a narrow spectrum with rather low diameter fibrils (up to 100 nm), while load-bearing tendons like the hamstring tendon show a broad

* Corresponding author at: Institute of Sports Medicine Copenhagen, Bispebjerg Hospital, Bispebjerg Hospital, Bispebjerg Bakke 23, Building 8, 2nd floor, 2400 Copenhagen, Denmark. Tel.: +45 3531 6091.
E-mail address: andreashe@sund.ku.dk (A. Herchenhan).

http://dx.doi.org/10.1016/j.ghir.2014.09.001
1096-6374/

spectrum with diameters reaching over 200 nm [14]. Adult tendon typically show a bimodal collagen fibril diameter distribution with one peak at low diameters of approximately 40 nm and a second peak around 140 nm [15,16].

Tendon cells experience continuous mechanical strain that has been proven to be vital for tendon development [12,17–20]. In addition, growth-stimulating signals can be elicited by local accumulation of growth factors such as Insulin-like Growth Factor-I (IGF-I) [3,4,21]. It has been demonstrated *in vivo* that local injection of IGF-I into the patellar tendon of humans yields an upregulation of matrix related genes such as collagen type I [22,23]. IGF-I has been shown to increase cell proliferation [4] and to promote matrix formation [3]. Furthermore, IGF-I inhibits cell death in isolated tendon cells by activating the protein kinase B signaling pathway [24]. Although these *in vitro* approaches using isolated tendon cells in 2D cultures have provided major insight into our understanding of tendon growth and development, it may not entirely represent the physiological responses *in vivo*. We aimed to study the effect of IGF-I on collagen development in the 3D tendon construct system *in vitro*, in which the cells are arranged more similar to their *in vivo* configuration [9,10,12,17,25].

In addition to growth factors, other substances in the cell culture medium used for the development of a tendon construct may affect the outcome. Fetal bovine serum (FBS) is routinely used for cell culture systems since it provides vital components for cells in culture, including growth factors, proteins, vitamins and hormones [26]. However, the detailed composition of FBS is difficult to determine and varies between different batches [27,28]. Surprisingly little attention has been given to the potential effect of the FBS concentration upon cell reactions in culture systems, and the fact that growth factor concentrations vary depending on the donor animal [29].

The aim of this study was to investigate the effect of IGF-I and FBS concentration upon tenocytes in a 3D cell culture. A very low level of FBS supplementation was chosen in order to pinpoint the effect of IGF-I on tendon constructs and collagen fibrillogenesis in absence of interacting factors that FBS contains. Therefore, tendon constructs were treated either with a standard dose of 10% FBS or a very low dose of 0.5%, with or without 250 ng/ml IGF-I. Construct development was monitored up to 4 weeks after seeding by means of construct ultrastructure, collagen fibril diameter, total collagen content and gene expression.

2. Materials and methods

2.1. Cell culture

Tendon fibroblasts were isolated from human semitendinosus and gracilis tendon as previously described in detail [9]. Briefly, patients (18–32 years old) undergoing reconstructive surgery after anterior cruciate ligament (ACL) rupture gave their informed consent to donate excess tendon tissue. The tissue was transported to a cell culture laboratory immediately following harvest. Under aseptic conditions, the tissue was minced into pieces ~2 mm^3 and digested overnight in DMEM/F12 (Gibco, Invitrogen) supplemented with 0.1% collagenase type II (Worthington) and 20% fetal bovine serum (FBS) (Gibco, Invitrogen). Following repeated washes in culture medium (DMEM/F12, 10% FBS), the cells were seeded into flasks and cultured until the next passage. Cells from at least five different donors in the 2nd to 6th passage were used for experiments. The present experiment was approved by the local ethical committee (ref. H-3-2010-070).

2.2. Tendon construct formation

Tendon constructs from human tenocytes were assembled as described previously with minor modifications [9]. Briefly, each well of a six-well plate was coated with ~1.5 ml SYLGARD (Dow-Chemicals) and allowed to set at 55 °C for 48 h. Next, two short silk sutures (0.5 cm, Ethicon) were pinned onto the coated plates with minutien insect pins (0.1 mm diameter) (Fine Science Tools GmbH) with a distance of 1.5 cm in between sutures. The plates were sterilized by immersion in 70% ethanol for 45 min. Human tendon fibroblasts were suspended in culture medium containing 4 mg human fibrinogen, 10 μg/ml aprotenin and 1 unit of human thrombin (all Sigma Aldrich) to a final concentration of 2.5×10^5 per 800 μl and rapidly spread over the complete surface of the coated wells. The cell embedded fibrin gel was allowed to set for 30 min at 37 °C, covered with medium and cultured until the matrix was fully contracted between the anchor points. Every other day, culture medium supplemented with 0.2 mM L-ascorbic acid 2-phosphate and 0.05 mM L-Proline (Sigma Aldrich) was replaced and adhesions to the side of the well were detached using a fine pipette tip to allow gel contraction. The constructs were divided into four treatment groups: DMEM/F12 medium supplemented with (1) 0.5% FBS, (2) 0.5% FBS + 250 ng/ml IGF-I, (3) 10% FBS and (4) 10% FBS + 250 ng/ml IGF-I. A first batch of constructs was analyzed at 21 and 28 days post seeding, where we could see an effect of IGF-I (denoted as first study part). In order to see the onset of the IGF-I effect, more constructs were grown with 0.5% FBS with or without IGF-I and analyzed at 7, 10 and 14 days, respectively, which were analyzed for collagen content and gene expression and are presented as results of the second part of the study.

2.3. Transmission electron microscopy

After discarding culture medium and rinsing in PBS, constructs were fixed in 2% Glutaraldehyde in 0.05 M phosphate buffer for 30 min at RT. The constructs were then cut in three equal pieces and fixed in fresh fixative for at least 2 h at 4 °C. After washing in 0.15 M phosphate buffer, the samples were postfixed with 1% OsO_4 in 0.12 M sodium cacodylate buffer for 2 h at room temperature. Following another washing in dH_2O, the samples were stained en bloc with 1% aqueous uranyl for 16 h at 4 °C, dehydrated in a graded serious of ethanol and embedded in Epon (Hexicon, Houston, Texas, USA) according to standard procedures.

Ultrathin cross sections were cut with a Reichert-Jung Ultracut E microtome using a diamond knife and were collected on one-hole copper grids with Formvar supporting membranes. Images were acquired in a Philips TM 100 transmission electron microscope, operated at an accelerating voltage of 80 kV, with a Megaview 2 camera and processed with the iTEM AnalySIS software package (ResAlta Research Technologies, Golden, USA). The NIH-based image-processing program, Image J, was used for measurement of collagen fibril diameters. On randomly selected micrographs, 300 fibrils were analyzed per specimen, cell line, treatment and time point, respectively.

2.4. Quantitative real-time PCR

The amount of mRNA for target genes was measured using quantitative real-time reverse transcriptase (RT) PCR. An overview over targets and primers sequences is provided in Table 1. First, tendon constructs were harvested and transferred to RNAse free tubes containing 1 ml TriReagent (Molecular Research Centre, Cincinnati, OH, USA), 5 stainless steel beads of 2.3 mm in diameter and 5 silicon-carbide sharp particles of 1 mm for mechanical disruption (BioSpec Products, Inc., Bartlesville, Oklahoma, USA). For RNA isolation, samples were mechanically

Table 1
PCR primer List.

mRNA	Sense	Antisense
RPLP0	GGAAACTCTGCATTCTCGCTTCCT	CCAGGACTCGTTTGTACCCGTTG
COL1A1	GGCAACAGCCGCTTCACCTAC	GCGGGAGGACTTGGTGGTTTT
COL3A1	CACGGAAACACTGGTGGACAGATT	ATGCCAGCTGCACATCAAGGAC
Scx	CAGCCCAAACAGATCTGCACCTT	CTGTCTTTCTGTCGCGGTCCTT
Tnm	GAAGCGGAAATGGCACTGATGA	TGAAGACCCACGAAGTAGATGCCA

disrupted using a FastPrep®-24 instrument (MP Biomedicals, Inc., Illkirch, France), and subsequently bromo-chloropropane (Molecular Research Centre) was added in order to separate the samples into an aqueous and an organic phase. Glycogen was added to the tendon samples to improve RNA precipitation (120 μg per ml TriReagent). Following isolation of the aqueous phase, RNA was precipitated using isopropanol, washed in ethanol and dissolved in RNAse-free water. RNA concentrations were determined by spectroscopy at 260 nm and RNA quality was confirmed by gel electrophoresis.

Synthesis of complementary DNA (cDNA) was performed using the Omniscript reverse transcriptase (Qiagen, Hilden, Germany) on 500 ng of tendon cell RNA. For each target mRNA, 5 μl of 20× diluted cDNA (in 1× Tris/EDTA buffer with 1 ng/μl salmon DNA) was amplified in 25 μl Quantitect SYBR Green Master Mix (Qiagen) with specific primers (100 nM each, Table 1) on a real-time PCR machine (MX3000P, Stratagene, La Jolla, CA, USA). The thermal profile was 95 °C, 10 min → (95 °C, 15 s → 58 °C, 30 s → 63 °C, 90 s) × 50 → 95 °C, 60 s → 55 °C, 30 s → 95 °C, 60 s. Signal intensity was acquired at the 63 °C step, and the threshold cycle (Ct) values were related to a standard curve made with the cloned PCR product. Specificity was confirmed by melting curve analysis after amplification (the 55 °C to 95 °C step). The large ribosomal protein P0 (RPLP0) mRNA, which was stably expressed relative both to GAPDH mRNA and total RNA (data not shown), was chosen as internal control. Values were normalized by RPLP0 expression and are presented as relative difference from 7-day 0.5% FBS to 21-day 0.5% FBS, respectively.

2.5. Collagen content analysis

Tendon constructs were snap frozen in liquid nitrogen and stored at −80 °C until further use. Subsequent to thawing, the samples were freeze dried and weighed at constant humidity using an ultra-microbalance scale (Mettler-Toledo GmBH, Gießen, Germany). The samples were hydrolyzed in 6 M HCl at 110 °C for 18 h, dried at 95 °C, followed by thorough washing in H_2O. The remaining samples were diluted in 600 μl acetate-citrate buffer (0.6% acetic acid, 130 mM citric acid, 440 mM sodium acetate, 425 mM sodium hydroxide) of which 150 μl were used for further analysis. Chloramine-T solution, 75 μl (60 mM chloramine-T in 50% 1-propanol), was added and incubated for 20 min at 20 °C. Aldehyde-perchloric acid solution, 75 μl (1 M 4-dimethylaminobenzaldehyde, 60% 1-propanol, 22% perchloric acid (70–72%)), was added and further incubated at 60 °C for 25 min. The reaction was stopped by putting the samples on ice, and the absorbance was measured using a multi-plate reader at a wavelength of 570 nm. The samples were correlated with a standard curve from pure hydroxyproline (Sigma, H1637), and collagen content values were calculated using the sample weight and an estimated hydroxyproline/collagen conversion number of 11.4% (the multiplying factor was calculated from the measured ratio between pure bovine tendon collagen mass and hydroxyproline mass).

2.6. Statistical analysis

The level of statistical significance was set for all tests at $p < 0.05$. The D'Agostino & Pearson omnibus normality test was applied to examine Gaussian distribution. Collagen content and collagen fibril diameter were analyzed using a 2-way analysis of variance (treatment group × time point) and post hoc tested using Tukey's multiple comparison test. Fibril diameter distributions (counts of fibrils within a certain diameter range) are presented as mean ± SEM per 5 nm group. For further analysis, the counts were grouped in 20 nm range groups (leading to 4 groups per treatment and time point) and analyzed separately for low or high FBS treatment using a 2-way analysis of variance (IGF-I × time point). Gene expression data were log-transformed and analyzed by a 2-way analysis of variance (treatment group × time point) and post hoc tested using Tukey's multiple comparison test. The statistical software package Prism 6 was used throughout the work for analysis and image preparation (GraphPad Software Inc.; La Jolla (Ca), USA). Data are presented as mean ± SEM.

3. Results

Within the first part of the study, constructs formed as described previously during 10–12 days. However, 0.5% FBS supplemented constructs were thinner, and the cell number was reduced compared to the other groups. In the second part of the study, cell proliferation in 0.5% FBS samples was lower, and the construct survival rate was reduced to approximately 75% (data not shown). All other treatments showed normal construct formation.

The microscopic structure of the developing tendon constructs is shown in Fig. 1 and shows representative cross-sectional images of tendon constructs of one cell line at 21 and 28 days with the four different treatments of 0.5% and 10% FBS with or without IGF-I, respectively. The cells in the constructs displayed distinct rough endoplasmic reticulum marking their activity (Fig. 1, arrow), and collagen fibrils are visible in the extracellular space (Fig. 1, arrowhead). Quantitative data for mean collagen fibril diameter and collagen content for these samples are presented in Fig. 2.

The total collagen content compared to dry weight is plotted in Fig. 2 as solid gray bars and shows three distinctive peaks for the values of the 21-day 0.5% FBS plus IGF-I, 28-day 0.5% plus IGF-I and 28-day 10% plus IGF-I treatment group, respectively. Samples with the low (0.5%) FBS treatment and supplementation with IGF-I showed a significantly higher collagen content of 12.14% (SEM: ±1.83%) and 15.62% (1.86%) at days 21 and 28 compared to both 0.5% FBS (6.40 ± 1.19% at 21 days and 9.39 ± 0.87% at 28 days) and 10% FBS (5.3 ± 1.04% and 7.05 ± 1.66%) treated constructs ($p < 0.05$). At 28 days, the group with 10% FBS plus IGF-I also shows a significantly higher collagen content than the groups without IGF-I ($p < 0.05$). In all groups, except the 10% FBS group, collagen content was higher at 28 days compared to 21 days ($p < 0.05$) (Fig. 2). IGF-I significantly increased the mean fibril diameter up to day 21 reaching 43.18 nm (4.11 nm) in the 0.5% FBS plus IGF-I group compared to 33.68 nm (4.78 nm) in the 0.5% group ($p < 0.05$) (Fig. 2; open bars). At 28 days, all treatments led to significantly increased diameters compared to 21 days ($p < 0.05$). Here the 0.5% FBS group showed the highest value of 52.23 nm (8.36 nm) that is significantly higher than the 0.5% FBS plus IGF-I (48.51 ± 5.71 nm), the 10% FBS group (47.77 ± 5.13 nm) and the 10% FBS plus IGF-I group (40.77 ± 2.53 nm) ($p < 0.05$). The lowest value of 40.77 nm (2.53 nm) is seen in the 10% FBS plus IGF-I group ($p < 0.05$).

The exact fibril diameter distributions of 0.5% FBS and 10% FBS with or without IGF-I supplementation, respectively, are presented in Fig. 3. The 0.5% FBS group shows a skewed fibril diameter distribution at 21 days, with fewer fibrils covering higher diameters of up to 75 nm. At 28 days, however, the fibrils spread over several diameters from <20 nm up to <95 nm (Fig. 3A). The group with 0.5% FBS plus IGF-I shows a similar development to the 10% FBS group, with a shift toward higher diameters after 28 days compared to 21 days. At 28 days, there is a second peak at about 30 nm visible, which indicates production of new, small diameter fibrils (Fig. 3A). Statistical analysis of the diameter groups shows that there is a significant effect of IGF-I on the two small diameter groups and the largest diameter group ($p < 0.05$). Furthermore, there is a significant effect of time on the low diameter group and the two high diameter groups ($p < 0.05$). The 10% FBS group shows a Gaussian distribution with the peak shifting from days 21 to 28 to the right (Fig. 3B). The treatment group with 10% FBS and IGF-I shows a Gaussian distribution with only a slight shift toward higher diameters at 28 days, which is consistent with the low diameter development from 36.75 nm (2.58 nm) at 21 days to 40.77 nm (2.53 nm) at 28 days (Fig. 2 open bars; Fig. 3B). Closer analysis shows a significant effect of time on all except the large diameter group ($p < 0.05$), while IGF-I only shows an effect on the 55–75 nm group ($p < 0.05$).

Please cite this article as: A. Herchenhan, et al., Insulin-like growth factor I enhances collagen synthesis in engineered human tendon tissue, Growth Horm. IGF Res. (2014), http://dx.doi.org/10.1016/j.ghir.2014.09.001

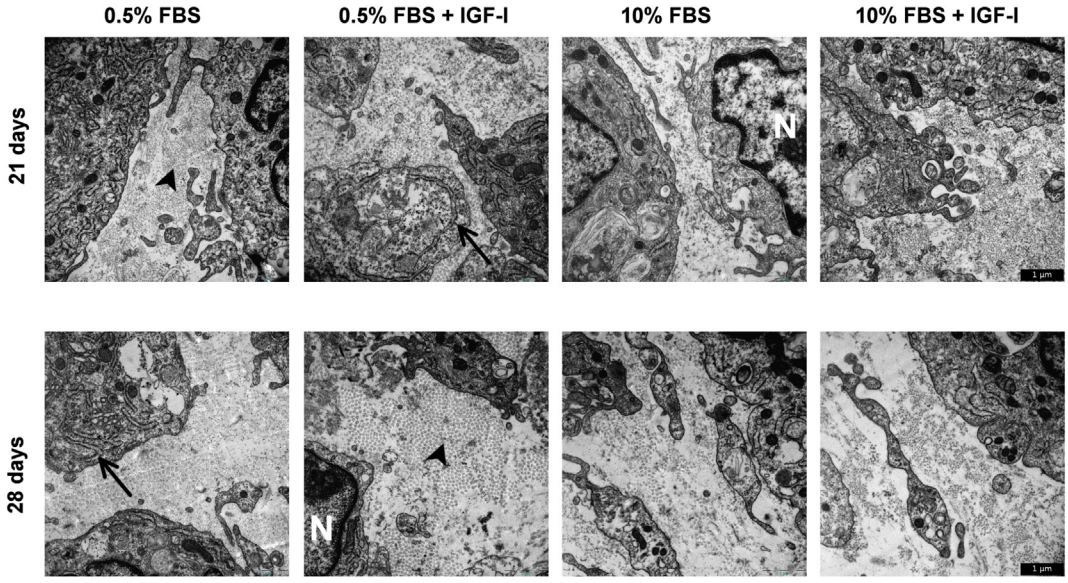

Fig. 1. Representative transmission electron micrographs showing transverse sections of tendon constructs at day 21 (top row) and 28 days post seeding (bottom row). The constructs are treated from left to right: 0.5% FBS, 0.5% FBS + IGF-I, 10% FBS, 10% FBS + IGF-I. Maturation of the extracellular matrix is visible in all groups over 1 week of development (arrowhead: collagen fibrils; arrow: rough endoplasmic reticulum; N: nucleus; scale bar, 1 µm).

During the early phase (days 7–14), the total collagen content develops over time from very low values of 0.67% (0.20%) at 7 days up to 9.10% (1.80%) at 14 days. Thereby, the 0.5% FBS plus IGF-I treatment group shows increased values at 10 and 14 days compared to the 0.5% FBS groups, with a significant effect of the treatment over time ($p < 0.05$) (Fig. 4).

Further, the mRNA for collagen types I and III and the tendon development marker tenomodulin rose in response to IGF-I treatment throughout day 21 to day 28 ($p < 0.05$ for IGF treatment and time), and for the early tendon marker scleraxis at days 10 and 14 ($p < 0.05$ for IGF treatment and time) (Fig. 5B). In contrast, mRNA for collagen, scleraxis and tenomodulin decreased at days 21 and 28 when FBS concentration was high (10%) compared to low (0.5%) irrespectively of the IGF-I concentration ($p < 0.05$ for low serum treatment) (Fig. 5A).

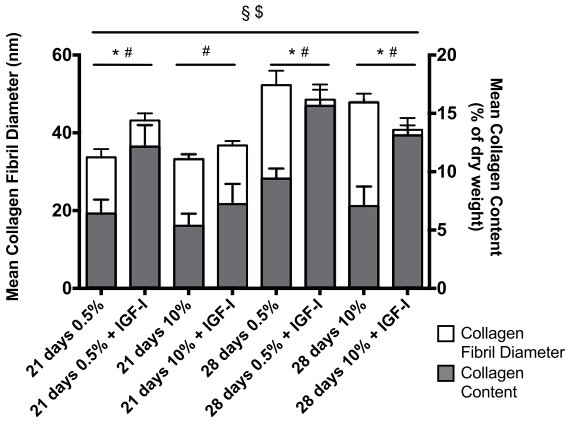

Fig. 2. Mean fibril diameters (open bars, primary *y*-axis) superimposed with mean collagen content (gray bars, secondary *y*-axis) at 21 and 28 days post seeding with the four different treatment groups. At 21 days, the patterns of content and diameter are similar with the highest value for 0.5% FBS + IGF-I-treated constructs. At 28 days, IGF-I supplemented constructs show significantly higher collagen content but reduced fibril diameter compared to only FBS-treated samples. Interestingly, the 0.5% FBS-treated samples at 28 days show the highest mean fibril diameter. All treatments show an increase in collagen content and fibril diameter from days 21 to 28 (mean ± SEM; $^{\S}p < 0.05$ effect of IGF-I on collagen content; $^{\$}p < 0.05$ effect of IGF-I on collagen fibril diameter; $^{*}p < 0.05$ difference in collagen content among pairs; $^{\#}p < 0.05$ difference in collagen fibril diameter among pairs).

4. Discussion

In this study, the data indicate that IGF-I had a stimulating effect upon collagen expression and collagen formation in human tenocyte derived tendon constructs. The fact that IGF-I is mostly found in the early period of tendon construct formation supports the view that growth factors are important for tendon development and regeneration (reviewed by Molloy et al. [30]). In addition, a reduction of the normal concentration of FBS in cell culture from 10% to 0.5% somewhat surprisingly resulted in elevated expression of extracellular matrix genes and led to high collagen fibril diameters 3–4 weeks after construct seeding.

Tendon constructs treated with IGF-I demonstrated an increased total collagen content, which corresponded with a higher mean fibril diameter at day 21. At 28 days, the total collagen content was still higher compared to non IGF-I-treated samples ($p < 0.05$), but the mean fibril diameter of 0.5% FBS-treated samples was higher compared to IGF-I stimulated samples. However, taking the fibril diameter distribution into account (Fig. 3), the 0.5% FBS samples showed an irregular distribution of fibril diameters, which does not correspond to physiological packing arrangements of collagen fibrils in tendon *in vivo* [15,31]. Comparable to the diameter distributions in the present study, it has been shown in developing tendons that collagen fibrils show a relatively uniform diameter and first develop a bimodal diameter distribution during maturation [31]. Further, we tried to further understand the effect of IGF-I supplementation during early construct formation. The results showed an earlier onset of collagen synthesis with IGF-I (Fig. 4), and thus possibly a positive effect on fibroblast proliferation as shown in earlier work [3,4].

IGF-I has been used on tendon cells [3,4], in 3-dimensional tissue cultures of engineered ligament [21,32] and in human subjects before [22,33,34]. Cells on 2D had a significantly increased collagen production and cell proliferation, particularly in combination with the growth factor PDGF-BB [3,4,35]. However, the production of intact collagen fibrils cannot be investigated optimally in 2D cells. Hagerty et al. [32] showed that IGF-I, in combination with transforming growth factor β1, had a collagen synthesis stimulating effect that resulted in higher maximal tensile load of the tendon constructs. We have focused on the ultrastructure of a newly synthesized collagen-rich tissue and showed for the first time that IGF-I also enhances collagen fibril diameter at an early developmental stage without affecting collagen structure or the cell configuration as proven by electron microscopy. Moreover, IGF-I

Please cite this article as: A. Herchenhan, et al., Insulin-like growth factor I enhances collagen synthesis in engineered human tendon tissue, Growth Horm. IGF Res. (2014), http://dx.doi.org/10.1016/j.ghir.2014.09.001

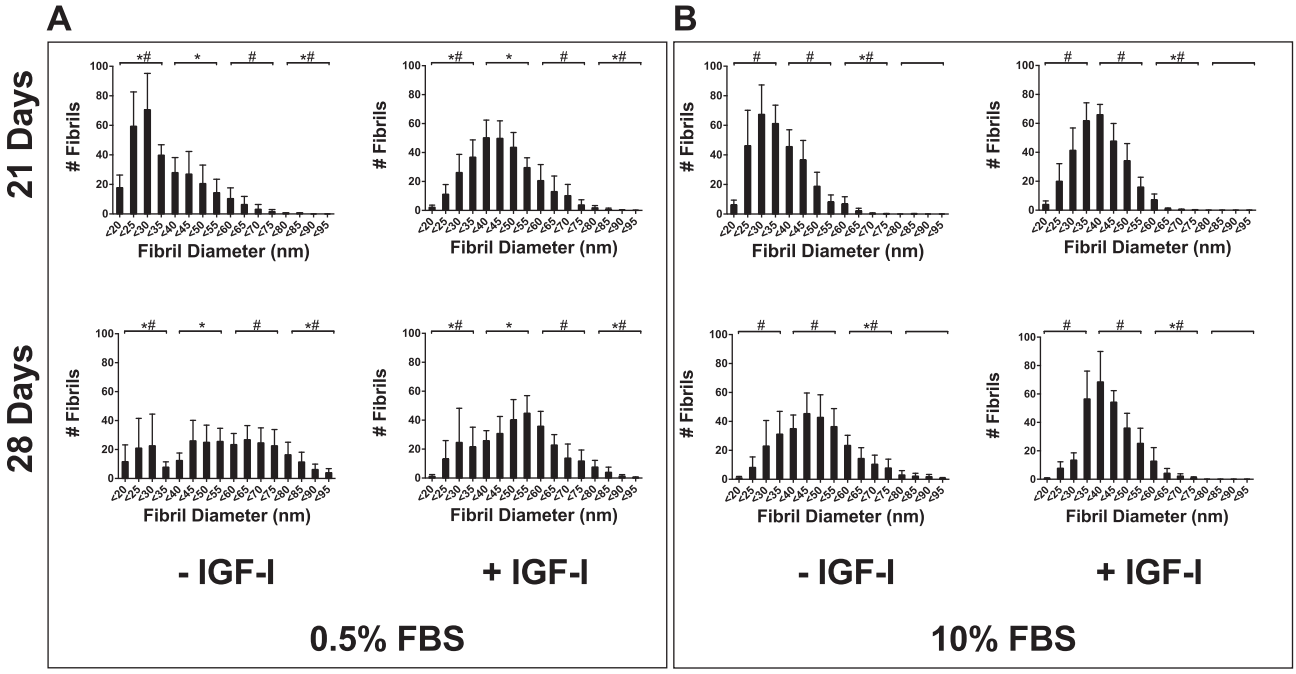

Fig. 3. Fibril diameter distributions of 0.5% FBS (A) and 10% FBS (B)-treated constructs. (A) 0.5% FBS-treated constructs show a skewed distribution with many low diameter fibrils at day 21 and a broad distribution at day 28. Constructs with 0.5% FBS + IGF-I show a Gaussian distribution at day 21, which is shifted to the right at day 28. (B) 10% FBS-treated constructs show a similar pattern with a broadening of the distribution without IGF-I supplementation from 21 to 28 days. FBS + IGF-I-treated constructs (10%) show a Gaussian distribution with very low variation that is shifted only marginally to higher diameters at 28 days. ($^{*}p < 0.05$ for IGF-I effect; $^{\#}p < 0.05$ for time effect).

has a rescuing effect on tendon constructs when treated with low levels of FBS.

In human subjects, IGF-I and human growth hormone (hGH) have been applied in different settings. Doessing et al. [34] have shown that growth hormone application leads to an increased local IGF-I production, which in turn stimulates collagen synthesis in tendon *in vivo*. Another recent study from our laboratory revealed a collagen synthesis enhancing effect of direct IGF-I application in human tendon *in vivo* [22]. Further, Boesen et al. 2013 showed that growth hormone had a matrix-stabilizing effect in elderly humans after 2 weeks of immobilization followed by 6 weeks of re-training [36]. Taken together, the findings from the present study support the notion that IGF-I plays an important role in growth, development and maintenance of tendon tissue. Specifically during collagen neosynthesis, IGF-I can enhance the cells productivity and might therefore be considered when new collagen formation is required.

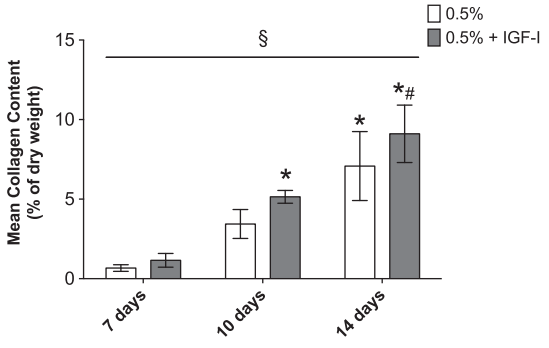

Fig. 4. Mean collagen content on days 7, 10 and 14, respectively. The collagen content rises over time and is significantly higher in samples supplemented with IGF-I (a; $^{*}p < 0.05$ compared to 7 days results; $^{\#}p < 0.05$ compared to 10 day results; $^{\S}p < 0.05$ overall effect of IGF-I).

In the current study, constructs supplemented with 0.5% FBS plus IGF-I showed higher tendon-specific gene expression and higher collagen fibril diameters over 10% FBS-treated samples. This demonstrates a rescuing effect by IGF-I over low FBS treatment and a more tendon-specific phenotype than those in 10% FBS-treated constructs. To what extend FBS contains blocking factors on extracellular matrix formation remains elusive. The survival rate of purely 0.5% FBS supplemented constructs was reduced, which was rescued by either higher serum levels or IGF-I supplementation. 10% FBS has for decades been used as standard supplement in cell culture media to promote cell survival and proliferation. The rationale for substantially reducing FBS concentrations in this study has two aspects. On the one hand, FBS contains high amounts of various growth factors including IGF-I, transforming growth factor-ß (TGF-ß), platelet-derived growth factor (PDGF) and fibroblast growth factor (FGF). Some of these have stimulating effects while others have blocking effects on collagen fibrillogenesis [37]. FBS reduction was therefore necessary to fathom the independent effect of IGF-I. On the other hand, FBS composition can vary substantially [26,29]. One study suggests a variation of IGF-I in FBS between 50 and 150 µg/l in FBS [29], while a different study could not detect IGF-I in FBS at all [27]. Growth hormone stimulates IGF-I production in cells and was shown to vary between 18.7 and 51.6 ng/ml in FBS [38]. Different lots of FBS can effect cell proliferation in dissimilar ways. Zheng et al. [27] detected similar concentrations of various FBS components in different lots but saw additional ingredients in proliferation-enhancing lots compared to others.

Our data suggest that with low serum, cell proliferation was profoundly impaired, but interestingly, we could demonstrate that a low FBS concentration had in fact a stimulating effect on collagen fibril diameter. Serum starvation blocks cell proliferation and locks cells in the G0/G1 phase, similarly to cells at 100% confluency [39]. The cells are therefore unable to actively organize the ECM, which might result in uncontrolled fusion of collagen fibrils leading to a broad fibril diameter spectrum. The low collagen content of FBS and IGF-I-deprived constructs demonstrates that the increased relative ECM gene expression

Please cite this article as: A. Herchenhan, et al., Insulin-like growth factor I enhances collagen synthesis in engineered human tendon tissue, Growth Horm. IGF Res. (2014), http://dx.doi.org/10.1016/j.ghir.2014.09.001

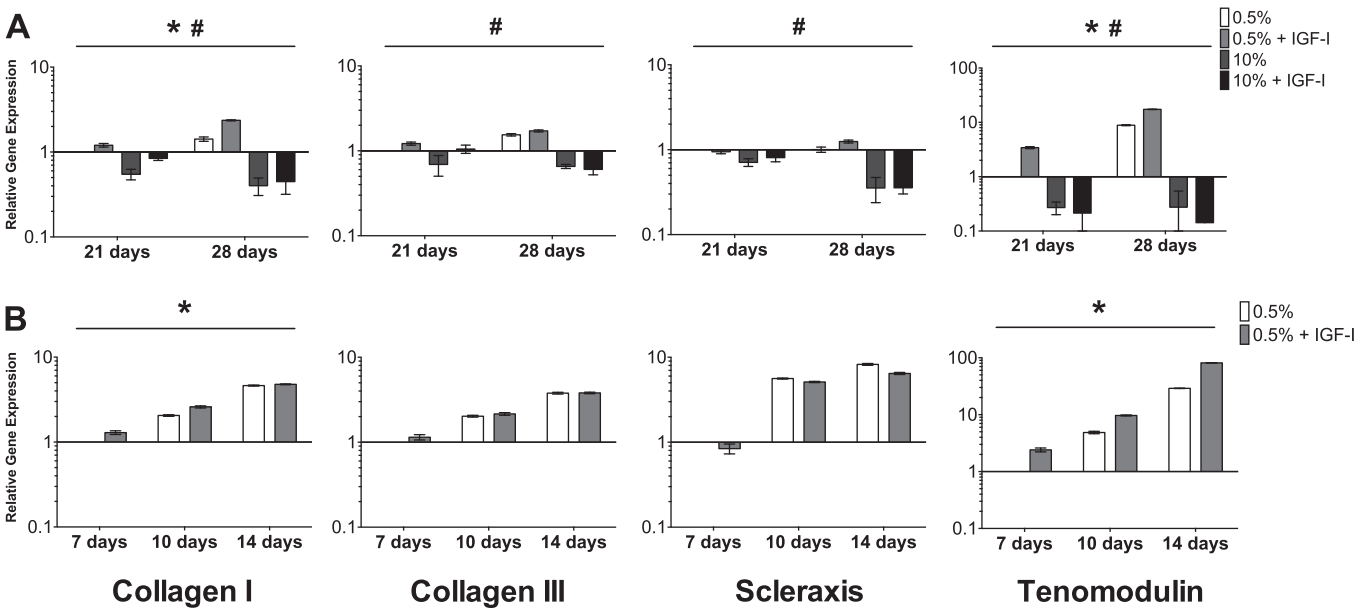

Fig. 5. Relative gene expression for collagen type I, collagen type III and the tendon development markers scleraxis and tenomodulin on days 21 and 28 (A) and days 7, 10 and 14 (B), respectively. Data are normalized to the corresponding 21-day 0.5% FBS without IGF-I (A) and 7-day 0.5% FBS without IGF-I (B) values. Across all treatments and time points, IGF-I has a significant effect on collagen type I and tenomodulin expression. Furthermore, low serum concentration has an enhancing effect on collagen type III and scleraxis gene expression.

is not translated to higher protein production. This phenomenon has been described before in vascular smooth muscle cells [40] and cardiac fibroblasts [41]. Another study has shown that elastin is upregulated in serum-deprived chick vascular smooth-muscle cells [40]. So far, there is no detailed explanation for this phenomenon. It has been suggested that the cells focus on matrix production when their proliferative capacity is blocked or the cells reach confluency, or that cells attempt to fill intercellular spaces with matrix to maintain cell communication [40,41]. However, in the present study, the upregulation does not lead to a higher collagen synthesis. The effect of FBS reduction on collagen fibrillogenesis warrants further investigation.

In conclusion, IGF-I supplementation promotes early onset of tensile strain induced collagen formation and tendon structural arrangement, whereas the FBS concentration normally used in cultures diminishes collagen expression, collagen content and fibril formation. This knowledge could be used in the future to design an improved collagen-stimulating environment in tendon tissue engineering approaches or treatment options after severe tendon injuries.

Conflict of interest

The authors have no conflict of interests to disclose.

Acknowledgments

The authors gratefully acknowledge the help with tissue acquisition of the department of orthopedic surgery at Bispebjerg Hospital. The Core Facility for Integrated Microscopy at the University of Copenhagen is thankfully acknowledged for support and access to electron microscopes. Funding is gratefully acknowledged from the Nordea Foundation (Healthy Aging grant), the University of Copenhagen, Department of Health Sciences and the Academy of Muscle Biology, Exercise and Health Research.

References

[1] J. Kastelic, A. Galeski, E. Baer, The multicomposite structure of tendon, Connect. Tissue Res. 6 (1978) 11–23.
[2] K.M. Heinemeier, et al., Lack of tissue renewal in human adult Achilles tendon is revealed by nuclear bomb (14)C, FASEB J. 27 (5) (2013) 2074–2079.
[3] S.-O. Abrahamsson, G. Lundborg, L.S. Lohmander, Recombinant human insulin-like growth factor-I stimulates in vitro matrix synthesis and cell proliferation in rabbit flexor tendon, J. Orthop. Res. 9 (4) (1991) 495–502.
[4] P.G.D.F.-B.B. Banes, IGF-I and mechanical load stimulate DNA synthesis in avian tendon fibroblasts in vitro, J. Biomech. 28 (12) (1995) 1505–1513.
[5] E. Cukierman, et al., Taking cell-matrix adhesions to the third dimension, Science 294 (5547) (2001) 1708–1712.
[6] C.S. Chen, et al., Geometric control of cell life and death, Science 276 (5317) (1997) 1425–1428.
[7] E. Dawson, et al., Biomaterials for stem cell differentiation, Adv. Drug Deliv. Rev. 60 (2) (2008) 215–228.
[8] D. Eyrich, et al., Long-term stable fibrin gels for cartilage engineering, Biomaterials 28 (1) (2007) 55–65.
[9] M.L. Bayer, et al., The initiation of embryonic-like collagen fibrillogenesis by adult human tendon fibroblasts when cultured under tension, Biomaterials 31 (18) (2010) 4889–4897.
[10] A. Herchenhan, et al., In vitro tendon tissue development from human fibroblasts demonstrates collagen fibril diameter growth associated with a rise in mechanical strength, Dev. Dyn. 242 (1) (2013) 2–8.
[11] N.S. Kalson, et al., An experimental model for studying the biomechanics of embryonic tendon: Evidence that the development of mechanical properties depends on the actinomyosin machinery, Matrix Biol. 29 (8) (2010) 678–689.
[12] N.S. Kalson, et al., Slow stretching that mimics embryonic growth rate stimulates structural and mechanical development of tendon-like tissue in vitro, Dev. Dyn. 240 (11) (2011) 2520–2528.
[13] J.Z. Paxton, et al., Optimizing an intermittent stretch paradigm using ERK1/2 phosphorylation results in increased collagen synthesis in engineered ligaments, Tissue Eng. A 18 (3–4) (2011) 277–284.
[14] J. Zhu, et al., Ultrastructural and morphological characteristics of human anterior cruciate ligament and hamstring tendons, Anat. Rec. (Hoboken) 295 (9) (2012) 1430–1436.
[15] S.P. Magnusson, et al., Collagen fibril size and crimp morphology in ruptured and intact Achilles tendons, Matrix Biol. 21 (4) (2002) 369–377.
[16] D.A. Parry, G.R. Barnes, A.S. Craig, A comparison of the size distribution of collagen fibrils in connective tissues as a function of age and a possible relation between fibril size distribution and mechanical properties, Proc. R. Soc. Lond. B Biol. Sci. 203 (1152) (1978) 305–321.
[17] M.L. Bayer, et al., Release of tensile strain on engineered human tendon tissue disturbs cell adhesions, changes matrix architecture, and induces an inflammatory phenotype, PLoS ONE 9 (1) (2014) e86078.
[18] C. Beckham, R. Dimond, T.K. Greenlee, The role of movement in the development of a digital flexor tendon, Am. J. Anat. 150 (1977) 443–460.
[19] M. Chiquet, et al., From mechanotransduction to extracellular matrix gene expression in fibroblasts, Biochim. Biophys. Acta (BBA) - Mol. Cell Res. 1793 (5) (2009) 911–920.
[20] N. Juncosa-Melvin, et al., Effects of mechanical stimulation on the biomechanics and histology of stem cell–collagen sponge constructs for rabbit patellar tendon repair, Tissue Eng. 12 (8) (2006) 2291–2300.

Please cite this article as: A. Herchenhan, et al., Insulin-like growth factor I enhances collagen synthesis in engineered human tendon tissue, Growth Horm. IGF Res. (2014), http://dx.doi.org/10.1016/j.ghir.2014.09.001

[21] T.L. McCarthy, M. Centrella, E. Canalis, Regulatory effects of insulin-like growth factors I and II on bone collagen synthesis in rat calvarial cultures, Endocrinology 124 (1) (1989) 301–309.
[22] M. Hansen, et al., Local administration of insulin-like growth factor-I (IGF-I) stimulates tendon collagen synthesis in humans, Scand. J. Med. Sci. Sports 23 (5) (2013) 614–619.
[23] R.H. Nielsen, et al., Increase in tendon protein synthesis in response to insulin-like growth factor-I is preserved in elderly men, J. Appl. Physiol. (1985) 116 (1) (2014) 42–46.
[24] A. Scott, K.M. Khan, V. Duronio, IGF-I activates PKB and prevents anoxic apoptosis in Achilles tendon cells, J. Orthop. Res. 23 (5) (2005) 1219–1225.
[25] Z. Kapacee, et al., Tension is required for fibripositor formation, Matrix Biol. 27 (4) (2008) 371–375.
[26] J. van der Valk, et al., Optimization of chemically defined cell culture media–replacing fetal bovine serum in mammalian in vitro methods, Toxicol. In Vitro 24 (4) (2010) 1053–1063.
[27] X. Zheng, et al., Proteomic analysis for the assessment of different lots of fetal bovine serum as a raw material for cell culture. Part IV. Application of proteomics to the manufacture of biological drugs, Biotechnol. Prog. 22 (5) (2006) 1294–1300.
[28] C.W. Boone, et al., Quality control studies on fetal bovine serum used in tissue culture, In Vitro 7 (3) (1971) 174–189.
[29] A. Honegger, R.E. Humbel, Insulin-like growth factors I and II in fetal and adult bovine serum. Purification, primary structures, and immunological cross-reactivities, J. Biol. Chem. 261 (2) (1986) 569–575.
[30] T. Molloy, Y. Wang, G. Murrell, The roles of growth factors in tendon and ligament healing, Sports Med. 33 (5) (2003) 381–394.
[31] G. Zhang, et al., Decorin regulates assembly of collagen fibrils and acquisition of biomechanical properties during tendon development, J. Cell. Biochem. 98 (6) (2006) 1436–1449.
[32] P. Hagerty, et al., The effect of growth factors on both collagen synthesis and tensile strength of engineered human ligaments, Biomaterials 33 (27) (2012) 6355–6361.
[33] A.P. Boesen, et al., Effect of growth hormone on aging connective tissue in muscle and tendon: gene expression, morphology, and function following immobilization and rehabilitation, J. Appl. Physiol. (1985) 116 (2) (2014) 192–203.
[34] S. Doessing, et al., Growth hormone stimulates the collagen synthesis in human tendon and skeletal muscle without affecting myofibrillar protein synthesis, J. Physiol. 588 (2) (2009) 341–351.
[35] M.A. Costa, et al., Tissue engineering of flexor tendons: optimization of tenocyte proliferation using growth factor supplementation, Tissue Eng. 12 (7) (2006) 1937–1943.
[36] A.P. Boesen, et al., Effect of growth hormone on aging connective tissue in muscle and tendon - gene expression, morphology and function following immobilization and rehabilitation, J. Appl. Physiol. (1985) 116 (2) (2013) 192–203.
[37] S.R. Caliari, B.A. Harley, The effect of anisotropic collagen-GAG scaffolds and growth factor supplementation on tendon cell recruitment, alignment, and metabolic activity, Biomaterials 32 (23) (2011) 5330–5340.
[38] P.J. Price, E.A. Gregory, Relationship between in vitro growth promotion and biophysical and biochemical properties of the serum supplement, In Vitro 18 (6) (1982) 576–584.
[39] R. Khammanit, et al., Effect of serum starvation and chemical inhibitors on cell cycle synchronization of canine dermal fibroblasts, Theriogenology 70 (1) (2008) 27–34.
[40] M.S. Kindy, C.J. Chang, G.E. Sonenshein, Serum deprivation of vascular smooth muscle cells enhances collagen gene expression, J. Biol. Chem. 263 (23) (1988) 11426–11430.
[41] M. Leicht, et al., Serum depletion induces cell loss of rat cardiac fibroblasts and increased expression of extracellular matrix proteins in surviving cells, Cardiovasc. Res. 52 (3) (2001) 429–437.

Please cite this article as: A. Herchenhan, et al., Insulin-like growth factor I enhances collagen synthesis in engineered human tendon tissue, Growth Horm. IGF Res. (2014), http://dx.doi.org/10.1016/j.ghir.2014.09.001

Manuscript III

Lysyl Oxidase controls collagen molecule aggregation during fibrillogenesis.

Lysyl Oxidase controls collagen molecule aggregation during fibrillogenesis

Andreas Herchenhan[a]*, Franziska Uhlenbrock[b], Pernilla Eliasson[a], MaryAnn Weis[c], David Eyre[c], Karl E. Kadler[d], S. Peter Magnusson[a], Michael Kjaer[a]

[a]*Institute of Sports Medicine Copenhagen and Center for Healthy Ageing, University of Copenhagen, Copenhagen, Denmark*
[b]*Section for Experimental Animal Models, Laboratory of Immunology, Faculty of Health and Medical Sciences, University of Copenhagen, DK-1870 Frederiksberg, Denmark*
[c]*Department of Orthopaedics and Sports Medicine, University of Washington, Seattle, Washington 98195-6500, USA*
[d]*Wellcome Trust Center for Cell-Matrix Research, Faculty of Life Sciences, University of Manchester, Oxford Road, Manchester M13 9PT, UK*
**corresponding author: Institute of Sports Medicine Copenhagen, Bispebjerg Hospital, Bispebjerg Bakke 23, 2400 Copenhagen, Denmark; email: andreas.herchenhan@gmail.com; tel.+45 3531 6091*

Abstract

Collagen is abundant in several tissues and ensures mechanical stability. Collagen molecules are enzymatically cross-linked by lysyl oxidase (LOX) to stabilise the fibrils. LOX activity can be inhibited by ß-aminoproprionitrile (BAPN), which results in mechanically weak tissues. Here we inhibited LOX in developing tendon constructs from primary human tenocytes and investigated the effects on the structure. The structure and strength of the constructs developed with time, but this mechanical maturation was inhibited by the LOX inhibition. The collagen was more soluble due to a lack of cross-links, which explains the lack the development of construct strength. Moreover, we show that LOX inhibition also leads to structurally abnormal collagen fibrils with irregular shapes and widely dispersed diameters, which resembles the Ehlers Danlos Syndrome phenotype. Interestingly, the total collagen content developed normally, and there was no difference in gene expression. This suggests that the cells do not sense the lack of cross-link formation and are unable to rescue the extracellular matrix from this severe intervention. Collagen type V, decorin, fibromodulin and tenascin-X proteins were unaffected by the cross-link inhibition, suggesting that LOX regulates fibrillogenesis independently of these molecules. Collectively, the data show the importance of LOX on the mechanical development of early collagenous tissues, and that LOX is essential for correct collagen fibril shape formation.

Key Words: Collagen cross-linking, enzymatic cross-links, BAPN, Ehlers Danlos Syndrome, tendon construct, tissue engineering, extracellular matrix

Introduction

Collagen is the most abundant protein in the human body and plays a major role in providing mechanical stability to many tissues and structures such as skin, blood vessels, bones and tendons [1-4]. Its mechanical integrity is based on a highly organized structure where three collagen molecules are helically arranged to form tropocollagen molecules, which are organized in a quarter-staggered arrangement to make collagen fibrils [5]. These fibrils can then either be randomly arranged, as for example in skin [6], or be included in further hierarchical levels such as in tendon [1]. Collagen fibrils are internally stabilized by enzymatic or non-enzymatic cross-links between the single tropocollagen molecules in a standardized fashion, respectively. Lysyl oxidase (LOX) is the major enzyme for enzymatic crosslink formation in collagen and elastin fibrils by deaminating particular lysine residues to form allysines in the telopeptide region of the tropocollagen molecule [7]. This enables the formation of crosslinks between two tropocollagens within a 4 D-period distance

among the helically arranged molecules [7]. During maturation, these crosslinks can connect to one more tropocollagen, building a trivalent crosslink [8]. It is unknown to what extend the cross-link formation during fibrillogenesis is crucial for mature tissue properties in humans.

Inactivation of the gene coding for LOX has earlier shown to be detrimental, leading to aortic aneurisms and thereby perinatal death in mice [9]. Also, LOX inactivation had a vast effect on the elastin and collagen fibrils of the respiratory tract and skin in these animals, which were disorganised and thereby hindered intact lung development [10]. LOX was recently discovered to also play a major role in tumour growth and metastasis by increasing the stiffness of tumour substrate and thereby promoting cancer cell proliferation [11, 12]. ß-Aminopropionitrile (BAPN) is a competitive inhibitor of LOX [13, 14] and has been shown to have detrimental effects upon several tissues. Early experiments have shown that BAPN injection into fertilized eggs leads to extremely fragile chick embryos after three days of incubation. Furthermore, collagen became extractible from all matrix rich tissues such as bone, skin and tendons [15]. Marturano and colleagues have elegantly shown that BAPN specifically inhibits LOX without affecting total collagen content, macroscopic fibril formation or cell fate in chick embryos. However, both the *in ovo* and *in vitro* treated chick tendons showed markedly reduced tensile moduli [16].

Apart from these considerable mechanical effects of LOX inhibition, very few studies have assessed the ultrastructure of these affected tissues. Mäki and colleagues [10] have shown disturbed collagen fibril bundles with slack packing density in lung and skin tissue from $LOX^{-/-}$ mouse embryos. Cell matrix constructs from chick embryonic corneal fibroblasts were further shown to develop impaired collagen fibril outlines when cultured with BAPN and transglutaminase inhibitor [17].

We have recently introduced and characterised a tendon construct system from adult human tendon fibroblasts that is ideal to investigate collagen fibril formation *in vitro* [18-20]. Primary fibroblasts from adult human tendon can produce new collagen fibrils *in vitro*, which increase in diameter with time and strengthen the structure [19]. In contrast to *in vitro* collagen self-assembly studies, the collagen fibrils are produced, aligned and modified in a controlled fashion by adult human fibroblasts [18]. This leaves the opportunity to specifically manipulate the cell-driven collagen modification during development.

In this study we investigate the role of LOX by blocking its activity with BAPN in the controlled tendon construct system. We hypothesise that LOX inhibition will lead to reduced tensile mechanical properties. Furthermore, we will investigate the effect of LOX inhibition on collagen fibril formation and thereby elucidate the role of LOX in collagen fibrillogenesis.

Materials and Methods

Cell Culture

Tendon fibroblasts were isolated from human semitendinosis and gracilis tendon as previously described in detail [18]. Briefly, patients (18-32 years old) who underwent reconstructive surgery after anterior cruciate ligament (ACL) rupture gave their informed consent to donate excess tendon tissue to the present study. The tissue was transported to a cell culture laboratory immediately following harvest. Under aseptic conditions the tissue was minced into pieces of ~ 2 mm^3 and digested overnight in DMEM/F12 (Gibco, Invitrogen) supplemented with 0.1% collagenase type II (Worthington) and 20% fetal bovine serum (FBS) (Gibco, Invitrogen). Following repeated washes in culture medium (DMEM/F12, 10% FBS) the cells were seeded into flasks and cultured until the next passage. Cells from at least five different donors in the 2^{nd} to 6^{th} passage were used for experiments. The present experiment was approved by the local ethics committee (ref. H-3-2010-070).

Construct Formation

Tendon constructs from human tenocytes were assembled as described previously with minor modifications [18]. Briefly, each well of a six-well plate was coated with ~1.5 ml SYLGARD

(Dow-Chemicals) and allowed to set at 55°C for 48 h. Next, two short silk sutures (0.5 cm, Ethicon) were pinned onto the coated plates with minutien insect pins (0.1 mm diameter) (Fine Science Tools GmbH) with a distance of 1 cm in between sutures. The plates were sterilized by immersion in 70% ethanol for 45 min. Human tendon fibroblasts were suspended in culture medium containing 4 mg human fibrinogen, 10 µg/ml aprotenin and 1 unit of human thrombin (all Sigma Aldrich) to a final concentration of $2x10^5$ per 800 µl and rapidly spread over the complete surface of the coated wells. The cell embedded fibrin gel was allowed to set for 30 min at 37°C, and cultured until the matrix was fully contracted between the anchor points. Every other day, culture medium supplemented with 0.2 mM L-ascorbic acid 2-phosphate and 0.05 mM L-Proline (Sigma Aldrich) was replaced and adhesions to the side of the well were detached using a fine pipette tip to allow gel contraction. After 12-14 days the cells contracted the structure to a rod-like structure in between the anchor points (Fig.1A).

Initially, constructs were treated with the LOX inhibitor BAPN (50 µM; Sigma Aldrich, A3134) from day 0. However, this treatment led to spontaneous rupture of the construct around the time of formation (Fig.1B, arrow indicates retracted construct), thus excluding any usable phenotype for further studies. Therefore, we used a regime where constructs were allowed to form initially (14 days) and were subsequently supplemented with 50 µM BAPN or left as control until harvesting (Fig.2A).

Mechanical Testing

Tensile testing of the tendon constructs at the different time points was performed in a PC-driven micromechanical rig with liquid chamber (20 N load-cell, sampling rate 10 Hz; Deben, Suffolk, UK). A stereoscopic microscope (SMZ1000, Nikon, Tokyo, Japan) with C-mount lens (x8), equipped with a 15 Hz digital camera (DFWX700, Sony, Tokyo, Japan; 640x480 Pixel) was used for imaging during the test to verify clamping length and monitor the rupture site of the construct.

The tendon constructs were glued on specimen plates with a mounting distance of 10 mm. The glue was left to dry for 5 min while the mid-portion was wrapped in PBS-soaked gauze. Subsequently, the specimen was transferred to a PBS-bath and after a short adaptation period, the test was started. The samples were stretched at 2 mm/min until the onset of force. After a 15 s relaxation period, the constructs were further stretched at 2 mm/min until failure.

The data analysis was based on the assumption that the construct had a circular cross-section. Construct diameter and mounting length were measured at the onset of force. For the calculation of ultimate tensile stress, the minimal diameter was used and the strain was determined from the onset of force until failure. Tensile modulus was calculated based on stress and strain from the onset of force up to the point of failure.

Three constructs per donor cell line were tested, and results of 6 (14 day control) and 8 cell lines (21 day control and BAPN), respectively, were compared.

Transmission Electron Microscopy (TEM)

After discarding culture medium and rinsing in PBS, constructs were fixed in 2% Glutaraldehyde in 0.05 M phosphate buffer for 30 min at RT. The constructs were then cut in three equal pieces and fixed in fresh fixative for at least 2 h at 4°C. After washing in 0.15 M phosphate buffer, the samples were postfixed with 1% OsO_4 in 0.12 M Sodium Cacodylate buffer for 2 h at room temperature. Following another washing in dH_2O, the samples were stained en bloc with 1% aqueous uranyl for 16 h at 4°C, dehydrated in a graded serious of ethanol and embedded in Epon (Hexicon, Houston, Texas, USA) according to standard procedures.

Ultrathin cross-sections were cut with a Reichert-Jung Ultracut E microtome using a diamond knife and were collected on one-hole copper grids with Formvar supporting membranes. Images were acquired in a Philips TM 100 transmission electron microscope, operated at an accelerating voltage of 80 kV, with a Megaview 2 camera and processed with the iTEM AnalySIS software package (ResAlta

Research Technologies, Golden, USA). The NIH-based image-processing program, Image J, was used for measurement of collagen fibril diameters. On randomly selected micrographs, 300 fibrils were analysed per specimen, cell line, treatment and time point, respectively.

3view

The samples were fixed as for TEM, but post-fixation was modified. Here, constructs were post-fixed in a solution of 1% OsO_4 and 1.5% K_4[Fe6] in 0.12 M sodium cacodylate buffer for 1 h. Subsequent to washing with water, samples were treated with 1% tannic acid in 0.12 M cacodylate buffer, washed and one more time incubated with 1% OsO_4 in 0.12 M cacodylate buffer for additional 30 min. Thereafter, samples were block stained, dehydrated and embedded as described above. Ultrathin sections were investigated by TEM in order to assure sample quality.

Samples were mounted on a Gatan 3view microtome within an FEI Quanta 250 scanning microscope as described in detail elsewhere [21]. Section thickness was 100 nm over a Z range of 50 µm, resulting in 500 images. Image processing was conducted using the IMOD software package (University of Colorado, Dept. of MCD Biology, 347 UCB, Boulder, CO 80309, USA) and videos were created.

Collagen Content Assay

Tendon constructs were snap frozen in liquid nitrogen and stored at -80°C until further use. Subsequent to thawing, the samples were freeze-dried and weighed at constant humidity using an ultra-microbalance scale (Mettler-Toledo GmBH, Gießen, Germany). The samples were hydrolysed in 6 M HCl at 110°C for 18 h, dried at 95°C, followed by thorough washing in H_2O. The remaining samples were diluted in 600 µl acetate-citrate buffer (0.6% acetic acid, 130 mM citric acid, 440 mM sodium acetate, 425 mM sodium hydroxide) of which 150 µl were used for further analysis. 75 µl chloramine-T solution (60 mM chloramine-T in 50% 1-propanol) were added and incubated for 20 min at 20°C. 75 µl aldehyde-perchloric acid solution (1 M 4-dimethylaminobenzaldehyde, 60% 1-propanol, 22% perchloric acid (70-72%)) were added and further incubated at 60°C for 25 min. The reaction was stopped by placing the samples on ice and the absorbance was measured using a multi plate reader at a wavelength of 570 nm. The samples were correlated with a standard curve from pure hydroxyproline (Sigma, H1637) and collagen content values were calculated using the sample weight and an estimated hydroxyproline/collagen conversion number of 11.4% (the multiplying factor was calculated from the measured ratio between pure bovine tendon collagen mass and hydroxyproline mass).

Gene Expression Analysis

The amount of mRNA for target genes was measured using quantitative real-time reverse transcriptase (RT) PCR. An overview over targets and primers sequences is provided in table 1. First, tendon constructs were harvested and transferred to RNAse free tubes containing 1 ml TriReagent (Molecular Research Centre, Cincinnati, OH, USA), 5 stainless steel beads of 2.3 mm in diameter and 5 silicon-carbide sharp particles of 1 mm for mechanical disruption (BioSpec Products, Inc., Bartlesville, Oklahoma, USA). For RNA isolation, samples were mechanically disrupted using a FastPrep®-24 instrument (MP Biomedicals, Inc., Illkirch, France) and subsequently bromo-chloropropane (Molecular Research Centre) was added in order to separate the samples into an aqueous and an organic phase. Glycogen was added to the tendon samples to improve RNA precipitation (120 µg per ml TriReagent). Following isolation of the aqueous phase, RNA was precipitated using isopropanol, washed in ethanol and dissolved in RNAse-free water. RNA concentrations were determined by spectroscopy at 260 nm and RNA quality was confirmed by gel electrophoresis.

Table 1. PCR Primer

Target	Sense	Antisense
RPLP0	GGAAACTCTGCATTCTCGCTTCCT	GCTCCTTGCCGAGAAGCAGAAC
COL1A1	GGCAACAGCCGCTTCACCTAC	GCGGGAGGACTTGGTGGTTTT
COL3A1	CACGGAAACACTGGTGGACAGATT	ATGCCAGCTGCACATCAAGGAC
COL5A1	AGCAGATGAAACGGCCCCTG	TCCTTGGTTAGGATCGACCCAGT
COL6A1	CACACCGCTCAACGTGCTCTG	GCTGGTCTGAGCCTGGGATGAA
COL11A1	ACCCTCGCATTGACCTTCCTCTT	ATCCCGTTGTTTTTGATATTCCCTCTG
COL12A1	CCCAGGTCCTCCTGGATACTGTGA	GCAGCACTGGCGACTTAGAAAATGT
COL14A1	AGCATGGGACCGCAAGGC	GACGCGCCACTGATCTCACC
Lysyl Oxidase	CGCTGTGACATTCGCTACACAGGAC	CATTGGGAGTTTTGCTTTGCCTTCT
LOXL1	GGTGAGATGCAACATTCACTACACAGG	GCCTGCTTTGGAAGGGGAGAGA
LOXL2	CCACCGCATCTGGATGTACAACTG	GAGCCCGCTGAAGTGCTCAAA
LOXL3	CTGGGTGCACAACTGCCACAT	TCAAACCTCCTGTTGGCCTCTTC
LOXL4	TATGATGGGCACCGGGTCTG	GGAGAGTTCTGCATTGGCTGGGTA
Transglutaminase 2	CGGGAGGATATCACCCACACC	CTCCTTCTCGGCCAGTTTGTTCA
Decorin	GGTGGGCTGGCAGAGCATAAGT	TGTCCAGGTGGGCAGAAGTCA
Fibrilin-I	CGCTGCAATCATGGTTTCATCCTTT	ATTCCCATTTCCACTTGCACATTC
Elastin	GGCTTCGGATTGTCTCCCATTTT	CCAACGTTGATGAGGTCGTGAG
BMP-I	CAGACGGCACACAGCTCGTAAGT	TGGCAGCTGGGGGTAGAAGTGT
Fibromodulin	CAGTCAACACCAACCTGGAGAACC	TGCAGAAGCTGCTGATGGAGAA
Tenascin-C	CAACCATCACTGCCAAGTTCACAA	GGGGGTCGCCAGGTAAGGAG
Tenascin-X	GGAGGACTATGCCCATGGTTTTG	CGCATGGAGTAGTCACCTGCCTGT
Biglycan	AGGCCAAGCTGACTGGCATCC	TGGCCTGGATTTTGTTGTGGTC
Lumican	CCCTGGTTGAGCTGGATCTGTC	CCAGGATCTTGCAGAAGCTCTTTATGT

Synthesis of complementary DNA (cDNA) was performed using the Omniscript reverse transcriptase (Qiagen, Hilden, Germany) on 500 ng of tendon cell RNA. For each target mRNA, 0.25µl of 20x diluted cDNA (in 1x Tris/EDTA buffer with 1ng/µl salmon DNA) was amplified in 25µl Quantitect SYBR Green Master Mix (Qiagen) with specific primers (100 nM each, Table 1) on a real-time PCR machine (MX3000P, Stratagene, La Jolla, CA, USA). The thermal profile was 95°C, 10 min → (95°C, 15 s → 58°C, 30 s → 63°C, 90 s) × 50 → 95°C, 60 s → 55°C, 30 s → 95°C, 60 s. Signal intensity was acquired at the 63°C step and the threshold cycle (Ct) values were related to a standard curve made with the cloned PCR product. Specificity was confirmed by melting curve analysis after amplification (the 55°C to 95°C step). The large ribosomal protein P0 (RPLP0) mRNA, which was stably expressed relative both to GAPDH mRNA and total RNA (data not shown), was chosen as internal control. Values were normalized by RPLP0 expression and are presented as relative difference from 21 day control.

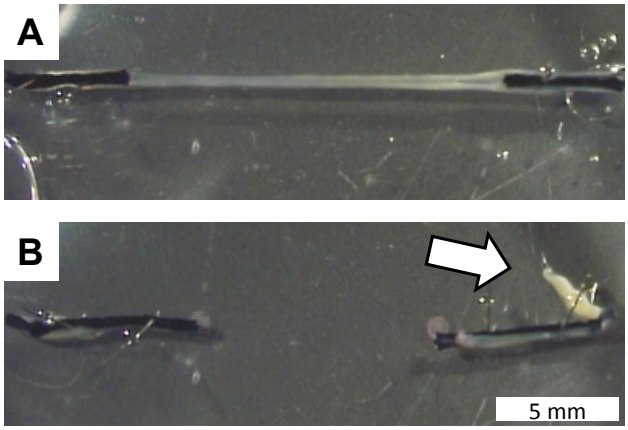

Figure 1. The tendon construct. A) Tendon construct grown for 14 days under control conditions. The black sutures at the ends anchor the structure to the base of the well. B) When treated with 50 µM BAPN, the construct ruptures spontaneously around the time point of formation. On the right hand side suture the retracted remnants of the construct is visible (arrow).

Collagen Cross-link Analysis

Tendon constructs were washed twice in PBS, blotted dry and subsequently heated in SDS-PAGE sample buffer (5 mg/ml) at 95°C for 3 min. Samples were run on 5% SDS-PAGE according to standard procedures [22]. For detection of type III collagen we used delayed reduction. Therefore, the gel was stopped after 20 min and 10 µl 0.5 M DTT (in water with

10% glycerol) were added. The gel was subsequently washed, stained with commassie brilliant blue, washed again and analyzed.

SDS-PAGE and Western Blotting

Tendon constructs for western blotting were washed in PBS and blotted dry. Constructs were lysed by mechanical disruption with a pistil and sonication for 3x5 s in sample buffer (NuPAGE® LDS sample buffer, Invitrogen, Carlsbad, CA, USA). Subsequently the samples were heated to 95°C for 10 min and centrifuged at 10000xg for 10 min and stored at -80°C until further use.

Samples were incubated at 70°C for 10 min and separated on a NuPAGE® criterion XT 4-12% Bis-Tris gel using 1xNuPAGE® MES SDS running buffer (Invitrogen) at 700 V for 70 min, blotted with an iBlot™ device (Invitrogen) on PVFD membranes (GE-healthcare, Little Chalfont, UK) and blocked with 5% milk powder in PBS plus 0.1% tween 20. Primary antibodies against LOX (1:1000; NB100-2530), collagen V (1:500; NBP1-19633), decorin (1:500; NBP1-84970), fibromodulin (1:500; NBP2-16494) and tenascin-X (1:500; H00007-D01P) were incubated over night at 4°C (all acquired from Novus biologicals, Littleton, CO, USA). The complementary HRP-conjugated secondary antibody (anti-rabbit, 1:1000 dilution, swine, DAKO, #P0399) was incubated for 1 h. Membranes were analysed using an Odyssey® FC system with complemented software (LI-COR Biotechnology, Lincoln, NE, USA).

Statistics

Construct mechanical data, total collagen content, mean fibril diameter and gene expression data were analysed by one-way ANOVA and individual differences were determined by Tukey's multiple comparisons test. Level of significance was set at $p<0.05$.

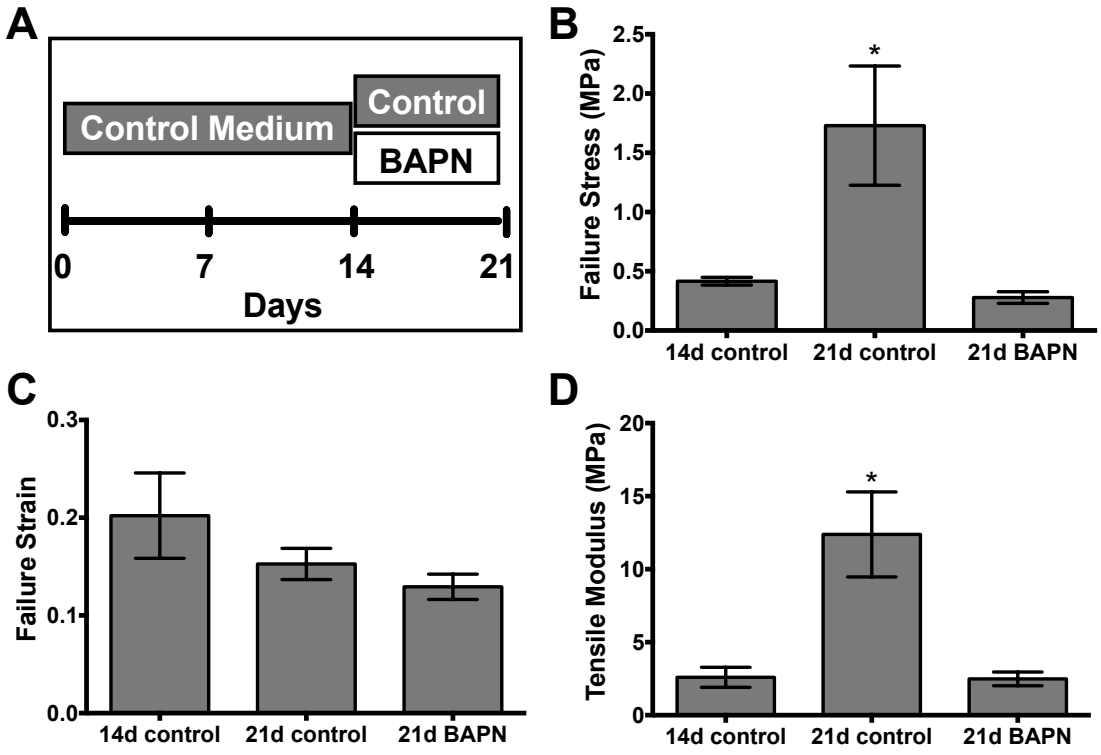

Figure 2. Construct mechanical data. A) Due to the rupture as shown in Fig.1, constructs were treated with control medium for 14 days and thereafter treated with 50 μM BAPN or left as controls, respectively, for 7 days. B) Failure stress of control constructs develops from day 14 to 21 by approximately 1.3 MPa. BAPN treatment inhibits abolishes this development completely. C) Despite a trend towards lower strains at 21 days, no statistical change in strain was found. D) The tensile modulus rises according to the increase in stress over similar strains by approximately 10 MPa. Again, the BAPN treatment prohibits this increase. (Data presented as Mean±SEM; *$p<0.05$ compared to other groups)

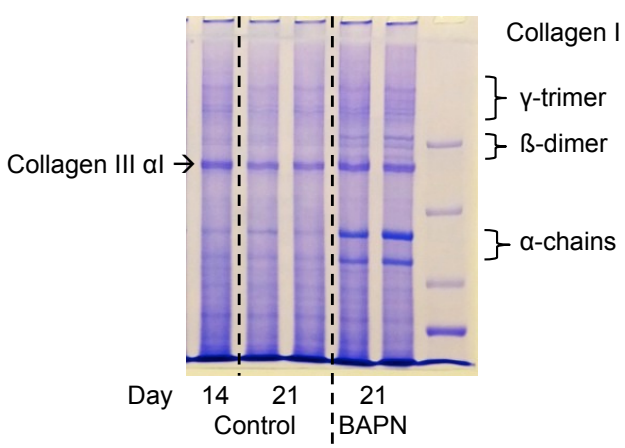

Figure 3. Collagen solubility. Equal amounts of tendon constructs were analyzed by SDS-PAGE in order to assess the collagen cross-link abundance in 14 and 21 day controls vs. BAPN treatment. The characteristic collagen type I pattern is shown with α monomers, β dimers and γ trimers. Overall, the BAPN samples show higher band intensity, particularly for monomers and dimers, suggesting higher collagen solubility due to fewer cross-links. Furthermore, the collagen type III αI chain is indicated. This shows similar amounts in all samples.

Results

Mechanical Testing

Ultimate failure stress developed from 14 to 21 days from 0.41 MPa (±0.03; mean ± SEM) to 1.73 MPa (±0.50) under control conditions, and this increase was completely abolished by BAPN (Fig.2B). The tensile strain at failure did not change significantly with time, and was unaffected by BAPN (Fig.2C). The stress/strain curve resulted in a tensile modulus of 2.59 MPa (±0.68) after 14 days and was increased to 12.38 MPa (±2.90) after 21 days in controls; whereas BAPN treated constructs did not show any development over 7 days and had a value of 2.48 MPa (±0.46) after 21 days (Fig.2D).

In an attempt to analyze the collagen cross-linking, equal amounts of homogenized tendon constructs were separated by SDS-PAGE. The characteristic pattern for collagenous tissue with collagen alpha monomers, beta dimers and gamma trimers is typically used as separation step for further HPLC analysis [23]. Representative data for one 14 day control, two 21 day control constructs and two 21 day BAPN-treated constructs are shown in Fig.3. The gel indicates that collagen from BAPN treated samples were more extractable than from control constructs as indicated by the higher band signal intensity, particularly for the alpha chains and beta dimer (Fig.3). The collagenIIIαI chain is visible due to the interrupted PAGE technique. Notably, this band was similar in the three groups. (Fig.3).

Tendon Construct Ultrastructure

The TEM data of the tendon constructs showed regular collagen fibril distributions with circular outlines, a uniform distribution of fibrils in the extracellular space and healthy cells (intact membranes, rough ER). At 14 days, control constructs show small collagen fibrils with similar diameters (Fig.4A) and after 21 days, the collagen fibrils were larger in diameter, yet still with rather uniform diameters (Fig.4B). At higher magnification the collagen fibrils of control constructs were not perfectly circular, but showed clear outlines with consistent fibril spacing (Fig.4D+E). Small dark circles in the ECM are microfibrils, which are characteristic for tendon tissue and fibripositors suggest novel collagen fibril development (indicated in image). In contrast, BAPN treated constructs showed irregular collagen fibril shapes with branching structures to different sides. The fibrils were of uneven size and spacing among fibrils varies highly. At high magnification, some fibrils appeared to fuse leading to very large fibril complexes, while other fibrils were very small (Fig.4C+F). The cells in BAPN treated samples looked nonetheless healthy, with rough ER indicating cell activity (Fig.4) and intact nuclei (compare supplemented videos). Microfibrils and fibripositors were also visible in BAPN samples, suggesting normal ECM composition except the described collagen fibril impairment.

Total collagen content was measured and normalised to construct dry weight in order to quantify the effect of BAPN on collagen synthesis. 14 day constructs had a mean collagen content of 7.0% (±1.5; mean ± SD), while constructs at 21 days had significantly higher collagen contents at 11.6% (±1.9)($p<0.05$). Though, BAPN treated constructs had similar total collagen contents to controls with 11.8% (±3.2)(Fig.5A). Similarly, the average fibril diameter developed significantly from 32.11 nm (±6.98; mean ± SD)

at 14 days to 44.87 nm (±9.61) at 21 days under control conditions. The BAPN treated samples showed a similar development to 44.78 nm (±13.83)(Fig.5B). In order to understand the effect of BAPN on collagen fibrillogenesis further, the fibril spectra for 14 day controls, 21 day controls and 21 day BAPN treated samples are shown in Fig.5C. 14 day constructs show a unimodal Gaussian distribution around the mean fibril diameter. The distribution of 21 day control constructs is shifted to the right with few fibrils reaching high diameters of above 60 nm. BAPN treated constructs have a similar distribution to 21 day controls, but have a more wide and flat distribution; i.e. the BAPN treated samples contain more very small diameter fibrils and a population of very large diameter fibrils as also visible in TEM images above. The ultrastructure was further assessed using three-dimensional electron microscopy (3view) to evaluate the tissue organisation in depth (supplementary videos 1+2). The videos show sections through a 21 day control construct (video 1) and a BAPN treated construct (video 2). Both samples show high cellular density, exhaustive cell connections and open ECM spaces. This space is partly covered by collagen fibrils that run longitudinally. The collagen fibrils move slightly in x and y direction, and yet they do not change course in z direction. This shows that BAPN treated fibrils are similar to control tissue despite being disrupted in shape. Importantly, also the large disrupted fibrils (recognisable by heavily stained larger structures in the ECM) appear to be consistent in shape over larger distances.

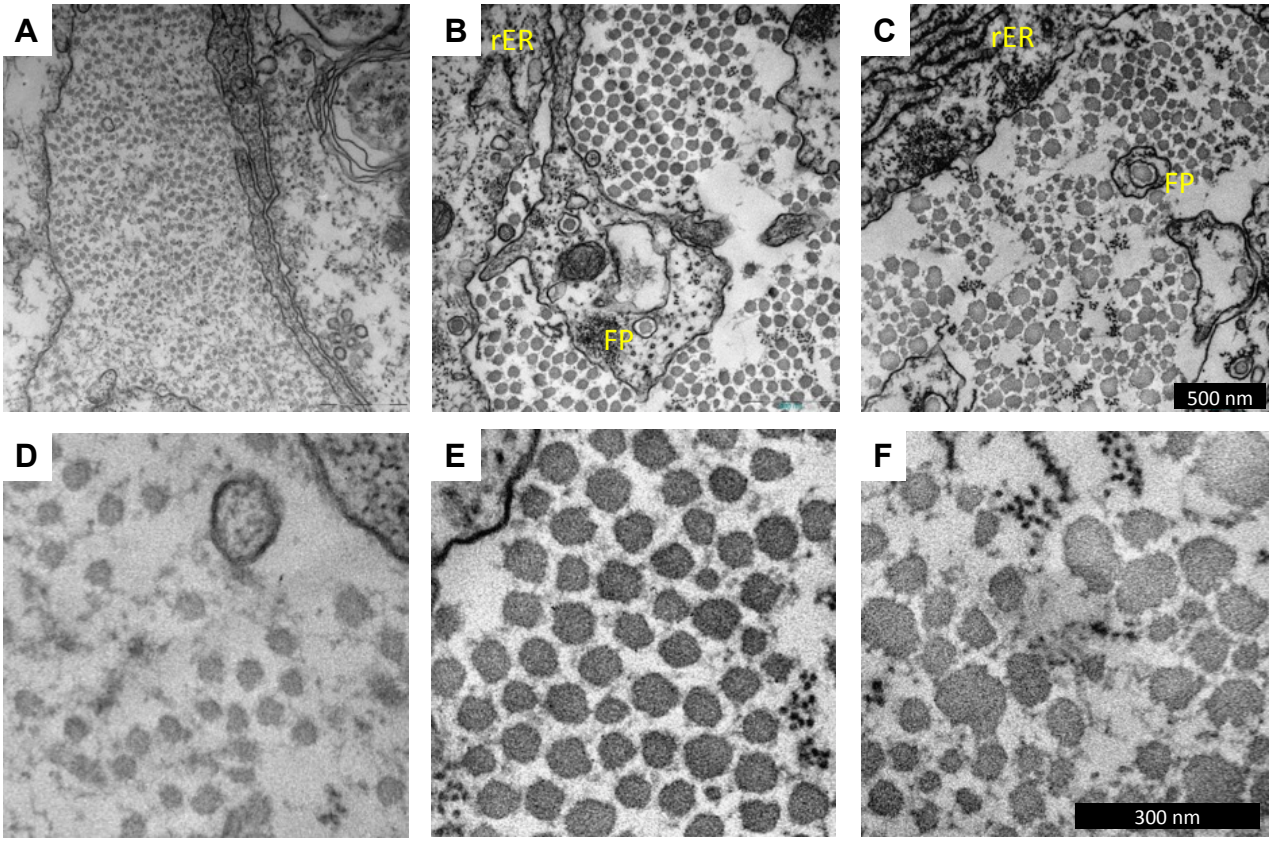

Figure 4. BAPN precludes correct collagen fibril formation. Tendon construct cross-sections were investigated by TEM for their ultrastructure. A+D) 14 day control constructs show small diameter fibrils distributed in the extracellular space. At high resolution (D) the fibrils show almost circular outlines with large spacing in between individual fibrils. B+E) At 21 days, the constructs show increased fibril diameters and tighter packing density. Moreover, the fibrils have similar fibril diameter with regular shapes. Rough endoplasmic reticulum (rER) indicate active cells and fibripositors (FP) hint towards cell-collagen interactions and collagen production. C+F) BAPN treated samples in contrast show heavily disrupted fibril shapes and irregular spacing in between individual fibrils. Fibril diameters vary considerably between very small and very large fibrils of up to 100 nm. Moreover, the very large fibrils totally lost their circular shape. Compare supplementary videos for a broader overview. (Scale bar 500 nm for A-C in C; scale bar 300 nm for D-F in F)

Gene Expression

To further address the response by the cells to LOX inhibition, gene expression of the different groups was analysed. At first, LOX and the LOX family members LOXL1-4 were investigated. Moreover, the collagen cross-linker transglutaminase 2 was included. As visible in Fig.6A, no significant changes in gene expression could be detected among the three groups. The group of established collagen fibrillogenesis regulators decorin, collagen V, fibromodulin and tenascin-X was analysed next. However, there was no significant change between groups for these parameters either (Fig.6B). Similarly, no changes could be detected in the group of important ECM molecules. This group included fibrillin I, Collagens I, III, VI, XI, XII, XIV, elastin, BMP-1, tenascin-C, biglycan and lumican. Despite that the data indicate an overall reduction in gene expression of these molecules, no statistical differences could be detected (Fig.6C). Moreover, as these data only were obtained after seven days of LOX inhibition, the immediate response of the cells to BAPN treatment was monitored over 1, 6, 12, 24 and 48 hours. Representatively for these experiments the expression profile for LOX over the time course is shown in Fig.6D. As for the above-mentioned experiments, no changes were observed. Collagen I, III, V, decorin, fibromodulin and tenascin-X did resemble this result with no change due to BAPN treatment (data not shown).

Western Blotting

Fig.7A shows the results for LOX and for the fibrillogenesis regulators decorin, fibromodulin and tenascin-X. LOX is not changed between the two treatments. The active form of LOX is thereby approximately 80 kDa (personal communication with Dr. Janine Erler, BRIC Copenhagen). Similarly, decorin and fibromodulin are not changed with very distinct bands (Fig.7A). Tenascin-X shows a band at approximately 75 kDa (indicated in figure) that depicts the tenascin-X protein, which is not changed due to BAPN treatment.

Collagen type V was analysed in direct comparison to a coomassie staining in order to analyse the cross-linking pattern of this collagen type simultaneously (Fig.7B). The rational in this experiment was to use the characteristic collagen monomer, dimer and trimer staining and directly evaluate the position of collagen type V in this context. There is, however, no difference detectable between controls and BAPN treated constructs (Fig.7B). This indicates no direct effect of LOX inhibition on collagen type V positioning within the collagen fibrils.

Discussion

LOX has previously been proven to be essential for the mechanical integrity of collagen [13, 15]. These data show here that this holds true for *in vitro* engineered tendon constructs from adult human tendon fibroblasts that present aligned collagen fibrils. Interestingly, blocking of LOX by BAPN leads to spontaneous rupture of constructs when introduced from early fibrillogenesis and it stops mechanical development when added to already formed- but still developing constructs (Fig.1+2). This effect is most likely due to a loss of intra- and possibly inter-fibrillar collagen cross-links, since collagen solubility was increased with BAPN treatment (Fig.3). Furthermore, we were able to show that LOX inhibition leads to impaired collagen fibril outlines and broad non-physiological fibril diameter distributions, despite no change in the total amount of collagen (Fig.4). The average fibril diameter remained also unchanged, but the irregular BAPN-treated fibrils manipulated this result. Because perfect circularity of fibrils was assumed, the minimal width was measured to obtain diameters. This underestimated the absolute size of the fibrils, as the simplified circles had a smaller area than the actual fibril had.

The effect of BAPN on tissues was for the first time shown by Levene et al. on chick embryos [15]. Injections of BAPN into fertilized eggs led to exceptionally weak connective tissues and high collagen solubility [13, 15]. Furthermore, constructs treated with BAPN from day 0

rupture at the time of formation (Fig.1). We have seen earlier that tendon constructs increase continuously in mechanical stiffness during five weeks post seeding [19]. Here we show that mechanical development of tendon-like tissue can be stopped by BAPN between days 14 and 21. Irrespective of BAPN treatment, the total collagen content increases similarly to controls during this phase (Fig.5). Therefore, our data suggests that in early development cross-links are an essential component to form mechanically and structurally intact collagen fibrils.

In line with the unaltered total collagen content, gene expression of various ECM targets like collagens I, III, V, IX and XII, biglycan, lumican, tenascin-C and elastin were equally expressed in BAPN treated samples compared to controls at all times (Fig.6). Gene expression of the cross-linking enzymes LOX, LOXL 1-4 and transglutaminase were also unaffected. This supports the notion that there is no effect of BAPN on the cells. It can also be hypothesized that the cells lack a mechanism to effectively manage collagen cross-linking. The fact that tendon constructs ruptured spontaneously when treated with BAPN from day 0 corroborates this theory. The fibroblasts applied a constant force that the impaired ECM could not withstand, leading to total rupture of the structure. Collagen fibril diameters and shapes are distinct markers of tissue integrity [24]. Throughout the body, the collagen network is shaped according to mechanical demands. This includes random networks of size-varying fibrils in skin [2, 25], fibrils interspersed with hydroxyapatite crystals in bones [4], highly organised layers of low-diameter fibrils in cornea [26, 27], strands of low-diameter fibrils in ligaments and strands of large diameter fibrils in tendons [24, 28]. Collagen fibrillogenesis starts with the production of tropocollagen molecules, which are extracellularly arranged into fibrils [5]. Early fibrils are about 20 nm in diameter, have circular outlines and tapered ends [5]. To date, collagen type V, decorin, fibromodulin and tenascin-X have been well established to have regulatory functions in collagen fibril diameter regulation [29-32]. Mutations in the collagen type 5 genes lead to classic Ehlers-Danlos disease (EDS), characterized by skin and joint hypermobility as well as frail bones [33-35]. Electron micrographs of tendons from classic EDS patients show dispersed fibril diameters and random "cauliflower-shaped" collagen fibrils [36]. Common theory suggests that collagen V fibrils are periodically included in collagen I fibrils and prohibit random accumulation of further collagen I molecules by sterical hindrance [29, 36].

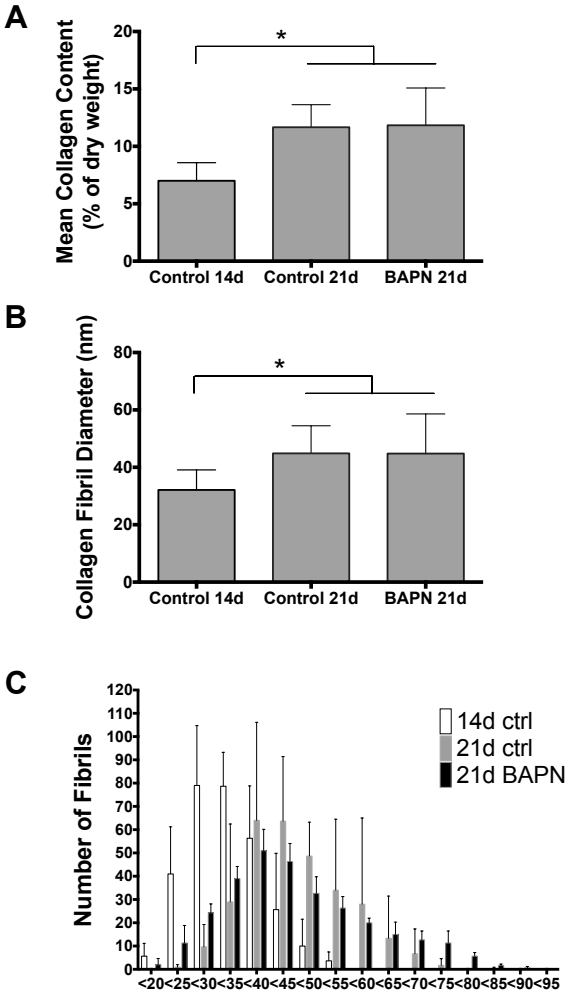

Figure 5. Collagen quantification. A) Total collagen content develops from 14 to 21 days by approximately 4.5% of dry weight. BAPN does not affect the increase in collagen content. B) Similarly, the mean collagen fibril diameter increases from day 14 to 21 by ca. 12 nm without any effect of BAPN. C) The distributions for controls shift as expected from days 14 to 21 towards higher diameters. BAPN treated constructs show a flattened distribution with more low- and high diameter fibrils compared to 21 day controls. However, the irregular shapes of BAPN treated fibrils are underestimated in size, as the minimal diameter was measured with the assumption of fibril circularity. (Mean±SEM; *$p<0.05$ towards other groups as indicated)

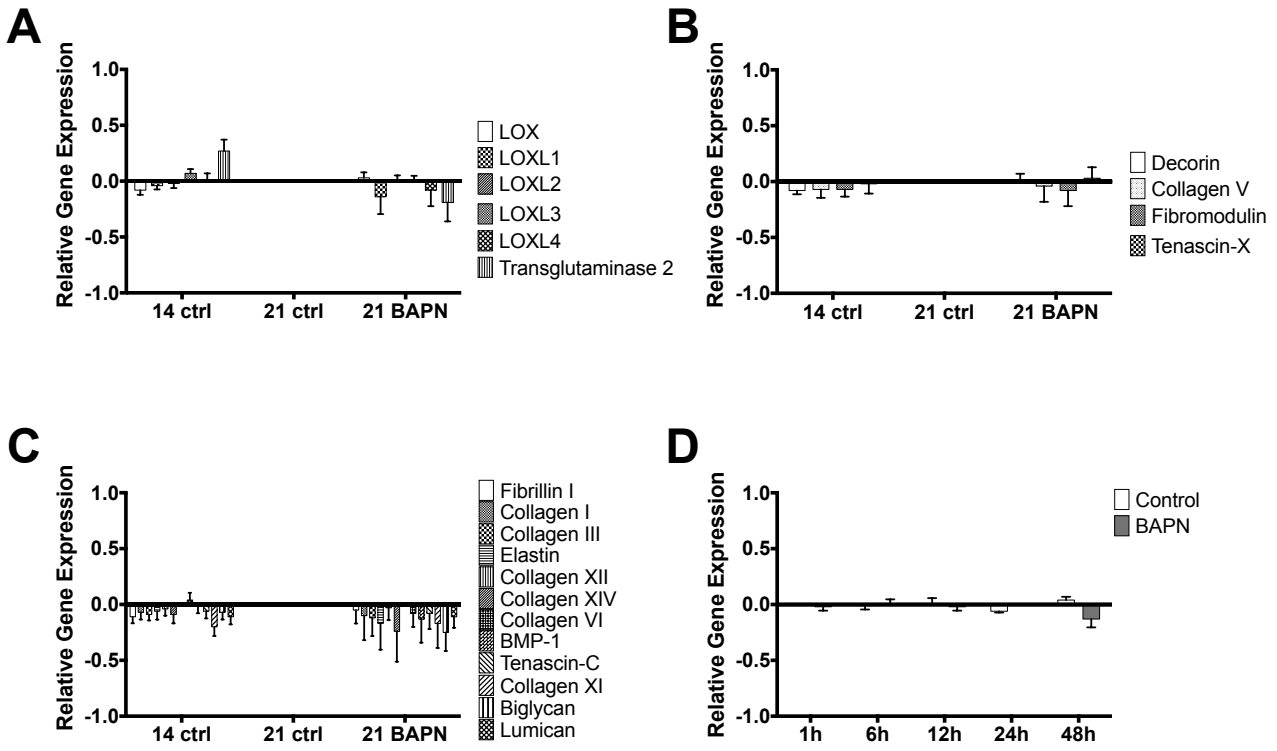

Figure 6. Gene expression analysis. Gene expression for 14 and 21 day controls, as well as 21 day BAPN treated samples was analyzed for (A) collagen cross-linking enzymes, (B) important fibrillogenesis regulators and (C) essential ECM components. Moreover, the immediate response towards BAPN treatment was analyzed as presented here for LOX gene expression (D). A similar pattern to (D) was observed for all other molecules. Overall, no changes in gene expression were found. (Mean±SEM)

Collagen types I and V are cross-linked to each other in theses heterotypic fibrils [37-39]. Lack of the small leucin-rich proteoglycan (SLRP) decorin has been shown to have a similar effect on collagen fibril formation as the above-described mutation in collagen V [30]. Decorin binds to collagen fibrils [40, 41] and it was proposed that it tightly controls collagen fibril structure by binding four single collagen molecules [42]. Fibromodulin also binds to collagen fibrils [43] and fibromodulin knockout mice show a similar phenotype to decorin knockout mice with irregular fibrils and super-flexible tissues [31]. These mice have – despite significantly weaker tendons – higher amounts of collagen cross-links [23]. It was proposed therefore that fibromodulin has a LOX-inhibiting role in order to prevent excessive cross-linking [23]. A different genetic cause of EDS is a mutation in the gene encoding tenascin-X [32], as also proven in tenascin-X deficient mice, which show elastic skin and irregular fibrils [44, 45]. Taken together, these studies present a very sensitive regulation system for collagen fibril formation by a close interplay of collagen V, decorin, fibromodulin and tenascin-X. This study showed that LOX inhibition leads to similarly disrupted collagen fibrils, adding LOX to this list of essential fibrillogenesis regulators.

To investigate connections between the here described results and knowledge about these fibril regulators, gene expression profiles were analysed. However, no change in gene expression was found for the collagen cross-link regulating proteins (Fig.6B). Thus, any possible interaction of the named molecules would occur extracellularly and without cellular control. Western blotting, though, resembled the gene expression data and did not show an effect on these proteins (Fig.7). Collagen type V was also directly compared to coomassie staining of the construct matrix to investigate whether cross-linking to type I collagen was altered. As this experiment did not show altered collagen type V

location (Fig.7B), LOX regulates fibril shape by another, yet to be discovered mechanism.

A recent study focussing on corneal development investigated the effects of LOX and transglutaminase (TG) induced cross-linking on cornea collagen fibrils [17]. 3-dimensional tissue constructs from chick corneal fibroblasts were manipulated with BAPN and TG inhibitor. TG inhibition had again a similar effect as the above described collagen V absence – collagen fibrils showed broadened diameter spectra and random shapes [17]. Interestingly, BAPN treatment had no effect on fibril shape in contrast to the present study. This might either be due to the fact that fibril formation is differently organised by tendon vs. cornea cells, or that the corneal constructs were not cultured under tensile tension as described here. Moreover, earlier studies of decorin deficient mice showed highly impaired collagen fibrils in tendons and skin but no change in corneal tissue, which supports the notion that collagen fibrillogenesis in cornea is regulated differently [46].

The novel 3view electron microscopy technique provided valuable insight into the 3 dimensional tissue architecture. The possible resolution is critical to follow single fibrils over a longer distance. The data show that the collagen fibrils in BAPN treated samples were similarly arranged to control tissue (supplementary videos). Fibril populations were in close proximity to the cells and moved moderately across the plane of view. Few large (probably irregular shaped) collagen fibrils were seen in the BAPN treated samples that appeared to be fusing with lower diameter fibrils. This observation and the overall structural differences were, however, difficult to quantify due to technical limitations.

In summary, we demonstrate that LOX is essential for correct collagen fibril shape formation and that it is important for collagen aggregation. Due to its capacity to establish cross-links, LOX also plays a significant role for mechanical stiffness and load resistance of tendons in human collagen fibrillogenesis.

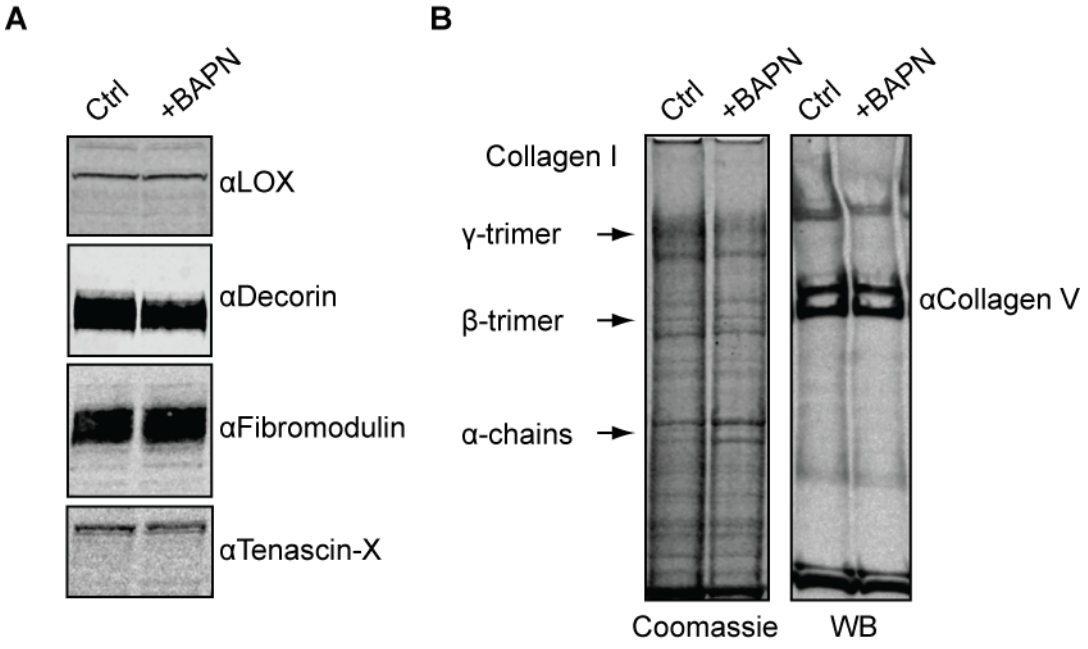

Figure 7. Western blotting results of 21 day controls and BAPN-treated samples were compared for LOX, decorin, fibromodulin and tenascin-X (A). The band for active LOX is not different between the treatments. Similarly, no change was found for decorin, fibromodulin and tenascin-X. (B) Direct comparison between a polyacrylamide gel stained with coomassie brilliant blue (left side) and western blot for collagen type V (right). The described pattern of collagen type I monomers, dimers and trimers is visible. The collagen type V alpha chain is indicated and is similarly positioned in both control and BAPN-treated construct. (Ctrl=Control, +BAPN=BAPN-treated)

Acknowledgements

The authors gratefully acknowledge the help with tissue acquisition of the department of orthopaedic surgery at Bispebjerg Hospital. The Core Facility for Integrated Microscopy at the University of Copenhagen is thankfully acknowledged for support and access to electron micro- scopes. Funding is gratefully acknowledged from the Nordea Foundation (Healthy Aging grant), the University of Copenhagen, Department of Health Sciences and the Academy of Muscle Biology, Exercise and Health Research.

References

1. Kastelic, J., G. A., and B. E., The Multicomposite Structure of Tendon, Connect Tissue Res 6 (1978) 11-23.
2. Silver, F.H., J.W. Freeman, and D. DeVore, Viscoelastic properties of human skin and processed dermis, Skin Res Technol 7(1) (2001) 18-23.
3. Wang, R., L.P. Brewster, and R.L. Gleason, Jr., In-situ characterization of the uncrimping process of arterial collagen fibers using two-photon confocal microscopy and digital image correlation, J Biomech 46(15) (2013) 2726-9.
4. Weiner, S. and W. Traub, Bone structure: from angstroms to microns, FASEB J 6(3) (1992) 879-85.
5. Kadler, K.E., et al., Collagen fibril formation, Biochemical Journal 316 (1996) 1-11.
6. Brown, I.A., Scanning electron microscopy of human dermal fibrous tissue, J Anat 113(Pt 2) (1972) 159-68.
7. Kagan, H.M. and W. Li, Lysyl oxidase: properties, specificity, and biological roles inside and outside of the cell, J Cell Biochem 88(4) (2003) 660-72.
8. Eyre, D.R., M.A. Paz, and P.M. Gallop, Cross-linking in collagen and elastin, Annu Rev Biochem 53 (1984) 717-48.
9. Maki, J.M., et al., Inactivation of the lysyl oxidase gene Lox leads to aortic aneurysms, cardiovascular dysfunction, and perinatal death in mice, Circulation 106(19) (2002) 2503-9.
10. Maki, J.M., et al., Lysyl oxidase is essential for normal development and function of the respiratory system and for the integrity of elastic and collagen fibers in various tissues, Am J Pathol 167(4) (2005) 927-36.
11. Baker, A.M., et al., Lysyl oxidase enzymatic function increases stiffness to drive colorectal cancer progression through FAK, Oncogene 32(14) (2013) 1863-8.
12. Cox, T.R., et al., LOX-mediated collagen crosslinking is responsible for fibrosis-enhanced metastasis, Cancer Res 73(6) (2013) 1721-32.
13. Pinnell, S.R. and G.R. Martin, The cross-linking of collagen and elastin: enzymatic conversion of lysine in peptide linkage to alpha-aminoadipic-delta-semialdehyde (allysine) by an extract from bone, Proc Natl Acad Sci U S A 61(2) (1968) 708-16.
14. Tang, S.S., P.C. Trackman, and H.M. Kagan, Reaction of aortic lysyl oxidase with beta-aminopropionitrile, J Biol Chem 258(7) (1983) 4331-8.
15. Levene, C.I. and J. Gross, Alterations in state of molecular aggregation of collagen induced in chick embryos by beta-aminopropionitrile (lathyrus factor), J Exp Med 110 (1959) 771-90.
16. Marturano, J.E., et al., Characterization of mechanical and biochemical properties of developing embryonic tendon, Proc Natl Acad Sci U S A 110(16) (2013) 6370-5.
17. Wang, L., et al., Lateral growth limitation of corneal fibrils and their lamellar stacking depend on covalent collagen cross-linking by transglutaminase-2 and lysyl oxidases, respectively, J Biol Chem 289(2) (2014) 921-9.
18. Bayer, M.L., et al., The initiation of embryonic-like collagen fibrillogenesis by adult human tendon fibroblasts when cultured under tension, Biomater 31(18) (2010) 4889-4897.
19. Herchenhan, A., et al., In vitro tendon tissue development from human fibroblasts demonstrates collagen fibril diameter growth associated with a rise in mechanical strength, Dev Dyn 242(1) (2013) 2-8.
20. Kapacee, Z., et al., Tension is required for fibripositor formation, Matrix Biol 27(4) (2008) 371-375.
21. Starborg, T., et al., Using transmission electron microscopy and 3View to determine collagen fibril size and three-dimensional organization, Nat Protoc 8(7) (2013) 1433-48.
22. Laemmli, U.K., Cleavage of structural proteins during the assembly of the head of bacteriophage T4, Nature 227(5259) (1970) 680-5.
23. Kalamajski, S., et al., Increased C-telopeptide Cross-linking of Tendon Type I Collagen in Fibromodulin-deficient Mice, J Biol Chem 289(27) (2014) 18873-18879.
24. Parry, D.A., G.R. Barnes, and A.S. Craig, A comparison of the size distribution of collagen fibrils in connective tissues as a function of age and a possible relation between fibril size distribution and mechanical properties, Proc R Soc Lond B Biol Sci 203(1152) (1978) 305-21.
25. Smith, L.T., K.A. Holbrook, and P.H. Byers, Structure of the dermal matrix during development and in the adult, J Invest Dermatol 79 Suppl 1 (1982) 93s-104s.
26. Birk, D.E. and R.L. Trelstad, Extracellular compartments in matrix morphogenesis: collagen fibril, bundle, and lamellar formation by corneal fibroblasts, J Cell Biol 99(6) (1984) 2024-33.
27. Komai, Y. and T. Ushiki, The three-dimensional organization of collagen fibrils in the human cornea

and sclera, Invest Ophthalmol Vis Sci 32(8) (1991) 2244-58.
28. Zhu, J., et al., Ultrastructural and Morphological Characteristics of Human Anterior Cruciate Ligament and Hamstring Tendons, Anat Rec (Hoboken) 295(9) (2012) 1430-6.
29. Wenstrup, R.J., et al., Type V collagen controls the initiation of collagen fibril assembly, J Biol Chem 279(51) (2004) 53331-7.
30. Zhang, G., et al., Decorin regulates assembly of collagen fibrils and acquisition of biomechanical properties during tendon development, Journal of Cellular Biochemistry 98(6) (2006) 1436-1449.
31. Svensson, L., et al., Fibromodulin-null mice have abnormal collagen fibrils, tissue organization, and altered lumican deposition in tendon, J Biol Chem 274(14) (1999) 9636-47.
32. Schalkwijk, J., et al., A recessive form of the Ehlers-Danlos syndrome caused by tenascin-X deficiency, N Engl J Med 345(16) (2001) 1167-75.
33. Malfait, F., et al., The molecular basis of classic Ehlers-Danlos syndrome: a comprehensive study of biochemical and molecular findings in 48 unrelated patients, Hum Mutat 25(1) (2005) 28-37.
34. Wenstrup, R.J., et al., COL5A1 haploinsufficiency is a common molecular mechanism underlying the classical form of EDS, Am J Hum Genet 66(6) (2000) 1766-76.
35. Nielsen, R.H., et al., Low tendon stiffness and abnormal ultrastructure distinguish classic Ehlers-Danlos syndrome from benign joint hypermobility syndrome in patients, FASEB J (2014).
36. Wenstrup, R.J., et al., Murine model of the Ehlers-Danlos syndrome. col5a1 haploinsufficiency disrupts collagen fibril assembly at multiple stages, J Biol Chem 281(18) (2006) 12888-95.
37. Birk, D.E., Type V collagen: heterotypic type I/V collagen interactions in the regulation of fibril assembly, Micron 32(3) (2001) 223-37.
38. Birk, D.E., et al., Collagen type I and type V are present in the same fibril in the avian corneal stroma, J Cell Biol 106(3) (1988) 999-1008.
39. Niyibizi, C. and D.R. Eyre, Structural characteristics of cross-linking sites in type V collagen of bone. Chain specificities and heterotypic links to type I collagen, Eur J Biochem 224(3) (1994) 943-50.
40. Fleischmajer, R., et al., Decorin interacts with fibrillar collagen of embryonic and adult human skin, J Struct Biol 106(1) (1991) 82-90.
41. Pringle, G.A. and C.M. Dodd, Immunoelectron microscopic localization of the core protein of decorin near the d and e bands of tendon collagen fibrils by use of monoclonal antibodies, J Histochem Cytochem 38(10) (1990) 1405-11.
42. Orgel, J.P., et al., Decorin core protein (decoron) shape complements collagen fibril surface structure and mediates its binding, PLoS One 4(9) (2009) e7028.
43. Hedbom, E. and D. Heinegard, Binding of fibromodulin and decorin to separate sites on fibrillar collagens, J Biol Chem 268(36) (1993) 27307-12.
44. Bristow, J., et al., Tenascin-X, collagen, elastin, and the Ehlers-Danlos syndrome, Am J Med Genet C Semin Med Genet 139C(1) (2005) 24-30.
45. Mao, J.R., et al., Tenascin-X deficiency mimics Ehlers-Danlos syndrome in mice through alteration of collagen deposition, Nat Genet 30(4) (2002) 421-5.
46. Danielson, K.G., et al., Targeted disruption of decorin leads to abnormal collagen fibril morphology and skin fragility, J Cell Biol 136(3) (1997) 729-43.

Supplementary Videos

Video 1. Video through the 3view dataset of a 21 day control. Cell nuclei are clearly visible and show invaginations. The cells and the collagen fibrils are longitudinally aligned. The magnification allows for differentiation among individual fibrils, but not for a clear view at the fibril shape. However, collagen fibrils are overall similar in shape and size as proven by TEM in Fig.4.

Video 2. Video through a serial stack of cross-sections of a BAPN-treated construct. Note the similarity in cells and nuclei compared to control constructs, suggesting that BAPN does not negatively affect the cells (video 1). Also, the ECM looks very similar. Large, heavily stained collagen fibrils can be observed that show dispersed shapes in TEM (compare Fig.4). Importantly, it appears like these fibrils are normally aligned with the longitudinal axis and are not the result of constant and uncontrolled branching/fusion of smaller fibrils.

Please find the videos under this link:

https://www.dropbox.com/sh/oy76udf1sc5rioy/AABJP9CZhsQ-Lyz3lWKfei9Ra?dl=0